Modelling and evaluation of ozone dry deposition

Dissertation

zur Erlangung des akademischen Grades
Doktor der Naturwissenschaften
am Fachbereich Geowissenschaften
der Freien Universität Berlin

Vorgelegt von

Dalma Szinyei

September 2014

Freie Universität Berlin

1. Gutachter: Prof. Dr. Peter Builtjes
2. Gutachter: Prof. Dr. Ulrich Cubasch

Tag der Disputation: 11. 12. 2014

Erklärung

Hiermit erkläre ich, dass ich die beigefügte Dissertation 'Modelling and evaluation of ozone dry deposition' selbstständig verfasst und keine anderen als die angegebenen Hilfsmittel genutzt habe.

Ich versichere außerdem, dass ich die beigefügte Dissertation nur in diesem und keinem anderen Promotionsverfahren eingereicht habe und, dass diesem Promotionsverfahren keine endgültig gescheiterten Promotionsverfahren vorausgegangen sind.

Dalma Szinyei

Berlin, den 23. 9. 2014

,,… dolgozni csak pontosan,
szépen,
ahogy a csillag megy az
égen,
ugy érdemes.''

,,… merely working
precisely and nice,
just like a star walks in the
sky,
is worth it.''

(József Attila)

To my Family and my Friends

Contents

I. Introduction

The changing seasons are the most spectacular manifestations of the connection between the atmosphere and the ecosystem. Almond trees in bloom, yellow rape fields and falling leaves are visible signs of changes in the lifecycle of plants in accordance with the annual courses of meteorological parameters. However, the relation between the atmosphere and ecosystem is not one-sided: it is not only the ecosystem that influences the atmosphere. The current composition of the atmosphere (nitrogen [N2] ~78%, oxygen [O2] ~21% and argon [Ar] ~0.93% relative fraction in dry air (Warneck, 2000)) has been formed by autotrophs to be favorable for terrestrial life, and this interaction between these two systems is still controlling our environment. Recently, experts - realizing the importance of the connection between these animate and inanimate systems (the biosphere and the atmosphere) - have turned toward the investigation of the boundaries of earth and life sciences such as the investigation of fluxes between the atmosphere and the ecosystem.

The trace gases, representing less than 1% of the atmosphere (e.g. carbon dioxide [CO_2], methane [CH_4], nitrous oxide [N_2O], ozone [O_3]) play a crucial role in the radiative balance of the Earth and in the determination of the chemical properties of the atmosphere. The presence of these gases can be traced back to geologic, biological, chemical and anthropogenic processes. The most important and most paradoxical trace gas of the atmosphere is ozone. In the stratosphere this trace gas plays the role of the protector of living organisms, meanwhile at the surface it can produce an adverse effect on human health and plants (Seinfeld and Pandis, 2012). Besides the direct effect of tropospheric ozone as a toxic pollutant, there is an indirect effect, which leads to the warming of the atmosphere (Sitch et al., 2007; Wittig et al., 2009), often referred to as the indirect radiative forcing of ozone. The process in the background of this hypothesis is that ozone entering into the plants through stomata modifies the cell exchange processes and the efficiency of photosynthesis (Fares et al., 2010a). Hence, it decreases the amount of CO_2 taken by plants and thus forces the greenhouse effect.

The role that CO_2 and tropospheric ozone play in the climate change has recently become one of the most important questions of atmospheric sciences. To answer these questions, interaction of processes on different scales has to be investigated, synthesizing knowledge from different fields of science from micrometeorology through climatology to life and plant sciences. Models and measurements are both common and necessary tools in the investigation of ecological processes. As a general requirement, estimations should rely on as many independent sources of information as possible in order to obtain correct results. Besides the use of wide range of information sources, quality check of the available data is of high importance. We cannot get reliable

conclusions using theories based only on model results, like building castles in the air. However, answering on some of important questions is not possible without the applyication of models. The goal of model applications is to estimate parameters far from measuring points and measurement periods (in the future or in the past). The confidence of the model results can be checked with measured data, physically non reliable model results have to be filtered using measurements from different locations. Besides interpretation and validation of model results and improving the models, attention has to be paid to the quality of measured data. In this process the quality control of the measurements and the knowledge about limitation of measuring techniques can help.

Due to the harmful effect of increasing human air pollution measuring and modelling of environmental load on surface ecosystems and publishing the results (e.g. Intergovernmental Panel on Climate Change (IPCC) assessment reports, www.ipcc.ch) of these researches are indispensable tasks of atmospheric scientists. The aim of this dissertation to investigate the structure and performance of ozone deposition models with a focus on model sensitivity and evaluation. After this brief introduction in the following subsections air pollution, the effect of tropospheric ozone, dry deposition processes, measurements and modelling efforts are discussed to have an overview on modelling and measuring methods and to highlight our research aims. In the second chapter of the thesis scientific publications are presented focusing on research questions. The general conclusions and outlook are described in the third and fourth chapters of this work.

I.1. Harmful effects of tropospheric ozone

The importance of deposition of atmospheric pollutants to the landscape was initially recognized with the start of scientific research on environmental effects of sulphur pollution in the 19th century (e.g. the effects of smoke on spruce and fir trees was reported by Stöckhardt in 1871). Environmental effects of atmospheric pollutants (e.g. sulphur and nitrogen oxides [SO_2, ..., NO, NO_2, or often referred to as SO_x, NO_x, respectively], ozone, ammonia [NH_3]) include eutrophication of natural ecosystems, acidification of soils, lakes and rivers and photochemical air pollution. Ozone is recognized as the most phytotoxic of the common air pollutants in the troposphere (Sandermann et al., 1998). However, in the stratosphere the maximum ozone concentration can vary between 4–8 ppm the background ozone concentration in the northern hemisphere is recently in the range of 35–40 ppb [~75–85 $\mu g\,m^{-3}$ at standard pressure and temperature] in the troposphere (Fowler et al., 2008). Henceforward, in this study the tropospheric ozone is in focus.

Due to increased emissions of the ozone precursor substances (NO_x, carbon monoxide [CO], volatile organic compounds [VOCs]) originated from local sources and trans-boundary pollution, national and international limits for surface air ozone concentrations

are regularly exceeded under certain meteorological conditions in North America and Europe and in Japan as well for either shorter episodic or longer periods. Excessive ozone pollution can have a marked effect on human health. It can cause breathing problems, lung diseases, trigger asthma, and reduce lung function. World Health Organization Air quality guidelines (WHO, 2006) recommend limits for the concentration of selected air pollutants, for ozone this value is 100 $\mu g\,m^{-3}$ (daily maximum 8-hour mean). During 2003 and 2006 summer, ozone concentration exceeded 140 $\mu g\,m^{-3}$ (daily maximum 8-hour mean) over large areas of Europe (EEA, 2007). In 2011 which was cooler and wetter year than the two years mentioned above, the EU's information threshold (one hour at 180 $\mu g\,m^{-3}$) was exceeded in 16 EU member states whilst the alert threshold of 240 $\mu g\,m^{-3}$ was exceeded in Bulgaria, France, Greece, Italy, Portugal and Spain (Mills et al., 2013). Samoli et al. (2009) have reported that the daily mortality rises by 0.3% and heart diseases by 0.4%, per 10 $\mu g\,m^{-3}$ increase in ozone exposure. Ground-level ozone causes cca. 22,000 excess deaths per year in Europe (Amann et al., 2005).

Terrestrial ecosystem (especially forests) can play an important role in long-term carbon storage (Schimel, 1995; Pan et al., 2011) and it is of high relevance to investigate all the effects which could influence this role. Climate change and air pollution interact in affecting forests by changes in soil processes, tree growth, species composition and distribution, increased plant susceptibility to stressors, increased fuel built-up and fire danger, water resources, recreation value (Bytnerowicz, 2007). Through its coupled feature ozone pollution has a huge influence also on carbon sequestration, biodiversity and food security. After entering the stomata, ozone reacts with the liquid components of the apoplast to create reactive oxygen species that can oxidize the cell walls to start a cascade of reactions which lead, at the final stage, to cellular death (Fares, 2010a). The effects of elevated ozone concentrations on vegetation can have visible symptoms (yellow or brownish spots on the leaf surface, Figure 1), can cause reduction in photosynthetic activity, damage the reproductive processes and cause early senescence (Felzer et al., 2007). Ozone deposition is usually associated with a decrease in productivity (Volk et al., 2006; Bassin et al., 2007) and in plant's growth and yield. Karnosky et al. (2003, 2005) reported significant ecosystem scale responses to elevated CO_2 and ozone levels in the Aspen FACE Experiment (open-air fumigation system). The changes were reflected in several ecosystem properties, including photosynthesis. They suggest that elevated ozone at relatively low concentrations can significantly reduce the growth enhancement by elevated CO_2.

Critical levels of ozone have been derived for vegetations, above which effects on yield can be expected (e.g. UN-ECE Workshops on Critical Levels of Ozone in 1994 and in 1996). In that time ozone exposures below 40 ppb were believed to be being detoxified by the plant's natural defence mechanisms and thus were not contributing to the damaging effects of ozone (Mills and Harmens, 2011). Recently the accumulated ozone flux via the stomatal pores on the leaf surface is considered to provide a biologically more appropriate method for describing the observed effects (detailed in Section I.4.1.)

Felzer et al. (2004) have found that carbon sequestration in the conterminous United States has been reduced due to the presence of ozone by 18–38 Tg carbon per year since the 1950s. Ozone effects can impact on the vitality of component species of plant communities, potentially altering plant biodiversity as well as that of the creatures that live in close association with plants (Mills et al., 2013). Effects of ozone on primary productivity are especially relevant for crop plants (Mills et al., 2013). The population of the world is predicted to increase to 9 billion by 2050, so the security of food supplies is one of the most important challenges for this century. Ozone damages cause reduced yield quantity and/or quality and reduced resilience of crops to other stress such as drought. Mills and Harmens (2011) quantified ozone impacts on wheat yield in Europe and predicted that losses would remain at 9% in 2020 amounting to €2 billion in EU27 (and Norway and Switzerland). Current ambient ozone levels in South Asia (discussed in the next chapter) are also considered to be reducing crop yield and quality for a range of important crops in the region, commonly within the range of 10% to 20%. In the USA in the 1980s the annual cost of loss of arable crop production due to ozone was estimated to be $2–4 billion (Fowler et al., 2008). Globally, crop yield losses for wheat, rice, maize and soybean in the year 2000 were estimated to be $14–26 billion (Van Dingenen et al., 2009).
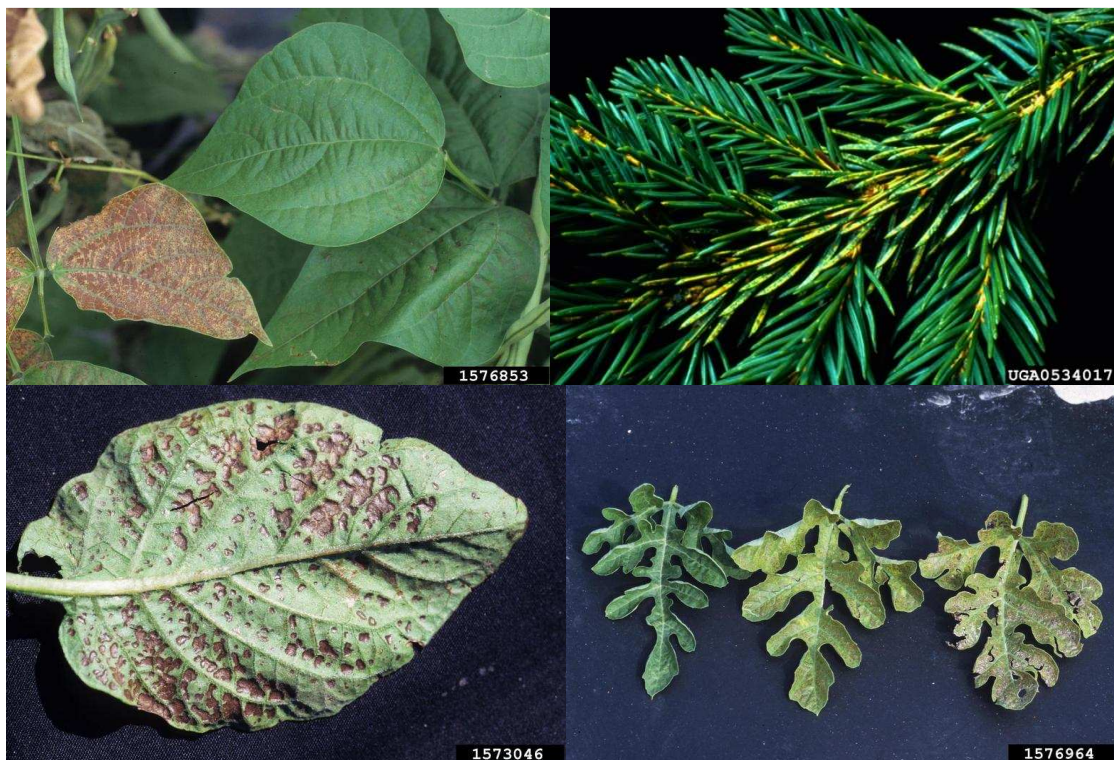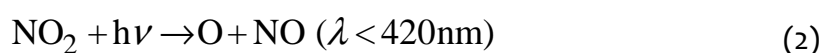

Figure 1. Ozone injury symptoms on leaves: common bean, Norway spruce, potato, watermelon (www.forestryimages.org).
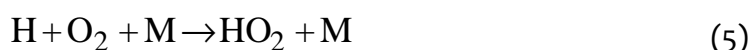
I.2. Tropospheric ozone

I.2.1. Formation and destruction

Tropospheric ozone is a secondary air pollutant, it has no direct surface source. Ozone can form by the recombination of an O_2 molecule and an O atom in the presence of a third body M (M is usually O_2 or N_2), which is required to carry away the energy released in the reaction (1). In the troposphere, NO_2 is the only known compound that can produce O atom during it's photodissociation at available radiation of wavelengths less than 420 nm (2):

$$O + O_2 + M \rightarrow O_3 + M \qquad (1)$$
$$NO_2 + h\nu \rightarrow O + NO \ (\lambda < 420 nm) \qquad (2)$$
$$O_3 + NO \rightarrow O_2 + NO_2 \qquad (3)$$

(1)–(3) only recycle ozone and NO_x, since during (3) NO destroys ozone and reproduces the NO_2. When other precursors, such as CO, CH_4 or certain organic compounds (VOC) are presented in the atmosphere then the reactions result net ozone production (7). Ozone production can be simulated by a simple reaction scheme, through the oxidation of CO, when NO is available and then during (1) and (2) reactions ozone is produced. In this reaction chain OH, HO_2, NO and NO_2 participate as catalysts:

$$CO + OH \rightarrow H + CO_2 \qquad (4)$$
$$H + O_2 + M \rightarrow HO_2 + M \qquad (5)$$
$$HO_2 + NO \rightarrow OH + NO_2 \qquad (6)$$
$$CO + 2O_2 \rightarrow CO_2 + O_3 \qquad (7)$$

Similar reaction chain occurs with the oxidation of methane in NO rich environment. Instead of methane, other organic compounds can also participate in this reaction chain, where carbonyl species or a ketone is formed besides the ozone.

Primary destruction processes of tropospheric ozone are the photochemical reaction when ozone molecules dissociate by solar radiation (8) or can be destroyed by the direct reaction with OH radical (9):

$$O3 + h\nu \ (\lambda < 320 \, nm) \rightarrow O_2 + O(^1D) \qquad (8)$$
$$OH + O_3 \rightarrow HO_2 + 2O_2 \qquad (9)$$
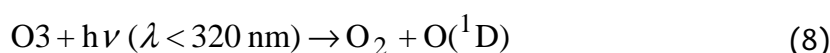
I. Introduction

In NO rich environment, the reaction (3) governs the ozone destruction. In NO poor environment, the oxidation of CO_2 can lead to ozone loss. In that case, after the reactions (4) and (5) instead of reaction (6) the generated HO_2 can react with ozone (10):

$$HO_2 + O_3 \rightarrow OH + 2O_2 \qquad (10)$$

I.2.2. Global budget, trends and climate effects

Besides chemical destruction, ozone can be removed from the atmosphere in the process of dry deposition when ozone is settling from the atmosphere to different surfaces by gravitation (detailed in Section I.3.). Besides the above detailed production ozone can enter the troposphere from the stratosphere. An often proposed way to quantify the magnitudes of these sources and sinks is the use of global chemistry transport models (CTMs) that simulate the chemical and dynamic processes controlling ozone production and destruction. By Stevenson et al. (2006) 26 atmospheric chemistry models have been intercompared and the model ensemble mean for year 2000 tropospheric ozone budget were resulted a net ozone influx of 550 ± 170 Tg yr^{-1} from the stratosphere, a surface removal of 1000 ± 200 Tg yr^{-1} by dry deposition, a net chemical production of 450 ± 300 Tg yr^{-1} and a burden of 345 ± 40 Tg.

The IPCC TAR (Smithson, 2002) presented that tropospheric ozone increases since the pre-industrial times have contributed somewhere between 0.25 and 0.65 W m^{-2} to global radiative forcing (Forster et al., 2007). On the basis of this direct forcing, ozone is ranked as the third most important anthropogenic greenhouse gas after carbon dioxide (1.49–1.83 W m^{-2}) and CH4 (0.43–0.53 W m^{-2}) (Fowler et al., 2008). IPCC AR5 (Hartmann et al., 2013) reported that there is medium confidence from limited measurements in the late 19th through mid-20th century that European surface ozone more than doubled by the end of the 20th century. There is medium confidence from more widespread measurements beginning in the 1970s that surface ozone has increased at most (non-urban) sites in the north hemisphere (1 to 5 ppb per decade), while there is low confidence for ozone increases (2 ppb per decade) in the south hemisphere. In this study it has been published that in recent decades, ozone precursor emissions have decreased in Europe and North America and increased in Asia, impacting ozone production on regional scales. Based on long-term records for the 1990–2010 period surface ozone trends vary regionally (Figure 2). In Europe tropospheric ozone concentration generally increased through much of the 1990s but since 2000 ozone it either levelled off or decreased at rural and mountaintop sites. In North America surface ozone concentration has increased in eastern and Arctic Canada, but is unchanged in central and western Canada. Surface ozone concentration has increased in the west coast of the USA and at half of the rural sites in the western USA during spring, meanwhile in the eastern USA surface ozone has decreased strongly in summer, is largely unchanged in spring and has increased in winter. East Asian surface

ozone concentration is generally increasing but decreasing in the subtropical western North Pacific. In the south hemisphere has increased significant at the four investigated available sites. No site or region showed a significant negative trend (Hartmann et al., 2013).
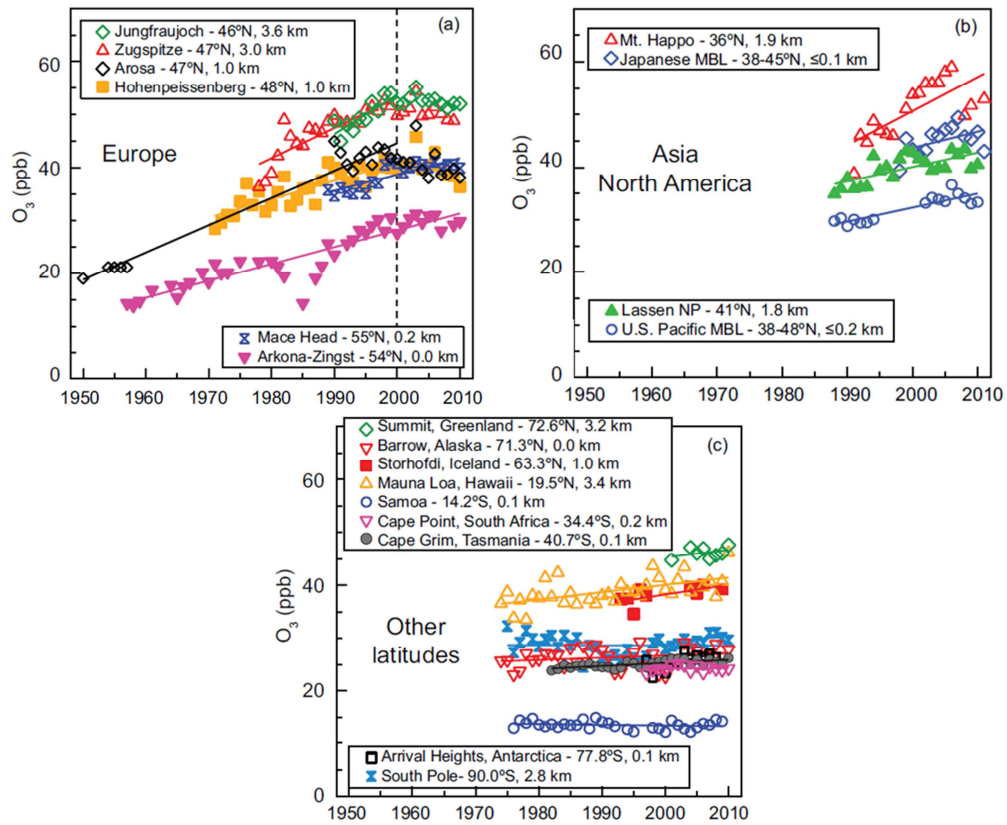

Figure 2. Annual average surface ozone concentrations from regionally representative ozone monitoring sites around the world. (a) Europe. (b) Asia and North America. (c) Remote sites in the Northern and Southern Hemispheres. The station name in the legend is followed by its latitude and elevation. Time series include data from all times of day and trend lines are linear regressions following the method of Parrish et al. (2012). Trend lines are fit through the full time series at each location, except for Jungfraujoch, Zugspitze, Arosa and Hohenpeissenberg where the linear trends end in 2000 (indicated by the dashed vertical line in (a)). Twelve of these 19 sites have significant positive ozone trends (i.e., a trend of zero lies outside the 95% confidence interval); the seven sites with non-significant trends are: Japanese MBL (marine boundary layer), Summit (Greenland), Barrow (Alaska), Storhofdi (Iceland), Samoa (tropical South Pacific Ocean), Cape Point (South Africa) and South Pole (Antarctica) (Hartmann et al., 2013).

To estimate future tropospheric ozone concentration, coupled chemistry–climate models can be used driven by future emissions projections. These models include description of ozone precursor emissions, atmospheric chemistry, transport and removal processes. The processes through which the climate system affects tropospheric ozone

levels are complex, and involve many interactions between the atmosphere, the land surface and ecosystems (Figure 3). Some of these processes are well-understood and are represented in the models. However, those involving the terrestrial biosphere, including biogenic emissions and dry deposition, are less understood, and are only represented simply in most models. For example the interactions of the global carbon cycle and ozone (indicated by dashed lines in Figure 3) have only recently been assessed, although these connections may be significant (Felzer et al., 2004; Sitch et al., 2007). Future changes in climate may not have a major global influence on tropospheric ozone concentrations (Fowler et al., 2008), but it is more important at the regional and local scales. Many of the processes creating or destroying ozone or delivering it to ground level are influenced by synoptic and local weather patterns, which also provide the pathways for the long range transport and for the ventilation of ozone and its precursors from the boundary layer to the free troposphere. Changes in environmental drivers (e.g. land cover, sunlight, temperature, humidity, precipitation, soil moisture) have the potential to change the evolution of near surface ozone.
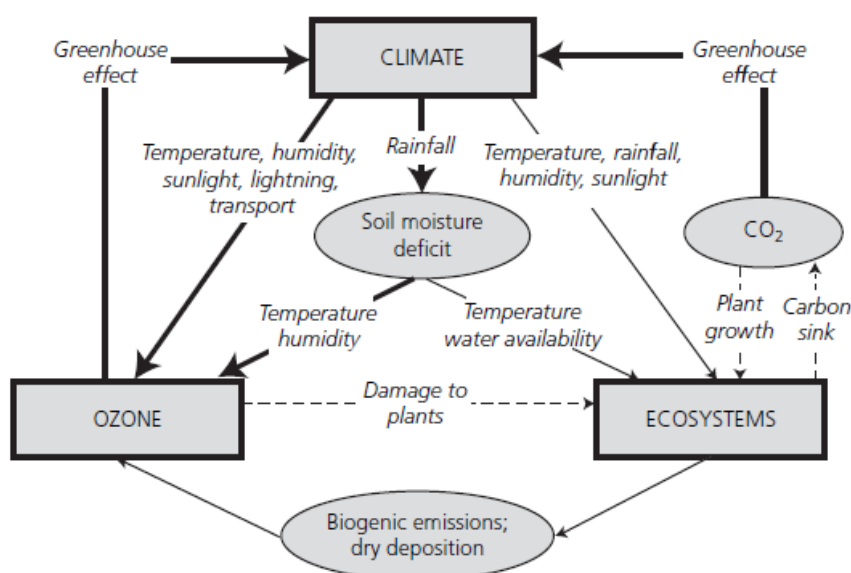

Figure 3. Schematic of the interactions between climate, ecosystems and tropospheric ozone. Thick solid lines denote processes that are generally well understood and represented in coupled chemistry–climate models. Thin solid lines denote processes that are understood but for which uncertainties exist and are only partially represented in models. Dashed lines correspond to links that are emerging as important but not generally included in model projections. This figure is a copy of Fig. 6.1 published in Fowler et al. (2008).

It is predicted based on A2 scenario (very heterogeneous world, continuously increasing global population, economic development is primarily regionally oriented) of Special Report on Emission Scenarios (SRES; Prather et al., 2001) that tropospheric daily ozone concentration in the northern midlatitudes will hit cca. 68 ppb by 2050 and 85 ppb

by 2100 compare to recent average 40 ppb (Anav et al., 2011). Based on this projection approximately 50% of forests, grasslands and croplands might be exposed to high ozone concentration levels by 2100 (Sitch et al., 2007; Wittig et al., 2009). Ashworth et al. (2013) simulated increase in ground-level ozone caused by changes in isoprene emission rates by replacing some present agricultural crops and grassland in Europe with 72 Mha short-rotation coppice in agricultural areas across Europe. Isoprene is the most significant biogenic VOC leading to enhanced ozone formation. The authors estimated an annual loss of ~7.1 Mt of wheat yield (3.5% of the crop yield in 2000) and ~0.8 Mt (1% of the yield in 2000) of maize caused by ozone. This is a ~50% increase in the wheat and maize yields estimated to be lost due to ozone damage in 2000. Besides, their model study suggests that the increase surface ozone concentration would result in 1,365 premature deaths per year, an increase of ~6% in the 22,000 deaths attributed to ozone effects in Europe. Sitch et al. (2007) demonstrated that the indirect radiative effects of ozone via reduced carbon sequestration could increase the total radiative forcing due to ozone over the period 1900–2100 by at least 70%. This work suggests that tropospheric ozone increase play an even more important role in global warming than previously assumed (Fowler et al., 2008).

I.2.3. Uncertainties

The damaging effect on living and non-living environment of tropospheric ozone is a central research topic of atmospheric sciences. This study focuses on the estimation of effect of surface ozone load on vegetation. Models developed for this application involves many uncertainties like describe the stomatal behaviour for elevated ozone concentration, accuracy of input parameters and parameterization of feed-back processes between ozone and carbon sequestration.

All the models mentioned in the previous chapter are based on the concept that plants damaged by ozone take up less carbon, and this process lead to an indirect radiative forcing. Challenging this theory, Hayes et al. (2012) reported that their observed results (i.e. for green leaves of some plant species, e.g. cocksfoot grasses (*D. glomerata*), ozone can inhibit stomatal closure) could lead to inaccuracies in global climate models since models assume that increasing ozone concentration closes stomata (Sitch et al., 2007; Collins et al., 2010), rather than opening the stomata further as described in their study. Globally, it has been estimated that ozone deposition to vegetation (by reaction with plant surfaces and uptake through the stomata) reduces tropospheric ozone concentrations by as much as 20% (Fowler et al., 2008). However, under water limited conditions, plants close stomata to conserve water and stomatal uptake of ozone is substantially reduced. Vieno et al. (2010) reported that the European summer heatwave in August, 2003 led to 20-30 ppb increase in ozone concentration.

Since these models are regional or global models, for spatial extensions detailed databased are required over many land surface categories. Non-linear models, like most of the deposition models, can magnify the uncertainties of some parameters and damp others. Without proper evaluation, models are not suitable for reliable large scale modelling in all situations. Detecting the global surface ozone trend also has uncertainties. It was presented before that only 12 of 19 regionally representative ozone monitoring sites show significant ozone concentration trends (Hartmann et al., 2013). This could lead to uncertainties in model evaluation. To proove the existance of any trend longer data set are needed. The investigation of the above mentioned model uncertainties are necessary. The aim of this study is to contribute to this process.

I.3. Dry deposition process, fluxes of trace gases

Every substance emitted into the atmosphere is eventually removed or destructed, i.e. has an atmospheric lifetime. The atmosphere presents two exits, precipitation or the surface, therefore the removal process of species can be grouped into wet deposition and dry deposition (Seinfeld and Pandis, 2012). Dry deposition refers to the direct sedimentation and/or diffusion of material to various terrestrial surfaces and uptake by the biota. Wet deposition refers to the uptake of material by cloud water and precipitation, and its subsequent transfer to the surface. There is a third type of deposition, namely occult deposition, when trace gases and particles are transferred from the atmosphere via fog particles to the ground.

In the deposition process, until the substance reaches the surface, it is moving through the bottom layer of the troposphere, the so-called planetary boundary layer (PBL). The PBL height varies in time and space, ranging from tens of meters in strongly statically stable situations, to several kilometers in convective conditions. Within the PBL, trace gases are transported horizontally by wind and vertically by turbulence via differently sized eddies, which are generally smaller towards the surface (Coyle et al., 2009). The bottom 10% of the PBL is called the surface layer or constant flux layer (Figure 4). Very close to the surface wakes are produced by rough surface elements leading to the roughness sub-layer. Above this layer is the inertial sub-layer where fluxes are constant with height. The term of flux density can be defined as the flow of a quantity per unit area per unit time. In this study ozone flux is in focus with a unit of $\mathrm{nmol\,m^{-2}s^{-1}}$ or $\mathrm{\mu g\,m^{-2}s^{-1}}$. Since ozone has no direct surface sources ozone flux is a one-way process from upper level of troposphere to the ground.
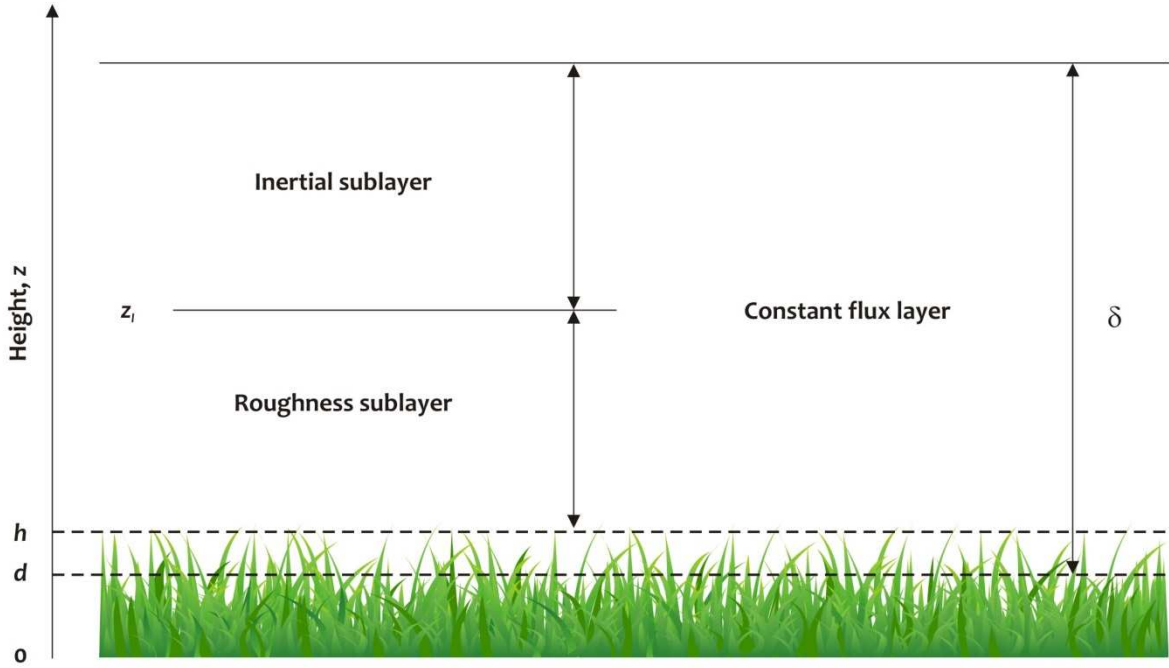
Figure 4. Structure of constant flux layer (not to scale). z_l represents the lower limit of the initial sublayer (e.g. 20-23m for a forest plantation and 3-3.5 m for a canopy of maize), h is the height of canopy and d stands for displacement height (see paper III in Chapter II)(Monteith and Unsworth, 2008).

The flux of given trace gases can be derived from the simplified form of the general budget equation (11) for trace gases (Foken et al., 1995).

$$\frac{\partial \overline{c}}{\partial t} + \nabla \cdot \left(\overline{u}_i \overline{c} \right) = -\nabla \cdot \left(\overline{u_i' c'} \right) + S_c$$

$$\quad \text{I} \qquad \text{II} \qquad\qquad \text{III} \qquad \text{IV}$$

(11)

In (11) the instantaneous values of components of wind vector (u_i) and concentration of trace gas (c) are decomposed into a mean (overbar) and a fluctuating component (comma), II describes convection (or advection), III is the divergence of turbulent flux and S_c presents the sum of chemical sinks and sources. Splitting the terms of (11), assuming horizontal homogeneous and steady-state conditions without source or sinks with zero mean vertical wind velocity, the turbulent flux (F) measured above the surface is the deposition flux:

$$\frac{\partial \left(\overline{w' c'} \right)}{\partial z} = 0$$

(12)

$$\left(\overline{w' c'} \right) = const. = F$$

(13)

Since the surface flux (*F*) of the given gas at a specified reference height is proportional to the mean concentration ($c(z_{ref})$), a proportional constant, the so-called deposition velocity ($v_d(z_{ref})$) was defined first by Chamberlain (1967) as (minus sign is required to make downward fluxes negative):

$$v_d\left(z_{ref}\right) = -\frac{F}{c\left(z_{ref}\right)}. \tag{14}$$

I.4. Methods to determine ozone deposition

I.4.1. Measurements and ozone metrics

To measure dry preposition a wide range of techniques have been used which can be divided into two groups: direct and indirect (Table 1). Direct methods are when the vertical flux is measured in the near of the surface or the deposited substance is collected. During the indirect methods a secondary quantity is measured (i.e. mean concentration or vertical gradients of the mean concentration of depositing material) and flux is derived related to this quantity. The choice of measurements methods depends on the properties of given substance, surface and air conditions (assumptions have to be made), if it is a field campaign or a laboratory measurements and the financial considerations.

Table 1. Measurement of dry deposition

Direct	Indirect
- surrogate surface method - natural surface (throughfall) method - box and cuvettes method - chamber method - eddy correlation (covariance) method - eddy accumulated method	- aerodynamic profile method - gradient method - modified Bowen-ratio energy balance method - variance method - inferential method

The first two papers focus on modelling, while in paper III deposition models based on inferential method were evaluated using measurements carried out by eddy correlation (EC) method. Therefore only these measurement techniques are mentioned in the next paragraphs.

During the eddy correlation method statistical correlations of the fluctuations in wind and concentration fields are measured to directly obtain values of the associated vertical fluxes. In the case of eddy correlation, high frequency measurements of vertical velocity and concentration are used to obtain fluctuating components of formula (13) and to

derive the vertical turbulent flux (*F*). This method is suitable for gaseous species, however very fast-response equipment is required (Seinfeld and Pandis, 2012). An example of an EC measuring system is presented in Figure 5. In the inferential method measured concentration of trace gas and the calculated rate of transfer from the atmosphere to the surface (deposition velocity) are used to express deposition flux.

Figure 5. Niwot Ridge Ameriflux tower: located in Colorado, USA (biocycle.atmos.colostate.edu) and eddy covariance system: ultrasonic anemometer and infrared gas analyser (en.wikipedia.org).

To quantify the levels of ozone load on ecosystem different metrics are used (Table 2). There are two main groups of these indices: concentration-based and flux-based metrics. In the previous decades concentration based metrics were commonly used but recently the flux based metrics takes part. Concentration-based metrics make no difference between climatic conditions and would not indicate the increased risk of damage in warm, humid conditions when stomata are more open than in hot, dry conditions. The flux-based metrics for ozone take into account the meteorological conditions, ozone concentration, plant development and land cover on the flux of ozone. They provide an estimate of amount of ozone entering through the stomata. Fares et al. (2010b) suggest that AOT40 (accumulated ozone over a threshold) and SUM0 (sum of all hourly ozone concentrations over an exposure period) are poor predictors of stomatal ozone uptake, and that a physiologically based metric would be more effective. Since stomata are partially open at night, the 24-h O3 exposure period of time should be used for both exposure–response and effective–dose models (Musselman et al., 2006).

Table 2. Metrics of ozone deposition (units and references)

Concentration based metrics

AOT [μmol mol^{-1} hours]	the sum of all daytime ozone concentrations >40 ppb	Panek, 2002
SUM0 [ppb-h]	the sum of all hourly ozone concentrations in a 14-h daytime period	Panek, 2002
SUM06 [ppb-h]	the sum of daytime ozone concentration hours >60 ppb	Panek, 2002
SUM08 [ppb-h]	the sum of daytime ozone concentration hours >80 ppb	Panek, 2002
W126 [ppb-h]	an index derived from sigmoidally weighting ozone concentrations	Panek, 2002
N100 [hour]	number of hourly average concentrations $\geq$ 0.10 ppm over the exposure period	Musselman et al., 2006

Flux based metrics

F [nmol m^{-2} s^{-1}]	the total flux to surfaces, including stomatal and non-stomatal surfaces such as the cuticles, and non-plant surfaces such as soils	Musselman et al., 2006
Fst [nmol m^{-2} PLA s^{-1}]*	instantaneous flux of ozone through the stomatal pores per unit PLA	LRTAP, 2010
FstY [nmol m^{-2} PLA s^{-1}]*	instantaneous flux of ozone above a flux threshold of Y nmol m^{-2} s^{-1}, through the stomatal pores per unit PLA	LRTAP, 2010
AFstY [nmol m^{-2} PLA]* or POD$_Y$ [mmol m^{-2} PLA]*	accumulated flux above a flux threshold of Y nmol m^{-2} s^{-1}, accumulated over a stated time period during daylight hours (global radiation greater than 50W m^{-2})	LRTAP, 2010
SUMFLUX [μmol m^{-2} h^{-1} 14 h]	measured ozone flux over the daylight period	Panek, 2002

*PLA stands for projected leaf area, which is the total area of the sides of the leaves that are projected towards the sun

I.4.2. Modelling efforts

Besides the measurements numerous models have been developed to describe the deposition processes of trace pollutants. The transport-deposition models can be effective tools to provide concentration and deposition data to facilitate the evaluation of effects of air quality on ecosystems. Various 3-dimensional CTMs (e.g. AURAMS (Smyth et al., 2009), CAMx (Emery et al., 2012), CHIMERE (Menut et al., 2013), EMEP MSC-W (Simpson et al., 2012), GEOS-CHEM (Bey et al., 2001), LOTOS-EUROS (Schaap et al., 2008), OFIS (Moussiopoulos and Douros, 2005), RCG (RemCalGrid) (Stern, 2009), TAMP (Hurley, 2008), WRF-CHEM (Grell et al., 2005)) have been developed to estimate and investigate the environmental load of air pollutants.

These models include embedded dry deposition modules (sub-models) that apply different approaches of parameterization schemes to calculate deposition of given trace gases or aerosols. The depositions models could be classified based on complexity of model in describing vegetation (one-, two- or multi-layered) and in the description and parameterization of exchange/deposition processes between the atmosphere and the surface (first order closure/K-theory, higher order closure, non-local closure).

The practical utility of a more complicated model is often limited by the need for complex parameters, which are often unknown or difficult to obtain. These parameters include vertical variations in leaf area index, canopy drag coefficients, the wind profile attenuation coefficient, and coefficients used to close higher order moment equations (Baldocchi et al., 1987). The choice is usually a compromise between application dependent requirements and data availability.

A main part of deposition models is in general a resistance submodel, which simulates the deposition or exchange of the given species between the atmosphere and surface. Deposition velocity can be calculated as the reciprocal value of the residual of the resistances (analogous to Ohm's low for electricity, Figure 6) via parameterization of the aerodynamic (R_a), the quasi-laminar boundary layer (R_b) and the canopy resistance (R_c):

$$v_d = \frac{1}{R_a + R_b + R_c},$$ (14)

These resistances are parameterized in terms of fundamental physical, chemical and vegetative factors (Wesely and Hicks, 2000). R_a is governed by micrometeorological parameters and depends mainly on the local atmospheric turbulence intensities. R_b is driven by diffusivity of the gaseous species and the air viscosity. The formulas for the calculation of the first two terms are similar in different deposition models, but the complexity of parameterization of the latter term varies by a great degree among the models and depends on the model application. R_c represents the capacity for a surface to act as a sink for a particular pollutant, and depends on the primary pathways for uptake such as diffusion through leaf stomata, uptake by the leaf cuticular membrane, and

deposition to the soil surface. Canopy resistance is parameterized by stomatal (R_{st}), cuticular (R_{cut}) and surface (R_{soil}) resistances (Figure 6). Futher detailed description of resistance models will be presented in Chaper II (paper I and paper III).
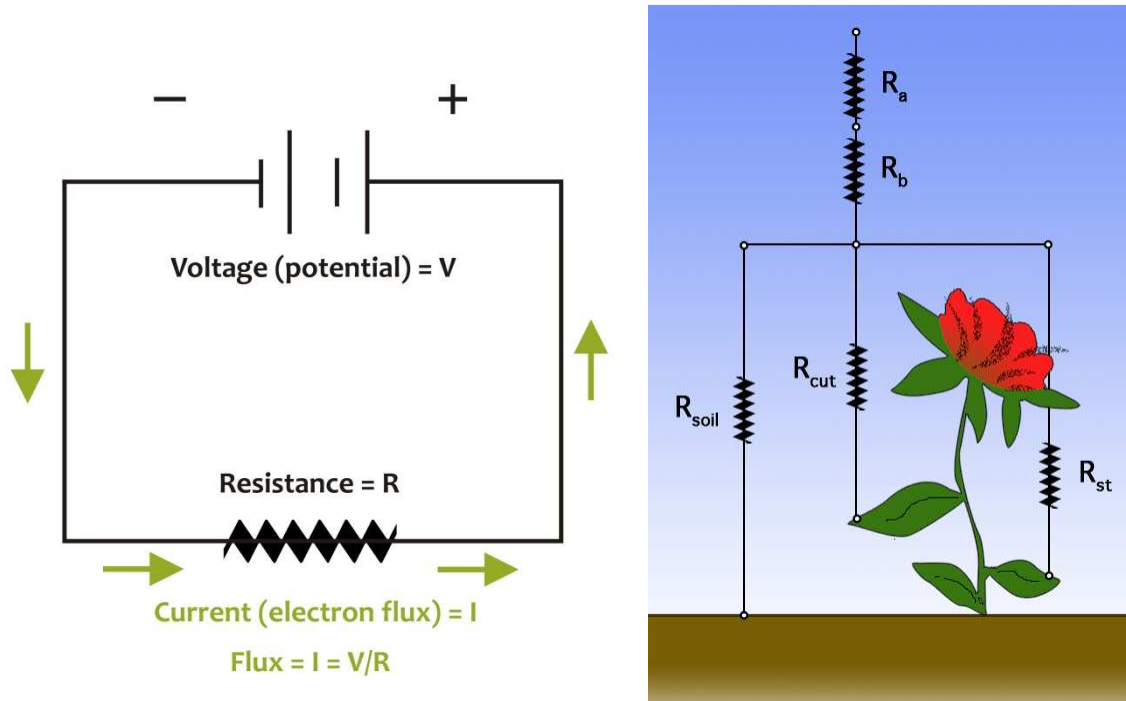

Figure 6. Schema of electrical circuit and resistance network.

I.5. Research questions

Based on the facts detailed in the previous sections, it has a high relevance to study the performance of deposition models in different environmental conditions and to compare the modelling results. Since the important and complex interactions between the surface and the atmosphere cannot be modelled on plot level, and, spatial extension requires modelling results as accurate as possible to avoid nonlinear accumulation of errors in the spatially representative results.

Dry deposition is very sensitive to surface conditions. To draw a picture on the effects of input data detailed statistical analyses of the investigated deposition model can help. A main aim of the first paper is to reveal the variability of some environmental parameters and data on the estimation of ozone deposition velocity, which can also help to understand the controlling mechanisms of deposition processes. The discussed questions in this context are:
- To what degree and how the meteorological variables and vegetation parameters influence the deposition model results?

Measurements using existing techniques are still neither accurate nor complete enough to obtain R_c values under most condition. As it was highlighted in paper I soil water content could be the limiting effect of on canopy (stomatal) resistance over climatic conditions. Therefore further investigations are needed on the parameterization of the canopy resistances. Within the second study of this thesis an investigation of different soil wetness state over Hungary is presented addressing the following research questions:

- How sensitive are the results of the improved model system to soil moisture variations in continental condition?

Since ozone deposition models are widely used for estimation of ozone deposition over large areas it is important to investigate model applicability over different land use categories (LUCs). The detailed in-depth evaluation of the discrepancies and their causes give an objective evaluation of performances of deposition schemes, and designate the direction of further improvements of the ozone deposition models. Besides this fact the investigation of ozone deposition effect on forest has a high relevance. From areas like Denver/Boulder Metropolitan (Colorado, US) upslope winds can bring high concentration ozone to the forest located in Rocky Mountains on sunny afternoon. Therefore these forests are exposited to high ozone deposition. The following questions are addressed in paper III:

- What environmental factors have impact on measured ozone deposition over a subalpine forest site?
- What are the weaknesses of the investigated models and how could they be improved?

To answer the research questions three papers are linked in this thesis.

I.6. Outline of the thesis

The first research question is addressed in paper I. Global sensitivity analyses using two different approaches were carried out to investigate the effect of six input parameters on deposition velocity. With the application of the Monte Carlo method, the nature of the relationship between each model input and output can be described, while the Morris investigation presents their sensitivities. Deposition velocity was calculated using a 'big-leaf' resistance deposition model over four different vegetation types. In this paper the values of both the total and the stomatal part of deposition velocity along with the determination of the probability density functions of the model results were presented.

In order to address the second research question a previously tested soil moisture model was built in a chemical transport model. The effect of soil moisture on modelled on stomatal ozone flux was investigated. Simulations with the developed set-up have been performed for two cases, with and without taking into account the effect of soil moisture stress on ozone deposition over Hungary for a hot, summer day.

Finally, the two last research questions are addressed in paper III. To explore the differences and to compare the models it is a good way to choose models belong to same type of methods. Follow this idea in paper III three widely used one-dimensional 'big-leaf' resistance submodels were evaluated using ozone flux measurements above a LUC (subalpine forest) for which none of the investigated models were calibrated. Based on the previous two papers is it obvious that the deposition models are sensitive to soil wetness moisture conditions. Model developments were carried out in all models focusing on soil moisture stress function.

II. Presentation of the papers

Paper I

Sensitivity analysis of an ozone deposition model

Mészáros R. [1], Zsély I. Gy. [2], Szinyei D. [1], Vincze Cs. [1], Lagzi I. [1]

[1] Department of Meteorology, Eötvös Loránd University, P.O. Box 32, H-1518 Budapest, Hungary
[2] Institute of Chemistry, Eötvös Loránd University, P.O. Box 32, H-1518 Budapest, Hungary

Abstract

In this study, sophisticated sensitivity analyses of a detailed ozone dry deposition model were performed for five soil types (sand, sandy loam, loam, clay loam, clay) and four land use categories (agricultural land, grass, coniferous and deciduous forests). Deposition velocity and ozone flux depend on the weather situation, physiological state of the plants and numerous surface-, vegetation-, and soil-dependent parameters. The input data and the parameters of deposition-related calculations all have higher or lower spatial and temporal variability. We have investigated the effect of the variability of the meteorological data (cloudiness, relative humidity and air temperature), plant- (leaf area index and maximum stomatal conductance) and soil-dependent (soil moisture) parameters on ozone deposition velocity. To evaluate this effect, two global methods, the Morris method and the Monte Carlo analysis with Latin hypercube sampling were applied. Additionally, local sensitivity analyses were performed to estimate the contribution of non-stomatal resistances to deposition velocity. Using the Monte Carlo simulations, the ensemble effect of several nonlinear processes can be recognised and described. Based on the results of the Morris method, the individual effects on deposition velocity are found to be significant in the case of soil moisture and maximum stomatal conductance. Temperature and leaf area index are also important factors; the former is

primarily in the case of agricultural land, while the latter is for grass and coniferous forest. The results of local sensitivity analyses reveal the importance of non-stomatal resistances.

Keywords:
Ozone fluxes, Deposition model, Sensitivity analyses, Monte Carlo method, Morris method

1. Introduction

Near-surface ozone plays an important role in the formation of photochemical air pollution (Krupa and Manning, 1988). During the last few years, in spite of the rigid emission reduction of ozone precursor compounds, ozone concentration still has high values in Europe (Jonson et al., 2006). Ozone and other compounds produced by photochemical cycles affect both vegetation and human health (Fiscus et al., 2005; Eller and Sparks, 2006; Black et al., 2007). In particular, elevated ozone concentrations can be potentially harmful to agricultural and natural vegetation. Occasional extreme concentrations may cause visible injury to the vegetation while the long-term, growing-season averaged exposure can result in decreased productivity and crop yield (Fuhrer et al., 1997). Recently it has also been shown that the indirect radiative forcing of climate change through ozone effects on the land carbon exchange could be an important factor and can induce a positive feedback for global warming (Ashmore, 2005; Stich et al., 2007).

From the biological aspect the response of vegetation to ozone is more closely related to the absorbed dose through the stomata than to external ozone exposure (Musselman et al., 2006; Paoletti and Manning, 2007). To characterize the vegetation damage caused by ozone, in the past decade, flux-based ozone exposure metrics have been favoured as opposed to concentration-based indices (Ashmore et al., 2004, Matyssek et al., 2007).

The ozone flux has been estimated by both more and less sophisticated deposition models for several types of vegetation and even for different climatic and geographic regions (in the last few years e.g. Emberson et al., 2000; Zhang et al., 2002; Nussbaum et al., 2003; Lagzi et al., 2004; 2006; Mészáros et al., 2006; Alonso et al., 2007; Ashmore et al., 2007; Keller et al., 2007; Pleijel et al., 2007; Schaub et al., 2007; Simpson et al., 2007; Tuovinen et al., 2007).

In such models, the ozone flux is controlled by ozone concentration and by deposition velocity via parameterization of the canopy and stomatal conductances. In general, in the models a multiplicative algorithm of stomatal conductance is applied. This method includes functions for the effects of photosynthetically active radiation, air temperature, soil water content and other parameters affecting stomatal conductance. Plant stomatal conductance and the calculation of deposition velocity play a key role in most deposition models applied to risk assessment and to estimation climatic effects of tropospheric ozone.

The main limitation of these deposition models lies in the uncertainty and variability of the model input data, such as the time- and species-dependent parameters. Therefore, these parameters may give rise to significant uncertainties in the simulation results, and it is very important to know the effect of the individual input parameters on model output. Nonlinear models, such as most of the deposition models, can magnify the uncertainties of some parameters and damp others. In many cases, the models may over- or underestimate the stomatal ozone fluxes through the calculation of deposition velocity. Sensitivity analysis is an effective tool for exploring the relation between the output of mathematical models and the input data which comprise the values of parameters as well as the initial conditions (Turányi et al., 2002; Zádor et al., 2005a, b; Zsély et al., 2005; Tomlin, S.A., 2006). To investigate the effects of six important model input parameters on total deposition and stomatal conductance of the ozone, the Monte Carlo and the Morris analyses (Saltelli et al., 2000) were performed for four vegetations and for five soil types. The following model input values were analyzed: air temperature and relative humidity at 2 m height, cloudiness, leaf area index, maximum stomatal conductance and root-zone soil water content. To explore the uncertainty of non-stomatal deposition, the effects of soil and cuticular resistance on deposition velocity were analysed in the frame of a local sensitivity analysis.

A main aim of this study is to reveal the variability of some environmental parameters and data on the estimation of ozone deposition velocity, which can also help to understand the controlling mechanisms of deposition processes. Detailed statistical analyses of a regional scale deposition model could draw a picture on the effects of input data: to which degree and how the meteorological variables and vegetation parameters influence the model results. With the application of the Monte Carlo method, the nature of the relationship between each model input and output can be described, while the Morris investigation presents their sensitivities.

In this paper we present the values of both the total and the stomatal part of deposition velocity along with the determination of the probability density functions of the model results.

2. Materials and methods

2.1. Description of the applied deposition model

For the purpose of estimating the environmental load caused by atmospheric pollutants, a high spatial resolution deposition model was developed and tested (Lagzi et al., 2004, 2006; Mészáros et al., 2006). Up to now, model applications have been carried out to simulate the turbulent fluxes of ozone from the atmosphere into the underlying surface. The total ozone flux (F_t) can be described as a product of the deposition velocity (v_d) and

the concentration (c_r) of ozone at a reference height (within the surface layer of the model):

$$F_t = v_d c_r.$$ (1)

The concentration fields are obtained from a transport model (Lagzi et al., 2004). However, in this study we have focused only on the deposition velocity and its dependence on some input parameters. Deposition velocity of ozone was estimated using a simple resistance method. In this process the deposition velocity is defined as the inverse of the sum of the atmospheric and surface resistances:

$$v_d = (R_a + R_b + R_c)^{-1}.$$ (2)

where R_a, R_b, and R_c are the aerodynamic resistance, the quasi-laminar boundary layer resistance, and the canopy resistance, respectively.

The aerodynamic resistance and the boundary layer resistance retard the turbulent gas-transport and molecular diffusion above the canopy and in a thin layer over surfaces, respectively. The aerodynamic resistance can be described by the Monin–Obukhov similarity theory taking into account the atmospheric stability (e.g. Lagzi et al., 2006), and it was parameterized iteratively from Monin–Obukhov length, friction velocity, sensible and latent heat fluxes. During the estimation of the energy budget components, a constant value for albedo was considered for each biome type (Table 1).

The boundary layer resistance is calculated by an empirical relationship after Hicks et al. (1987).

The canopy resistance depends on both meteorological data and the physiological soil and plant characteristics, and it is parameterized by the following equation:

$$R_c = \frac{1}{R_{st}^{-1} + R_s^{-1} + R_{cut}^{-1}},$$ (3)

where R_{st}, R_s, and R_{cut} are the stomatal, the surface and the cuticular resistances, respectively. Surface dependent values of R_s and R_{cut} are presented in Table 1. The stomatal resistance can be obtained from the widely used, empirical formula of Jarvis (1976) referring to a vegetation canopy:

$$R_{st} = \frac{1}{G_{st}(PAR) f_t(t) f_e(e) f_\theta(\theta) f_{D,i}},$$ (4)

24

where $G_{st}(PAR)$ is the unstressed canopy stomatal conductance, a function of PAR (photosynthetically active radiation). In this parameterization, the canopy is divided into sunlit and shaded leaves, and G_{st} is calculated with the following form:

$$G_{st}(PAR) = \frac{LAI_s}{r_{st}(PAR_s)} + \frac{LAI_{sh}}{r_{st}(PAR_{sh})}, \tag{5}$$

$$r_{st}(PAR_s) = r_{st,min}(1 + b_{st} / PAR_s), \tag{6}$$

$$r_{st}(PAR_{sh}) = r_{st,min}(1 + b_{st} / PAR_{sh}), \tag{7}$$

where LAI_s and LAI_{sh} are the total sunlit and shaded leaf area indices, respectively, PAR_s and PAR_{sh} are PAR received by sunlit and shaded leaves, respectively. The term $r_{st,min}$ is defined as a reciprocal value of the so-called maximum stomatal conductance (g_{max}) and b_{st} is a plant species dependent constant. LAI_s, LAI_{sh}, PAR_s and PAR_{sh} terms are parameterized after Zhang et al. (2001).

The stress factors in the denominator in equation (4) range between 0 and 1 and modify the stomatal resistance: $f_t(t)$, $f_e(e)$ and $f_\theta(\theta)$ describe the effect of temperature, vapour pressure deficit and soil water stress on stomata, respectively (Fig. 1), while $f_{D,i}$ modifies the stomatal resistance for the pollutant gas of interest (for ozone, $f_{D,i} = 0.625$).

The temperature stress function is described by the following relation:

$$f_t = \frac{t - t_{min}}{t_{opt} - t_{min}} \left(\frac{t_{max} - t}{t_{max} - t_{opt}} \right)^{b_t}, \tag{8}$$

where

$$b_t = \frac{t_{max} - t_{opt}}{t_{max} - t_{min}}. \tag{9}$$

Here t_{min}, t_{max} and t_{opt} are the vegetation dependent minimum, maximum and the optimal temperature (Table 1).

The stress of the vapour pressure deficit can be parameterised by the following form:

$$f_e = 1 - b_e(e_s - e), \tag{10}$$

where b_e is a vegetation dependent constant, e and e_s are the water vapour pressure and the saturated water vapour pressure, respectively.

The soil water stress function $f_\theta(\theta)$ is calculated with root-zone soil water content (θ):

$$f_\theta = \begin{cases} 1 & \text{if } \theta > \theta_f \\ \max\left\{\dfrac{\theta - \theta_w}{\theta_f - \theta_w}, 0.05\right\} & \text{if } \theta_w < \theta \leq \theta_f \\ 0.05 & \text{if } \theta \leq \theta_w \end{cases}, \qquad (11)$$

where θ_w and θ_f are the soil moisture contents at wilting point and at field capacity, respectively. These terms depend on the soil texture. The following soil texture categories were used in the model: sand, sandy loam, loam, clay loam and clay. Table 2 contains θ_w and θ_f values for the soil textures used in this study. Root-zone soil water content, θ was modelled by a simple water-budget model (Mészáros et al., 2008).

Four different vegetation types (agricultural land, grass, coniferous forest and deciduous forest) were distinguished in this study. The vegetation-dependent parameters are presented in Table 1.

The stomatal conductance or in other words, the stomatal deposition velocity means the reciprocal value of the stomatal resistance (R_{st}), which characterizes the flux through the stomata, similarly to total deposition velocity (v_d) in Eq. (2), which describes the total flux in the near surface layer.

2.2. Data sources

The effects of the six model inputs were investigated by the analyses; two plant parameters (leaf area index, maximum stomatal conductance), three atmospheric variables (cloudiness, relative humidity, temperature) and the root-zone soil moisture content, which expresses the effect of soil type on dry deposition velocities.

All the plant parameter values (average, minimum, maximum and standard deviation) were taken from a significant work of Breuer et al. (2003), which contains plant-specific parameter values for four main land cover types; crops, pasture (herbs, forbs, grasses), coniferous and deciduous trees both in global and European temperate ecosystems. The plant parameters (maximum stomatal conductance and leaf area index) concerning the European vegetation summarised in this overview were used as data for the sensitivity analysis (Table 3a).

The meteorological data were taken from the ALADIN meso-scale limited area numerical weather prediction model used by the Hungarian Meteorological Service (Horányi, et al., 1996). In this case, 12 UTC analysis fields for July, 1998 were used (Table 3b). For this period, the statistical values (average, minimum, maximum and standard deviation) of the variables (temperature, relative humidity and cloudiness) were calculated from grid data over a region that covers Hungary (φ: 45.7°N – 48.6°N, λ: 16.1°E – 23.0°E, with resolution: 0.1° × 0.15°).

The input value of daily root-zone soil moisture was calculated by a simple bucket model (Mészáros et al, 2008) on a rectangular grid with a 0.1° × 0.15° resolution over Hungary for July, 1998. The soil texture data were obtained using a Hungarian soil-map (Várallyay et al., 1980). The grid cell soil texture was represented by the dominant soil texture. The meteorological data (mean daily temperature and relative humidity, as well as precipitation amount) utilised in root-zone soil moisture calculation were generated by the ALADIN model. The upper limit of soil moisture was the saturated soil moisture (θ_s) applied for each soil type (Table 2). Based on the estimation of the bucket model, the statistical parameters of soil moisture were determined for five soil categories using the spatial average of the results for each soil type over the whole period (Table 3c). The investigated parameters, meteorological and soil statistical data are shown in Table 3a-3c.

Though the above presented statistical datasets are for Hungary and its surrounding area, our results are characteristic for the behaviour of the deposition models used for the temperate region. Moreover, meteorological data for a typical summer month were used in this study.

2.3. Global sensitivity analysis

In this investigation two different methods were applied. Both of them are global techniques (i.e. they explore the whole parameter space, the parameters are not fixed at their mean values). The first method is the Monte Carlo Analysis with Latin Hypercube Sampling (LHS-MC) (Saltelli et al., 2000; Moore and Londergan, 2001; Zádor et al., 2005a, b; Zsély et al., 2005; 2008). For this method, the probability density functions of the input data (see Section 2.2.) were assumed to have a normal distribution truncated at the minimum and maximum values.

According to these functions a large number (10,000) of parameter sets were generated and the model was run with each of these parameter sets. Model calculations were carried out for an arbitrarily chosen geographical point ($\varphi = 46.97°$, $\lambda = 19.55°$) for July, 1998 at 12 UTC for each day. All these 31 daytime deposition velocities were averaged and used as the representative deposition velocity for the given dataset. Simulations with the same parameter set were performed for the 20 combinations of the 5 soil and 4 vegetation types. Additionally, both total and stomatal deposition velocities were calculated. This means 40 (20 for total and 20 for stomatal velocities) output datasets for the six examined model parameters.

This method provides a good estimation of the attainable minimum and maximum values of the calculated results (Zádor et al., 2005b; Zsély et al., 2005; 2008), while the parameters change in their possible intervals. The Latin hypercube sampling ensures that the parameter space is represented with a good approximation of full coverage. The LHS-MC analysis provides accurate and unbiased (McKay et al., 1979) information about the sensitivity of models, while it does not reveal the individual contributions.

The second method was the Morris one-at-a-time method (Morris, 1991; Saltelli et al., 2000; 2004; Zádor et al., 2005b; Campolongo et al., 2007). The estimation of probability density functions of the input values is not required, only their possible intervals are used (see Section 2.2.). In this method $N + 1$ parameter sets are generated (where N is the number of parameters) using the algorithm of Morris, so that a given parameter takes precisely two values throughout the sets: in every run, just one parameter is changed randomly compared to the previous run, and every parameter is changed precisely once during the $N + 1$ runs. The values of the parameters are selected from the whole range of the parameter values by setting out a small number of equidistant points. The procedure was repeated 10 times, so new $N + 1$ parameter sets were designed in the same way. The elementary effect of changing a parameter can be calculated as the difference between the calculated results using different values of the parameter, while the other parameters remain unchanged (but not at their mean values). The means and the standard deviations of these effects are plotted against each other. Parameters with a high mean effect are influential, whereas a low mean effect shows that variability in that parameter does not affect the given output variable significantly. Low standard deviation represents the parameter has an approximately linear effect; whereas a high value means that the effect of that parameter is nonlinear or depends to a large extent on the actual values of the other parameters (interaction).

2.4. Sensitivity for non-stomatal resistances

The deposition process depends on the local weather conditions, surface and soil type as well as plant physiological state. Here the effects of the variation of non-stomatal deposition pathways (cuticular and surface resistances) were also analysed using the local sensitivity technique. For this purpose, the deposition model runs were performed with appropriate fixed (mean) values of plant, meteorological and soil data (Table 3a–3c). The effects of the changes of non-stomatal resistances on the deposition velocity of ozone were calculated separately. The cuticular and surface resistances – which are dominantly constant in deposition models – were considered. The cuticular resistance was modified individually from 1000 up to 10000 s m^{-1}. The surface resistance (which represents the soil pathways) was varied between 100 and 1500 s m^{-1}. These are usual ranges for both resistances obtained from the literature (e.g. Massman, 2004).

3. Results and discussion

3.1. Monte Carlo analysis

The main advantage of these statistical simulations is the comprehensive approach: with a large number of parameter sets, the ensemble effect of several nonlinear processes can be recognised and described. The only weakness is that this method treats the parameters as independent variables, even though some of them related to others. It is well known that meteorological variables are not always independent of each other. For example, in general there is a correlation between temperature and relative humidity. However, a wide range of temperature values can occur in the case of a given relative humidity and vice versa. During the analysis, the whole range of realistic values of meteorological elements was covered, with respect to the specified area and period. Nevertheless, the application of the Monte Carlo analysis is a useful tool to investigate the behaviour of the applied model.

The application of sensitivity analysis often reveals errors in the model or its unexpected behaviour. Usually in the deposition models LAI is below 10. However, the achievable maximum value of this index is larger in case of some vegetation (see Table 3a). The Monte Carlo calculations showed that the model does not give an adequate response when LAI is larger than a threshold value. This value depends on some model parameters and the day of the year. The reason for this behaviour is due to the insufficient parameterization of photosynthetically active radiation (Zhang et al., 2001). As it can be seen in Fig. 2a, PAR_{sh}, that is PAR received by shaded leaves (see Eq. (9) in Zhang et al., 2001), decreases as LAI increases. In the function of incoming solar radiation, PAR_{sh} could become lower than zero. The higher the solar radiation is, the lower the value of LAI when PAR_{sh} reaches zero. In our investigations, for July, 1998, the threshold LAI was found to be around 14.5. Therefore, above this value of LAI the deposition velocity was not estimated. The characteristic shape of total deposition velocity as a function of LAI can be seen in Fig. 2b.

Fig. 3 presents the distribution of the total and the stomatal deposition velocities as the function of the given parameter. All diagrams in the figure refer to loam soil and agricultural land. This combination of soil and vegetation types was chosen arbitrarily and similar distribution patterns were obtained in the case of the other 19 pairs of soil/vegetation. Based on the distributions, soil moisture and maximum stomatal conductance have a near-linear relationship with deposition velocity in both total and stomatal cases. The relative humidity has a small linear effect. The actual value of the total deposition velocity is primary affected by both meteorological data (through R_a, R_b and R_{st}) and plant physiological parameters. However, the distribution of the deposition velocity is mainly governed by the variability of temperature via temperature stress function (Eq. 8), which has a local maximum as can be shown in Fig 1a. In this case the deposition velocity has an optimal shape distribution, where for optimal temperature

29

(when the stomatal conductance is not limited) the highest deposition velocities can be found (Fig. 3).

In the case of *LAI*, the distribution of deposition velocity shows a similar pattern. The higher the *LAI* is, the higher the v_d is until a maximum value (this is around *LAI* = 6 in Fig. 2). A further increase of *LAI* causes a decrease of deposition velocity because of stomatal conductance, G_{st} (5) also decreases with higher *LAI* through the parameterization of photosynthetically active radiation, *PAR* received by sunlit and shaded leaves (*PAR_s* and *PAR_sh*). As it can be seen in the graphs, cloudiness, which affects the incoming solar radiation and the net radiation, has no significant coherence with the deposition velocities.

The distributions of total and stomatal deposition velocity in the case of the same parameters show some similarities, but the ranges of attainable values are different. Minimum values of stomatal deposition velocities can approach zero when some effects block the uptake through the stomata. Stomatal deposition velocity (stomatal conductance) has greater variability than total deposition velocity. Under some conditions, when one or more environmental stresses hit the vegetation, the stomatal uptake is nearly zero, and when almost no environmental stress appears the stomatal deposition velocity approaches its vegetation dependent maximum.

Fig. 4 shows the summarized results of the Monte Carlo analysis together with the average and statistical parameters of both the total and the stomatal deposition velocities. The results characterize the whole range of parameter values. For a given spatial and temporal situation, the calculated values related to given vegetation and soil, as well as the differences among these values could be very different. Even so, based on Fig. 4, some similar properties of the deposition processes can be recognised. First of all, the averages of both total and stomatal deposition velocities are quite similar over each soil type, and they depend more on vegetation. Very different ratios between total and stomatal deposition velocity were found for each vegetation type; the greatest for coniferous forest, while the lowest was in the case of agricultural land.

Low stomatal deposition velocity of coniferous forest is due to its physiological properties (e.g. high temperature stress for summer, low maximum stomatal conductance). The highest stomatal values can be observed for agricultural land due to the highest value for maximum stomatal conductance and the given temperature range is the most favourable (no temperature stress) for this vegetation in this period. In the case of grass the high temperature stress caused by high optimal temperature can compensate the effects of the high maximum stomatal conductance and high *LAI* values. At the same time, lower G_{st} and *LAI* are balanced by lower temperature stress for deciduous forest (see Table 3a). Therefore, the stomatal deposition velocities for the latter forms of vegetation are quite similar.

The distribution of deposition values are plotted by frequency hystogram (Fig. 5). All curves illustrate a similar pattern: after a quick growth a slow falloff can be seen, particularly in the stomatal cases.

3.2. Morris method

While the Monte Carlo method presents accurate and unbiased information about the sensitivity of model results, it does not reveal the individual contributions. The Morris method can trace back the semi-quantitative individual effects of the parameters on deposition velocity and the inefficient parameters can be separated from the effective. However, in this case – in contrast to the Monte Carlo method – the probability density functions of the parameters are not used, so the calculated individual contributions are not unbiased.

Since there are no significant differences among the results of the Morris method for any of the soil types, we have arbitrarily chosen one of them (loam) for the presentation. Fig. 6 contains six graphs, the standard deviation of the elementary effects are plotted against the mean of the elementary effects. The points situated in the bottom left corner of each graph (low means together with low standard deviations) represent vegetation in which cases the given parameter is less important and the effect is linear between input and output. A higher value of mean denotes a greater effect of the input value on the results. High standard deviation refers to a nonlinear or interaction effect.

Similar results for each soil types were evaluated. The mean effects over the soil types were averaged and the parameters were classified using these values (Table 4). The numerical limits used for classification are in the caption. Leaf area index has a weak effect irrespective of the vegetation. Cloudiness and relative humidity have medium effects only in case of coniferous forest. Temperature has a significant effect only in agricultural land for both total and stomatal deposition velocities. Maximum stomatal conductance has medium effect in most cases. However, soil moisture is the most significant parameter for both the total and stomatal deposition velocities for each vegetation type. These results of the Morris method can be summarized in that cloudiness and relative humidity are less important parameters. Leaf area index and temperature are important parameters in some cases, and maximum stomatal conductance and soil moisture are influential parameters in all cases.

3.3. Local sensitivity analysis

In the former analyses the sensitivity of total and stomatal deposition velocity was investigated with global methods. However, the variability of the non-stomatal deposition pathways in contrast to stomatal uptake could also significantly affect ozone deposition. Therefore, to explore the effect of cuticular (leaf surface) and surface (soil) resistances on total deposition velocities a local sensitivity analysis was carried out. Fig. 7 presents the effect of the variability of non-stomatal resistances on deposition velocity. Results show that an increase in both resistances involves a decrease of total deposition velocity. It can also be recognised that the effect of surface resistance is more

pronounced, because the range of realistic values of this resistance is lower than in the case of cuticular resistance. The variation of cuticular resistance from 1000 to 10000 s m^{-1} causes only less than 10% variability in the total deposition velocity. However, variation of surface resistance from 100 to 1500 s m^{-1} produces a two- or three-times variation in deposition velocity. In several models, the surface resistance is parameterized with a constant value. However, it has large degree of uncertainty because of its dependence on soil moisture, soil nitric oxide emission, surface roughness as well as the structure of the vegetation (Massman, 2004). Therefore, the importance of surface resistance in modelling deposition velocity plays a crucial role and further investigation is required.

4. Summary

The behaviour of a deposition model in a temperate climate in the Central European region and the effects of input parameters on the calculated total and stomatal depositions are investigated in this paper. Two global statistical methods, the Monte Carlo and the Morris analyses were used. With the Monte Carlo method it was possible to characterize the probability distribution of the total and stomatal depositions. The Morris method provided individual contributions of the investigated input variables to the daytime total and stomatal deposition velocity (or in other words the stomatal conductance) of ozone. Additionally, a local sensitivity analysis was carried out to reveal the contribution of non-stomatal pathways. The results correspond to Central Europe for July, 1998, which represents a hot, summer period. Based on our sensitivity analyses, important and unimportant input data were defined. This information is very useful when creating an input database for deposition as well as dispersion models. For the estimation of the effective load caused by near surface ozone or to determine its projected effect for the future, these analyses tell which input values of the models need to be determined with high accuracy or need further refinement and in which cases the variability of the parameters is negligible. These results can be helpful for both actual environmental and climate-change studies. Since long-term prediction of atmospheric variables and feedbacks are very difficult to determine precisely, the sensitivity analyses can be effective tools to decrease the uncertainty of estimations.

The main results of this investigation are summarized in the following:

1. In former qualitative investigations (e.g. Mészáros et al., 2006) only local sensitivity analyses were carried out, and linear perturbations were applied on chosen model values. Results of these earlier investigations showed that the temperature is the most effective input parameter of the model. This linear approach cannot explore, on the one part, the whole parameter space, and, on the other part, the possible interactions between the parameters and does not provide quantitative information about the probability distribution functions of the model results. Instead of these former analyses, in this investigation two different methods were applied. The combined

application of the Monte Carlo and the Morris methods is an appropriate tool to describe the sensitivity of a deposition model, and so general and specific properties of the deposition process can be recognized.

2. The results emphasize the importance of the deposition velocity estimation. Although average values of the deposition velocities (total and stomatal, respectively) over different vegetations are quite similar, very different ranges around the averages were found for each surface type. The large variability of the deposition velocities is due to the change of meteorological conditions, vegetation and surface dependent parameters.

3. The stomatal deposition velocity (stomatal conductance) has a larger variability than the total deposition velocity. Under some conditions, when environmental stresses hit the vegetation, stomatal uptake is nearly zero, while under optimum circumstances the stomatal deposition approaches its vegetation dependent maximum.

4. The type of the soil slightly affects the deposition velocity; however, root-zone soil moisture is one of the most crucial factors of deposition in the continental climate region.

5. Based on the results of the Morris method, the individual effects on deposition velocity are precisely determined and found to be significant in the case of soil moisture and maximum stomatal conductance.

6. The local sensitivity analysis pointed out that variation of surface resistance can involve differences in variability of total deposition velocity of up to two or three times. Therefore, more sophisticated parameterization of surface resistance is required in deposition models.

References

Ács, F., 2003. On the relationship between the spatial variability of soil properties and transpiration. Időjárás 107, 257–272.

Alonso R., Bermejo, V., Sanz, J., Valls, B., Elvira, S., Gimeno, B.S., 2007. Stomatal conductance of semi-natural Mediterranean grasslands: Implications for the development of ozone critical levels. Environmental Pollution 146, 692–698.

Ashmore, M.R., 2005. Assessing the future global impacts of ozone on vegetation. Plant, Cell and Environment 28, 949–964.

Ashmore, M.R., Emberson, L., Karlsson, P.-E., Pleijel, H., 2004. New direction: a new generation of ozone critical levels for the protection of vegetation in Europe. Atmospheric Environment 38, 2213–2214.

Ashmore, M.R., Büker, P., Emberson, L.D., Terry, A.C., Toet, S., 2007. Modelling stomatal ozone flux and deposition to grassland communities across Europe. Environmental Pollution 146, 659–670.

Baldocchi, D.D., Hicks, B.B., Camara, P., 1987. A canopy stomatal resistance model for gaseous deposition to vegetated canopies. Atmospheric Environment 21, 91–101.

Black, V.J., Stewart, C.A., Roberts, J.A., Black, C.R., 2007. Ozone affects gas exchange, growth and reproductive development in Brassica campestris (Wisconsin Fast Plants). New Phytologist 176, 150–163.

Breuer, L., Eckhardt K., Frede H., 2003. Plant parameter values for models in temperate climates. Ecological Modelling 169, 237–293.

Brook, J.R., Zhang, L., Di-Giovanni, F., Padro, J., 1999. Description and evaluation of a model of deposition velocities for routine estimates of air pollutant dry deposition over North America. Part I: model development. Atmospheric Environment 33, 5037–5051.

Campolongo, F., Cariboni, J., Saltelli, A., 2007. An effective screening design for sensitivity analysis of large models. Environmental Modelling & Software 22, 1509-1518.

Eller, A.S.D., Sparks, J.P., 2006. Predicting leaf-level fluxes of O_3 and NO_2: the relative roles of diffusion and biochemical processes. Plant, Cell & Environment 29, 1742–1750.

Emberson, L.D., Ashmore, M.R., Cambridge, H., Simpson, D., Tuovinen, J.-P., 2000. Modelling ozone flux across Europe. Environmental Pollution 109, 403–412.

Fiscus, E.L., Booker, F.L., Burkey, K.O., 2005. Crop responses to ozone: uptake, modes of action, carbon assimilation and partitioning. Plant, Cell & Environment 28, 997–1011.

Hicks, B.B., Baldocchi, D.D., Meyers, T.P., Hosker, R.P. Matt, D.R., 1987. A preliminary multiple resistance routine for deriving dry deposition velocities from measured quantities. Water, Air and Soil Pollution 36, 311–330.

Horányi, A., Ihász, I., Radnóti, G., 1996. ARPEGE/ALADIN: A numerical Weather prediction model for Central-Europe with the participation of the Hungarian Meteorological Service. Időjárás (Journal of the Hungarian Meteorological Service) 100, 277–301.

Jarvis, P.G., 1976. The interpretation of the variations in leaf water potential and stomatal conductance found in canopies in the field. Philosophical Transactions of the Royal Society of London, Series B, 273, 593–610.

Jonson, J.E., Simpson, D., Fagerli, H., Solberg, S., 2006. Can we explain the trends in European ozone levels? Atmospheric Chemistry and Physics, 6. 51–66.

Keller, F., Bassin, S., Ammann, C., Fuhrer, J., 2007. High-resolution modelling of AOT40 and stomatal ozone uptake in wheat and grassland: A comparison between 2000 and the hot summer of 2003 in Switzerland. Environmental Pollution 146, 671–677.

Krupa, S.V., Manning, W.J., 1988. Atmospheric ozone: formation and effects on vegetation. Environmental Pollution 50, 101–137.

Lagzi, I., Mészáros, R., Horváth, L., Tomlin, A., Weidinger, T., Turányi, T., Ács, F., Haszpra, L., 2004. Modelling ozone fluxes over Hungary. Atmospheric Environment 38, 6211–6222.

Lagzi, I., Mészáros, R., Ács, F., Tomlin, A.S., Haszpra, L., Turányi, T., 2006. Description and evaluation of a coupled Eulerian transport-exchange model. Part I: Model development. Időjárás (Journal of the Hungarian Meteorological Service) 110, 349–363.

Matyssek, R., Bytnerowicz, A., Karlsson, P.-E., Paoletti, E., Sanz, M., Schaub, M., Wieser, G., 2007. Promoting the O_3 flux concept for European forest trees. Environmental Pollution 146, 587–607.

Massman, W.J., 2004. Toward an ozone standard to protect vegetation based on effective dose:a review of deposition resistances and a possible metric. Atmospheric Environment 38, 2323–2337.

McKay, M.D., Conover, W.J., Beckman, R. J., 1979. A Comparison of Three Methods for Selecting Values of Input Variables in the Analysis of Output from a Computer Code. Technometrics 21, 239–245.

Mészáros, R., Lagzi, I., Juhász, Á., Szinyei, D., Vincze, Cs., Horányi, A., Kullmann, L., Tomlin, A.S., 2006. Description and evaluation of a coupled Eulerian transport-exchange model. Part II: Sensitivity analysis and application. Időjárás (Journal of the Hungarian Meteorological Service) 110, 365–377.

Meyers, T.P., Finkelstein, P., Clarke, J., Ellestad, T.G., Sims, P.F., 1998. A multilayer model for inferring dry deposition using standard meteorological measurements. Journal of Geophysical Research 103, 22645–22661.

Moore, G.E., Londergan, R.J., 2001. Sampled Monte Carlo uncertainty analysis for photochemical grid models. Atmospheric Environment 35, 4863–4876.

Morris, M.D., 1991. Factorial sampling plans for preliminary computational experiments. Technometrics 33, 161–174.

Musselman, R.C., Lefohn, A.S., Massman, W.J., Heath, R.L., 2006. A critical review and analysis of the use of exposure- and flux-based ozone indices for predicting vegetation effects. Atmospheric Environment 40, 1869–1888.

Nussbaum, S., Remund, J., Rihm, B., Mieglitz, K., Gurtz J., Fuhrer J., 2003. High-resolution spatial analysis of stomatal ozone uptake in arable crops and pastures. Environment International, 29, 385–392.

Paoletti, E., Manning, W.J., 2007. Toward a biologically significant and usable standard for ozone that will also protect plants. Environmental Pollution 150, 85–95.

Pleijel, H., Danielsson, H., Emberson, L., Ashmore, M.R., Mills, G., 2007. Ozone risk assessment for agricultural crops in Europe: Further development of stomatal flux and

flux–response relationships for European wheat and potato. Atmospheric Environment 41, 3022–3040.

Saltelli, A., Scott, E.M., Chen, K. (Eds.), 2000. Sensitivity analysis. Wiley, Chichester.

Saltelli, A., Tarantola, S., Campolongo, F., Ratto, M., 2004. Sensitivity analysis in practice. Wiley, Chichester.

Schaub, M., Emberson L., Büker, P., Kräuchi, N., 2007. Preliminary results of modeled ozone uptake for Fagus sylvatica L. trees at selected EU/UN-ECE intensive monitoring plots. Environmental Pollution 145, 636–643.

Simpson D., Ashmore M.R., Emberson L., Tuovinen J.-P., 2007. A comparison of two different approaches for mapping potential ozone damage to vegetation. A model study. Environmental Pollution 146, 715–725.

Stich, S., Cox., P.M., Collins, W.J., Huntingford, C., 2007. Indirect radiative forcing of climate change through ozone effects on the land-carbon sink. Nature 448, 791–794.

Tomlin, S.A., 2006. The use of global uncertainty methods for the evaluation of combustion mechanisms. Reliability Engineering and System Safety 91, 1219–1231.

Tuovinen, J.-P. Simpson, D., Emberson, L. Ashmore, M., Gerosa, G., 2007. Robustness of modelled ozone exposures and doses. Environmental Pollution 146, 578–586.

Turányi, T., Zalotai, L., Dóbé, S., Bérces, T., 2002. Effect of the uncertainity of kinetic and thermodinamic data on methane flame simulation results. Physical Chemistry Chemical Physics 4, 2568–2578.

Várallyay, Gy., Szűcs, L., Murányi, A., Rajkai, K., Zilahy, P., 1980. Map of soil factors determining the agro-ecological potential of Hungary (1:100 000) II. Agrokémia és Talajtan, 29, 35–76 (In Hungarian).

Zádor, J., Wagner, V., Wirtz, K., Pilling, M.J., 2005a. Quantitative assessment of uncertainties for a model of tropospheric ethene oxidation using the European Photoreactor (EUPHORE). Atmospheric Environment 39, 2805–2817.

Zádor, J., Zsély, I.Gy., Turányi, T., Ratto, M., Tarantola, S., Saltelli, A., 2005b. Local and Global Uncertainty Analyses of a Methane Flame Model. Journal of Physical Chemistry A 109, 9795–9807.

Zhang, L., Moran, M.D., Brook, J.R., 2001. A comparison of models to estimate in-canopy photosynthetically active radiation and their influence on canopy stomatal resistance. Atmospheric Environment 35, 4463–4470.

Zhang, L., Moran, M.D., Makar, P.A., Brook, R., Gong, S., 2002. Modelling gaseous dry deposition in AURAMS: a unified regional air-quality modelling system. Atmospheric Environment 36, 537–560.

Zsély, I.Gy., Zádor, J., Turányi, T., 2005. Uncertainty Analysis Backed Development of Combustion Mechanisms. Proceedings of the Combustion Institute 30, 1273–1281.

Zsély, I.Gy., Zádor, J., Turányi, T., 2008. Uncertainty analysis of NO production during methane combustion. International Journal of Chemical Kinetics 40, 754–768.

Table 1 Vegetation-dependent parameters used in the simulations.

Vegetation type	Albedo	Surface resistance R_s (s m^{-1})	Cuticular resistance R_{cut} (s m^{-1})	Radiation correction term b_{st} (W m^{-2})	Optimal temperature t_{opt} (°C)	Minimum temperature t_{min} (°C)	Maximum temperature t_{max} (°C)	Vapour pressure deficit b_e (hPa)
Agricultural land	0.17	400	1500	60	25	5	45	0.02
Grass	0.19	300	2000	20	40	10	55	0.02
Coniferous forest	0.12	300	2000	44	15	−5	40	0.03
Deciduous forest	0.16	300	2000	43	27	0	45	0.04

(Sources: Baldocchi et al., 1987; Hicks et al., 1987; Meyers et al., 1998; Brook et al., 1999)

Table 2 A summary of the soil moisture contents used in this study (Based on Ács, 2003).

Soil type	Soil moisture at wilting point θ_w (m^{3}m^{-3})	Soil moisture at field capacity θ_f (m^{3}m^{-3})	Saturated soil moisture θ_s (m^{3}m^{-3})
Sand	0.03	0.15	0.40
Sandy loam	0.11	0.29	0.45
Loam	0.14	0.33	0.50
Clay loam	0.18	0.36	0.53
Clay	0.25	0.41	0.55

Table 3a A summary of the statistics of model input data – plant parameters (Source: Breuer et al., 2003).

Variables		Vegetation	Input data for the probability density function			
Vegetation parameters			Mean	Min	Max	SD
LAI	Leaf area index	Agricultural land	3.7	1.8	10.0	1.5
		Grass	7.2	0.5	16.2	3.8
		Coniferous forest	6.2	1.1	14.0	3.3
		Deciduous forest	5.8	2.5	10.0	1.7
g_{max} (mm s^{-1})	Maximum stomatal conductance	Agricultural land	5.7	2.9	10.0	2.6
		Grass	5.4	1.2	12.5	2.7
		Coniferous forest	1.8	0.5	4.0	0.9
		Deciduous forest	4.2	1.6	8.5	1.8

Table 3b A summary of the statistics of model input data – meteorological data (sources: Aladin numerical mesoscale model).

Variable		Input data for the probability density function				Period	Resolution	Area	Source
Meteorological data		Mean	Min	Max	SD				
N (%)	Cloudiness	12.70	0.00	100.00	14.26	1998 July	0.1° × 0.15°	45.7°N – 48.6°N,	ALADIN numerical
RH (%)	Relative humidity at 2 m	69.37	35.00	100.00	10.88			16.1°E – 23.0°E	meso-scale model
T (K)	Air temperature at 2 m	297.52	277.55	309.65	5.00				12UTC

Table 3c A summary of the statistics of model input data – soil data (calculated by a bucket model).

Variable			Input data for the probability density function				Period	Resolution	Area	Source
Soil data			Mean	Min	Max	SD				
$\theta\,(\mathrm{m^3m^{-3}})$	Soil moisture	Sand	0.111	0.037	0.236	0.037	1998 July	0.1° × 0.15°	45.7°N – 48.6°N,	Calculated daily values
		Sandy loam	0.215	0.124	0.355	0.038			16.1°E – 23.0°E	by a bucket-model
		Loam	0.259	0.136	0.500	0.044				
		Clay loam	0.296	0.209	0.420	0.036				
		Clay	0.369	0.230	0.550	0.071				

Table 4 Classification of the parameters based on the average effect of parameters to the deposition velocities. The results corresponding to the total and stomatal deposition velocities were classified separately. All cases were handled together (results of Morris method).

Land use categories		Agricultural land		Grass		Coniferous forest		Deciduous forest	
Input variable		total	stomatal	total	stomatal	total	stomatal	total	stomatal
Cloudiness		+	+	•	+	•	•	++	+
Relative Humidity		+	+	+	+	•	•	++	+
Leaf Area Index		•	•	+	+	+	+	•	•
Temperature		++	+++	•	+	•	•	+	+
Maximum stomatal conductance		+	++	+	++	+	+	++	++
Soil moisture		+++	+++	+	++	+	+	++	++

•, Very weak effect; $mean_{total} \leq 0.04$ cm s^{-1}; $mean_{stomatal} \leq 0.05$ cm s^{-1}.

+, Weak effect; 0.04 cm s$^{-1} < mean_{total} \leq 0.07$ cm s^{-1}; 0.05 cm s$^{-1} < mean_{stomatal} \leq 0.13$ cm s^{-1}.

++, Medium effect; 0.07 cm s$^{-1} < mean_{total} \leq 0.15$ cm s^{-1}; 0.13 cm s$^{-1} < mean_{stomatal} \leq 0.25$ cm s^{-1}.

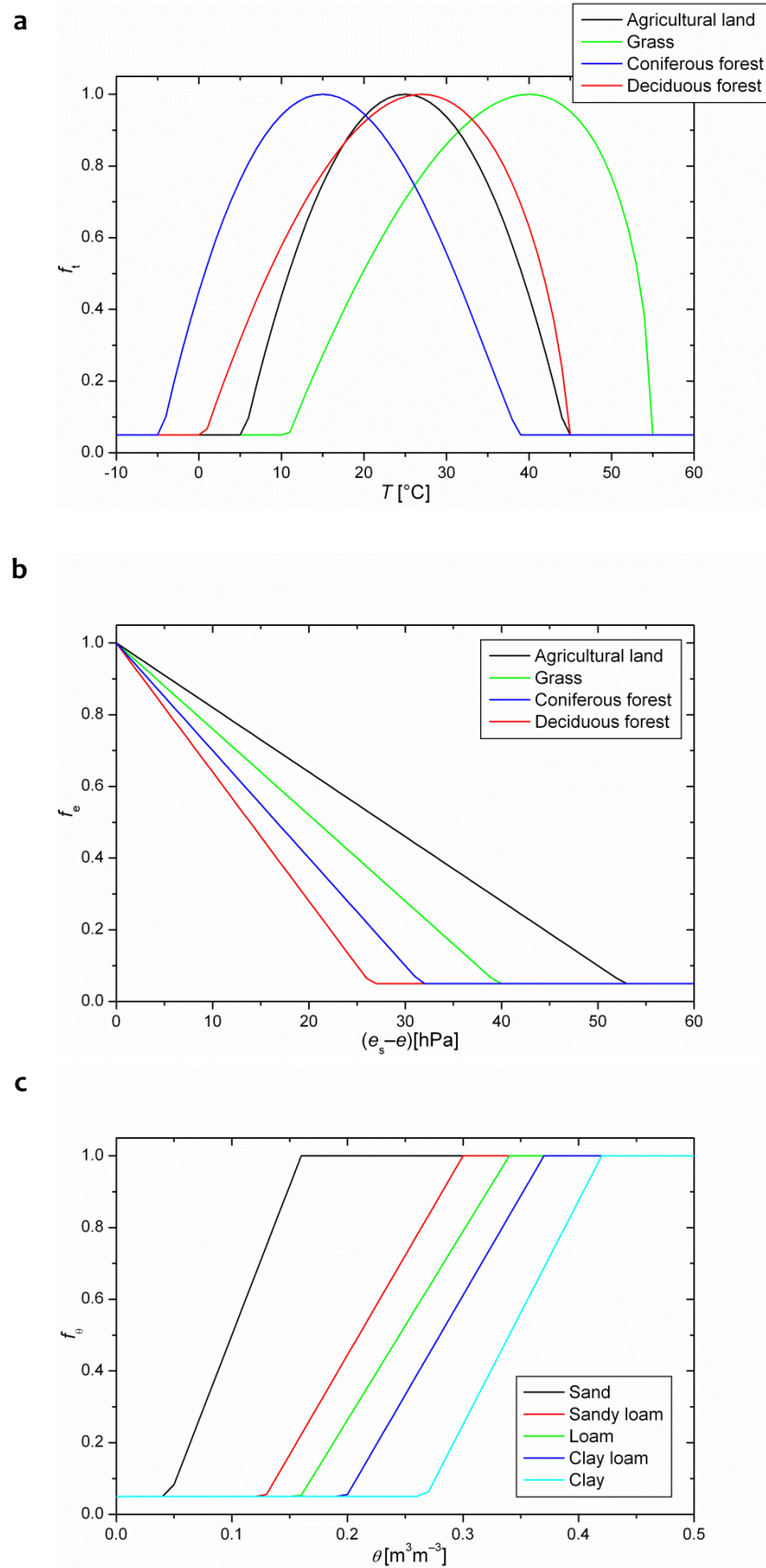+++, Strong effect; $mean_{total} > 0.15$ cm s^{-1}; $mean_{stomatal} > 0.25$ cm s^{-1}.

Fig. 1. Stress function for the estimation of stomatal resistance: temperature stress (a), water vapour stress (b) and soil moisture stress (c), respectively.
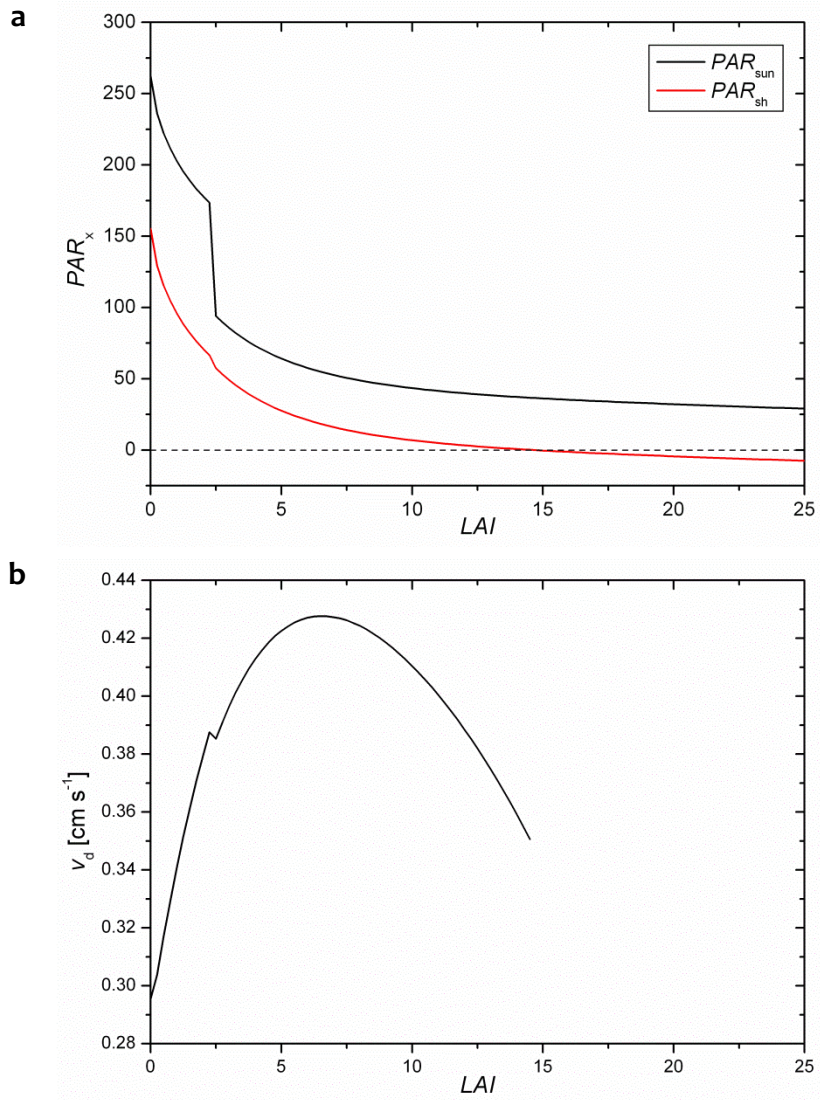
Fig. 2. Parameterization of PAR_{sun} and PAR_{sh} functions (a) and v_d (b) as a function of LAI using the mean values for the input parameters (Table 3a–c). The discontinuities at LAI = 2.5 are due to the different parameterization of these functions in the Zhang model (Zhang et al., 2001).
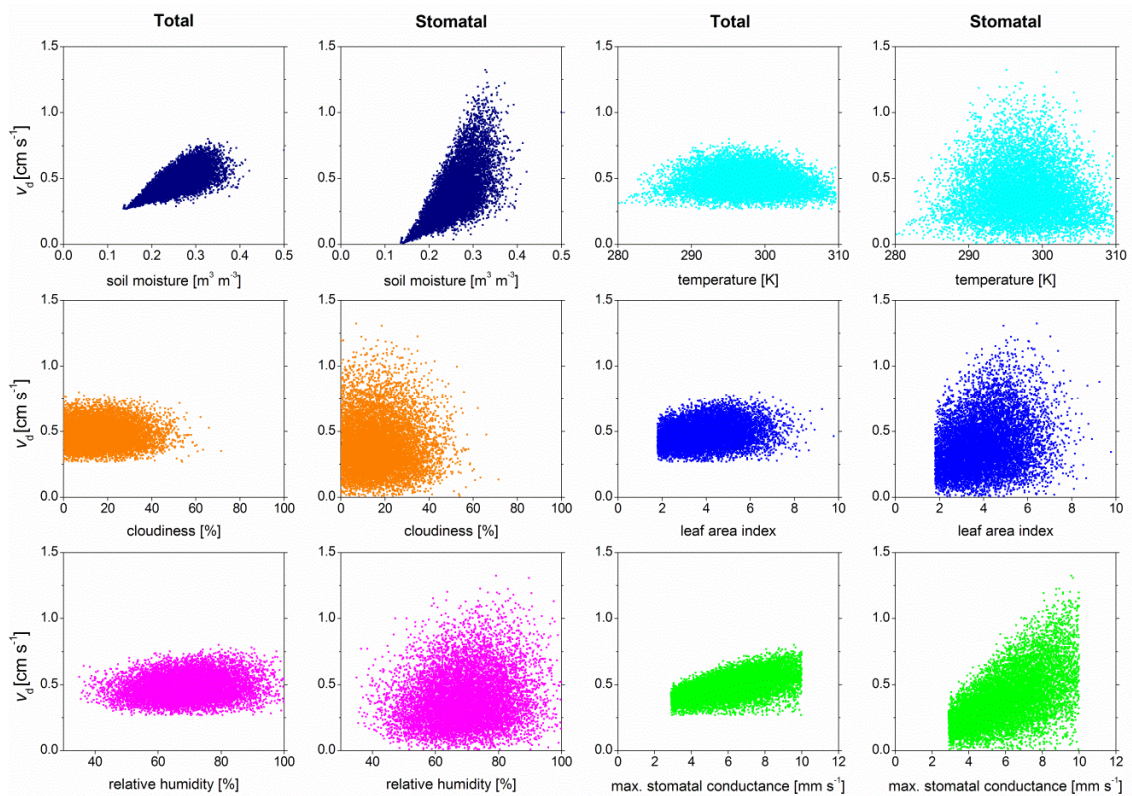
Fig. 3. Distribution of the total and the stomatal deposition velocities over loam soil and agricultural land. Results obtained from Monte Carlo analysis.
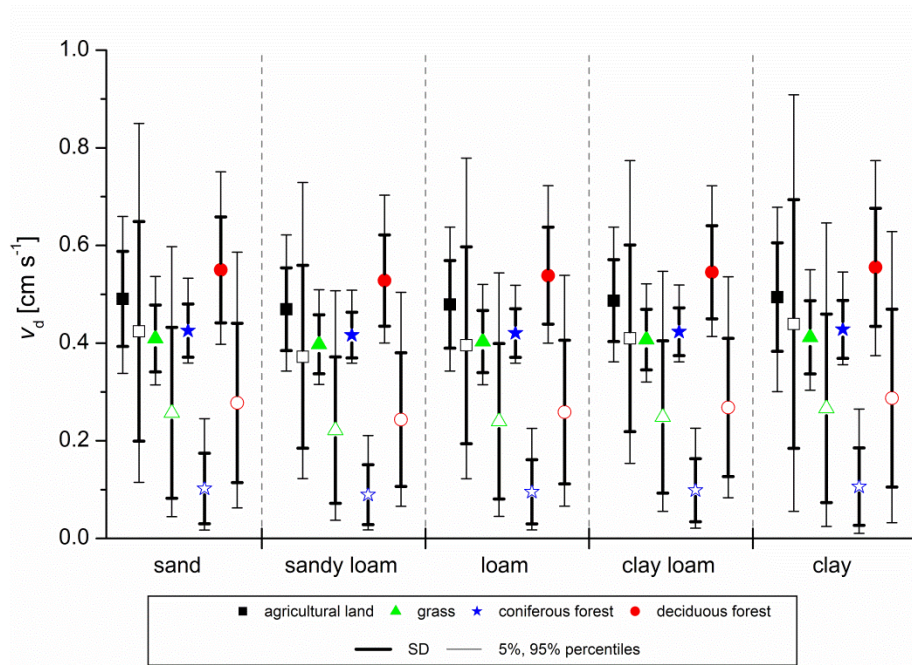

Fig. 4. Average, standard deviation and percentiles of the total and the stomatal deposition velocities over the various soil and surface types. The stomatal deposition velocities are presented by empty symbols. Results obtained from Monte Carlo analysis.
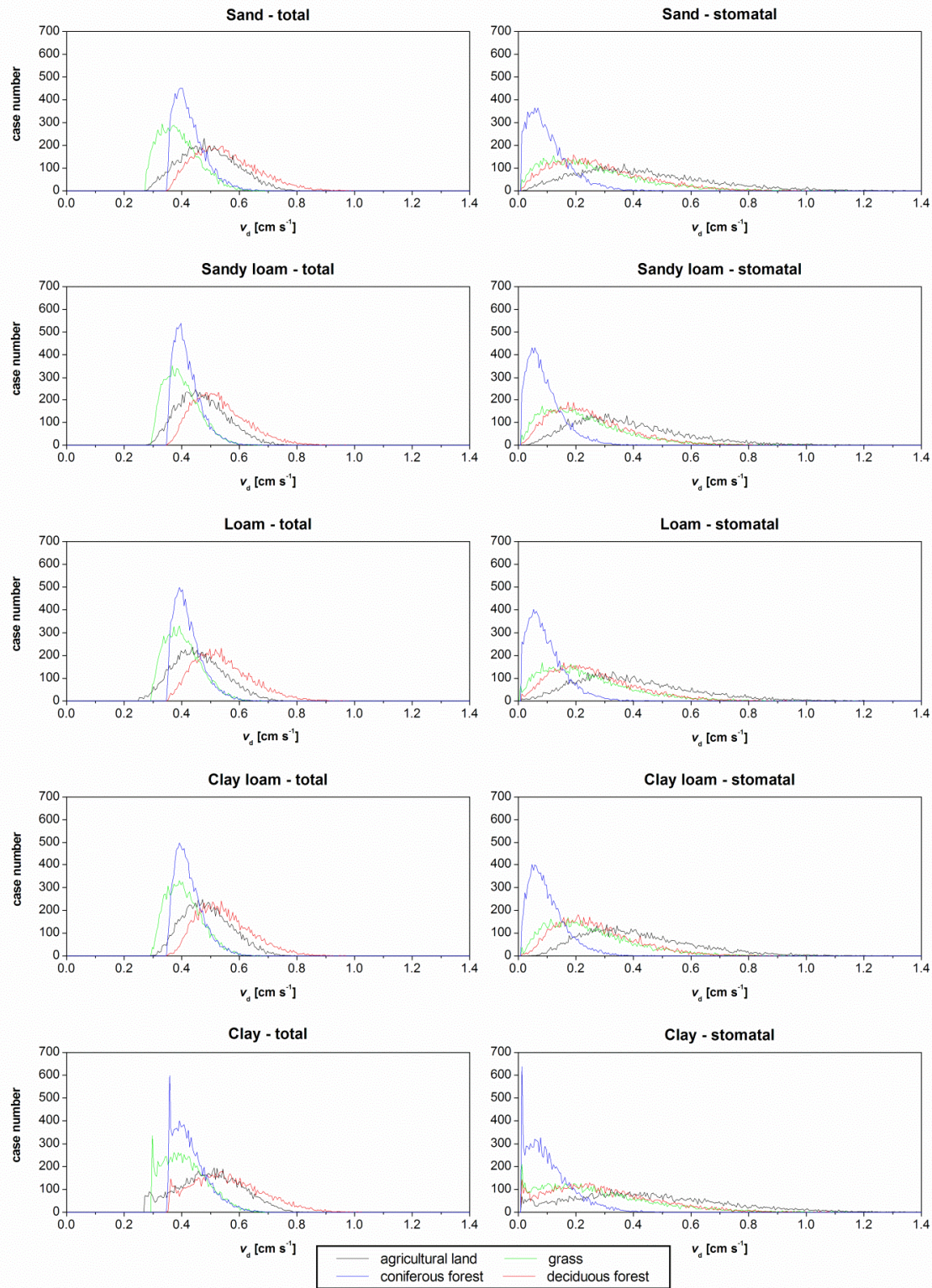
Fig. 5. Frequency distributions of the total and the stomatal depositions over five soil and four vegetation types. Results obtained from Monte Carlo analysis.
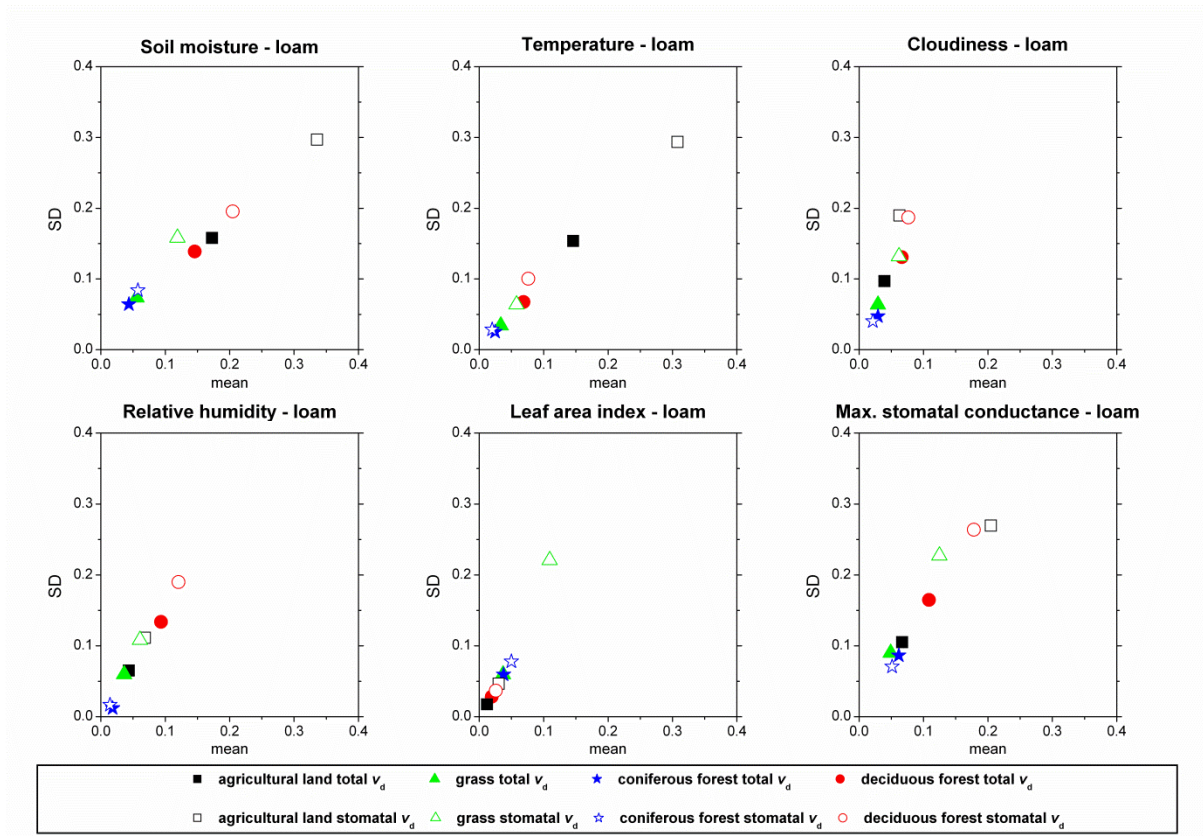
Fig. 6. Mean and standard deviation of the total and the stomatal deposition velocities over loam soil and four surface types obtained from the Morris method. The stomatal deposition velocities are indicated by empty symbols.
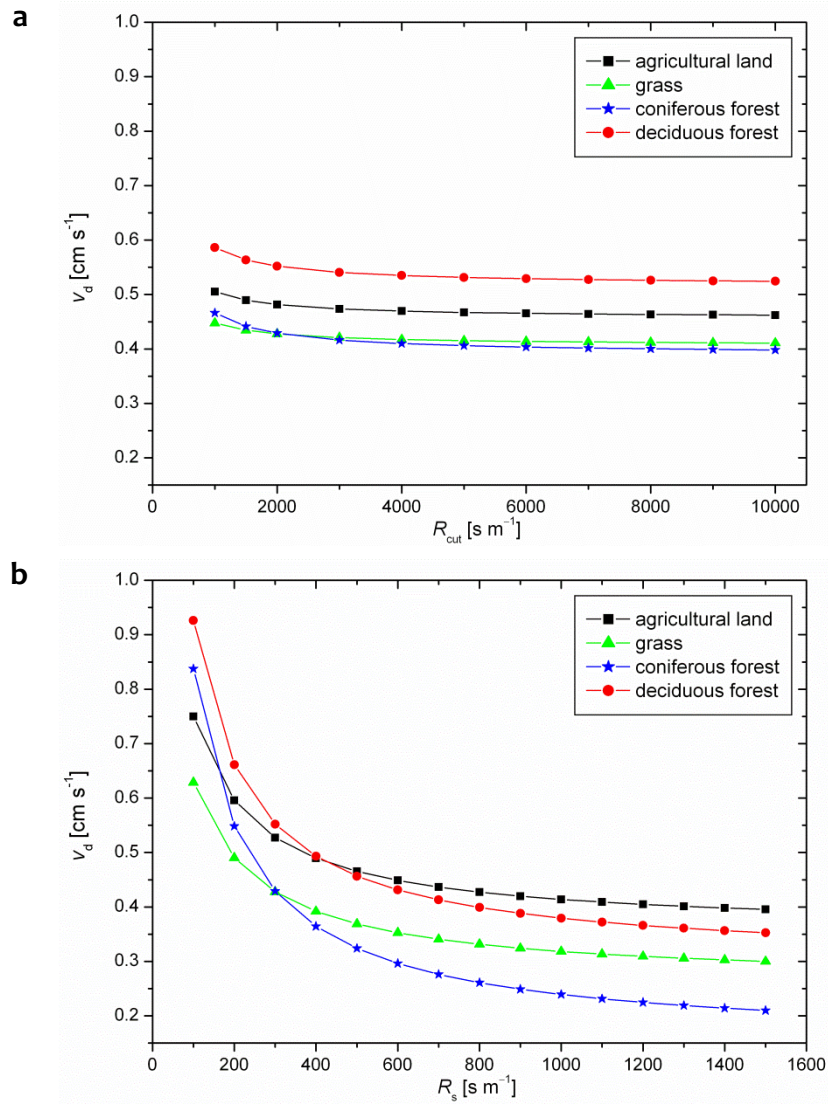
Fig. 7. Results of the local sensitivity analysis for loam soil: effect of cuticular resistance on total deposition velocity (a), and the effect of surface resistance on total deposition velocity (b) using the mean values for the input parameters (Table 3a–c).

Paper II

Effect of the soil wetness state on the stomatal ozone fluxes over Hungary

Mészáros R.[1], Szinyei D.[1], Vincze Cs.[1], Lagzi I.[2], Turányi T.[2], Haszpra L.[3], Tomlin A. S.[4]

[1] Department of Meteorology, Eötvös Loránd University, H-1518 Budapest, P.O. Box 32, Hungary
[2] Department of Physical Chemistry, Eötvös Loránd University, H-1518 Budapest, P.O. Box 32, Hungary
[3] Hungarian Meteorological Service, P.O. Box 39, Budapest H-1675, Hungary
[4] School of Process, Environmental and Materials Engineering, University of Leeds, Leeds, LS2 9JT, U.K.

Abstract

A coupled Eulerian photochemical reaction–transport model and a detailed ozone dry deposition model have been utilized for the estimation of stomatal ozone fluxes over Hungary. Ozone concentrations were modelled on an unstructured triangular grid using a method of lines approach to the solution of the reaction–diffusion–advection equations describing ozone formation, transport and deposition. The model domain covers Central-Europe including Hungary, which was located at the centre of the domain and covered by a high resolution nested grid. The dry deposition velocity of ozone was calculated based on the aerodynamic, quasi-laminar boundary layer and canopy resistance for five dominant vegetation types based on a land use map for Hungary. The coupled models were then used to analyse the effect of soil water content on the stomatal ozone flux. The stomatal ozone flux calculations were performed for two cases, with and without taking into account the effect of the soil moisture stress on the ozone deposition. The meteorological data utilized in the model were generated by the ALADIN meso-scale limited area numerical weather prediction model used by the Hungarian Meteorological Service. In contrast to earlier studies, when prescribed soil water fields were used, in this case, the soil water content for Hungary was estimated on a rectangular grid with a resolution of 0.10 × 0.15 degrees. The soil texture data were obtained using a Hungarian soil-map. It was found that soil water deficiency can strongly reduce the stomatal conductance and hence the ozone flux through it.

Keywords: dry deposition model, photochemical air pollution model, root-zone soil water content, ozone, stomatal flux

1. Introduction

Due to substantial emissions of ozone precursor species across Europe, elevated ozone concentrations may cover large areas of Europe for either shorter episodic or longer periods under certain meteorological conditions [1]. These elevated concentrations can be harmful to agricultural and natural vegetation. Air quality measures based on accumulated exposure over a threshold (AOT) such as AOT40 were therefore developed based on experiment in order to try to mitigate damage [2]. However, since ozone enters plants through the stomata, the response of vegetation to changes in atmospheric ozone concentrations is more directly influenced by the stomatal ozone flux than the atmospheric concentration itself. Therefore, it has been suggested that the stomatal ozone flux is a more appropriate measure for ozone damage than the AOT 40 value [3]. This flux depends on several factors including the soil wetness state in moderate soil water availability conditions. To this end the goal of this study was to analyse the sensitivity of stomatal ozone flux to the soil wetness state over Hungary.

Root-zone soil water content plays an important role in stomatal conductance. In the Soil-Vegetation-Atmosphere (SVAT) models, the effect of available soil moisture on stomata in general is described in two different ways. Some of these models use the leaf water potential [4–7], and others the soil water potential or soil water content [8–12]. Ács [13] showed, that these two different estimations should give the same results for a consistent soil parameter set. Since the latter method is simpler than the former one, it is more suitable for routine applications. It must be noted that in some other models [14] the effect of soil moisture stress is omitted. This approximation can be suitable in well-watered regions, but under continental climate conditions, especially during the summer months, soil wetness cannot be neglected.

Based on a previous investigation [15], it seems that in continental regions, soil water deficiency can strongly reduce the stomatal conductance and so the ozone flux through it. This former study has been pointed out that in Hungary the dry deposition velocity of ozone depends on the soil water content during the daytime, when stomatal deposition is dominant. For high soil water contents, deposition is also influenced by atmospheric and surface characteristics and can be highly spatially variable. However in earlier studies only prescribed soil water fields were used. In contrast, in this study the soil water field has been calculated using a simple water-budget model developed by Mintz and Walker [16]. Utilizing results of this model, an Eulerian photochemical reaction–transport model coupled with a detailed ozone dry deposition model was applied for estimating the stomatal deposition of ozone over Hungary. The combined model was tested for a sunny, summer day (23rd July, 1998). The stomatal ozone flux was estimated with and without

taking into account the effect of the soil moisture stress. Results show that under continental climate conditions the soil state can be a crucial factor in determining the extent of stomatal ozone deposition.

2. Materials and methods

2.1. The coupled dipersion–deposition model

An Eulerian reactive transport and a deposition model have been coupled for estimating the effective ozone load over Hungary. The deposition velocity of ozone was calculated as the inverse of the sum of the atmospheric and canopy resistances, where this latter term was parameterized by stomatal, mesophyll, surface and cuticular resistances. The reaction–diffusion–advection equations relating to ozone formation, transport and deposition were solved on an unstructured triangular grid using the 'method of lines' technique. This approach reduced the partial differential (reaction–diffusion–advection) equation set to a system of ordinary differential equations where the independent variable is the time. The two main steps of 'method of lines' were the spatial discretization and time integration. Our model uses a flux limited, cell centred finite volume scheme on an unstructured triangular mesh [17-20]. The resulting system of ordinary differential equations can then be solved as an initial value problem using the code SPRINT2D [17-20]. The model domain covers Central-Europe including Hungary, which was located at the centre of the domain and covered by a high resolution nested grid. The model grid structure during the simulations included a fixed fine nested grid over Hungary (980 km × 920 km), which had edge size of 12.5 km and a coarse grid outside of the rectangle covering Hungary. This coarser grid was characterized by edge length of 100 km. The model applies Dirichlet and Neumann type boundary conditions depending on the advective fluxes over boundary edge. The boundary conditions are imposed through the approximate Riemann solver. The vertical stratification is presented using four horizontal layers. These are the surface, the mixing, the reservoir and the free-troposphere layer, respectively. The vertical mixing of pollutants is approximated by a parameterized description of mixing between the layers. This is achieved by parameterization of the vertical eddy diffusion (set of coupled ordinary differential equations) between the surface and mixing layers, and fumigation between the mixing layer, and either the reservoir or upper layer above it. The coupled air quality model used the Emission Inventory for Budapest (1 km × 1 km), the National Emission Inventory (20 km × 20 km) for Hungary and EMEP inventory data for outside the country. The model uses the GRS (Generic Reaction Set) gas-phase chemical kinetic scheme to describe the photooxidant formation [21]. This mechanism represents 7 species interacting in 7 reactions. Although, the model also allows the utilisation of larger reaction schemes.

Photolysis rate constants are expressed as mth order rate constants with units (molecule cm^3) $m^{-1}s^{-1}$.

The dry deposition velocity of ozone was estimated over different types of vegetation. The land-cover map was generated using a Hungarian land-use map (Figure 1) [22]. The model was applied on the grid of the meso-scale limited area numerical weather prediction model ALADIN [23]. The time and space resolution of the data was 6 hours and 0.10 × 0.15 degrees, respectively.

The total ozone flux (F_t) was calculated as a product of the deposition velocity of ozone (v_d) and the ozone concentration (C_r) at a reference height (within the surface layer of the model):

$$F_t = v_d\, C_r.$$
(1)

The deposition velocity is defined as the inverse of the sum of the atmospheric and surface resistances, which retard the ozone flux:

$$v_d = (R_a + R_b + R_c)^{-1},$$
(2)

where R_a, R_b and R_c are the aerodynamic resistance, the quasi-laminar boundary layer resistance, and the canopy resistance, respectively.

The aerodynamic resistance is calculated using Monin-Obukhov's similarity theory taking into account the atmospheric stability. The procedure is described in detail in the work of Ács and Szász [24]. The boundary layer resistance is calculated by an empirical relationship after Hicks et al. [25]. The canopy resistance R_c is parameterized by equation:

$$R_c = \frac{1}{(R_{st} + R_{mes})^{-1} + (R_s)^{-1} + (R_{cut})^{-1}},$$
(3)

where R_{st}, R_{mes}, R_s, and R_{cut} are the stomatal, mesophyll, surface and cuticular resistances, respectively.

The stomatal resistance can be calculated from the empirical formula of Jarvis [26] referring to a vegetation canopy. This parameterization requires knowledge of the soil and plant physiological characteristics:

$$R_{st} = \frac{1}{G_{st}(PAR)f_t(t)f_e(e)\,f_\theta(\theta)f_{D,i}},$$
(4)

where $G_{st}(PAR)$ is the unstressed canopy stomatal conductance, a function of PAR, the photosynthetically active radiation. This term is estimated after Zhang et al. [27]. The factors in the denominator range between 0 and 1 and modify the stomatal resistance:

$f_t(t)$, $f_e(e)$ and $f_\theta(\theta)$ describe the effect of temperature, the vapour pressure deficit and plant water stress on stomata [15], while $f_{D,i}$ modifies the stomatal resistance for the pollutant gas of interest (for ozone, $f_{D,i} = 0.625$ after Wesely [28]).

The mesophyll resistance for ozone in the model is taken to be zero. Cuticular resistance, R_{cut} and surface resistance, R_s for ozone deposition were obtained as in Lagzi et al. [15].

Ozone basically reacts by vegetation through the stomata. Therefore it is important to know the part of the total flux which represents the stomatal uptake. Since we assumed that the flux is constant between the reference height and the top of the canopy, the total flux can be written as follows:

$$F_t = C_r (R_a + R_b + R_c)^{-1} = C_c R_c^{-1}, \qquad (5)$$

where C_c is the concentration at the top of canopy. For estimating stomatal ozone flux, the total flux at the canopy top level is divided into stomatal (F_{st}) and non-stomatal (F_{nst}) deposition pathways:

$$F_t = F_{st} + F_{nst}, \qquad (6)$$

and

$$F_t = C_c R_{st}^{-1} + C_c R_{nst}^{-1}. \qquad (7)$$

Accordingly from Eq. (5), the stomatal flux is calculated separately:

$$F_{st} = C_r R_c (R_a + R_b + R_c)^{-1} R_{st}^{-1}. \qquad (8)$$

2.2. The water-budget model

Previous investigations [15] have shown that soil water content can strongly affect the stomatal flux. This influence is described by Eq. (4) with the soil water stress function term $f_\theta(\theta)$. This can be parameterized using soil water content (θ):

$$f_\theta = \begin{cases} 1 & \text{if } \theta > \theta_f \\ max\left\{ \dfrac{\theta - \theta_w}{\theta_f - \theta_w}, 0.05 \right\} & \text{if } \theta_w < \theta \leq \theta_f \\ 0.05 & \text{if } \theta \leq \theta_w \end{cases}, \qquad (9)$$

where θ_w and θ_f are the wilting point and the field capacity soil moisture contents, respectively. These terms depend on the soil texture of the grid cell. The soil texture was determined from the work of Várallyay et al. [29]. The grid cell soil texture was

represented by the dominant soil texture (Figure 2). The following soil texture categories were used in the model: sand, sandy loam, loam, clay loam and clay. The θ_w and θ_f values for different soil textures were taken from Ács [30].

In Hungary, under continental climate conditions, deposition is frequently obstructed by soil water deficiency. Soil water content, θ can be modelled by a simple bucket model [16]. The model estimates the soil water content in the root-zone using a daily time step. Vegetation can take up water from the root-zone. Horizontal water transport in the root-zone and interaction with deeper soil layers are neglected. Water surplus overflows at the surface.

The soil water content on the ith day (θ_i) is calculated as the sum of the soil water content and the water budget component on the (i–1)th day:

$$\theta_i = \theta_{i-1} + (P_{i-1} - I_{i-1}) - (T_{i-1} + E_{i-1}), \tag{10}$$

where P_{i-1}, I_{i-1}, T_{i-1} and E_{i-1} are the precipitation, the interception, transpiration and vaporation on the (i–1)th day, respectively (all terms expressed in mm). Interception is parameterised as:

$$I_{i-1} = \min(P_{i-1}, PE_{i-1}), \tag{11}$$

where PE_{i-1} is the potential evapotranspiration. There are a number of possible parameterizations for potential evapotranspiration, but a common one used for Hungary has been constructed by Antal [31]:

$$PE_{i-1} = \frac{1 - (f / 100)}{2 - (f / 100)} \cdot t_n, \tag{12}$$

where f [%] and t_n [°C] are the average daily values of relative humidity and temperature on the (i–1)th day, respectively. For temperatures below 0°C, the potential evapotranspiration is equal to zero in the model. In this case water cannot diminish in the bucket and can only increase by precipitation.

The term $T_{i-1} + E_{i-1}$ (transpiration + evaporation) is expressed by a $\beta_{T,E}$ stress coefficient:

$$(T_{i-1} + E_{i-1}) = \beta_{T,E} \cdot (PE_{i-1} - I_{i-1}), \tag{13}$$

where

$$\beta_{T,E} = \frac{\theta_{i-1} - \theta_\omega}{\theta_f - \theta_\omega} z_r. \tag{14}$$

Here θ_{i-1} is the soil water content on the previous day, and z_r is the root-zone in mm.

3. Results and discussions

The coupled transport-deposition model was applied for a simulation period from noon 22nd July to midnight 23rd July, 1998. This case study was chosen since during the selected days, the high temperature, low cloud cover and low wind speed resulted in high photooxidant levels in Hungary. The initial concentrations of the major species were 0.4 ppb for NO_2, 2.0 ppb for NO, 80 ppb for O_3, and 4.1 ppb for VOC, which corresponded to typical daytime species concentrations. The initial concentrations were equal in each layer across the whole simulated domain.

To analyze the influence of soil moisture on the ozone flux, the soil water content has been calculated by a simplified water-budget model. This model was started from 1th July, 1998 to obtain a realistic value of soil moisture content for the simulation day (23rd July, 1998). The initial θ values were chosen for each grid cell as the average of the wilting point and the field capacity soil moisture contents with respect to the given soil types. Distribution of soil water content is shown in Figure 3. The results indicate a good correlation with Figure 2, because the meteorological conditions before the simulation day had been optimal for soil water content (precipitation and evaporation were roughly in balance) and therefore the soil water content was mainly determined by soil type. The lowest soil moisture content values occur in the region where the soil type is sand, whereas the highest ones occur in the case of clay soil.

Figure 4 shows the simulated spatial distribution of ozone concentration at 12 UTC on 23rd July, 1998. The chosen period was the same as described in our previous paper [15], where model results were compared with measurement data. We have pointed out that the soil moisture practically does not affect the calculated ozone concentration. High ozone concentrations are obtained in the north-western, and eastern parts of Hungary, and also in southeast of the city of Budapest. In this region, elevated ozone concentrations are appeared due to the formation of a plume from the city's emissions. At the same time, low concentrations are observed in the city of Budapest, because of high concentrations of nitrogen oxide in the urban atmosphere which titrates a large proportion of the ozone transported into the city.

The distribution of the deposition velocities at 12 UTC on 23rd July, 1998 is presented in Figure 5. The calculated deposition velocities of ozone over different vegetation types are shown to vary between 0.1 and 0.6 cm s^{−1}, showing good agreement with published observed data (see Lagzi et al. [15]). The spatial variability within this range is quite high due to varying land use and soil types through soil wetness state.

The total ozone flux is the product of the deposition velocity and ozone concentration. Figure 6 shows the distribution of total ozone flux, where the effects of both concentration and deposition fields are apparent. For example, the highest values of the total ozone flux (around 1 μg m^{−2} s^{−1}) can be seen in the Eastern and North-Eastern parts of the country. In these regions both the concentration of ozone and its deposition velocity are higher. In the South Eastern region, the ozone concentrations were predicted

to be high (> 80 ppb). However, the predicted total ozone flux is relatively low due to low deposition velocities in this region, demonstrating possible flaws in the assumption that damage can be directly related to ozone concentrations.

To utilize the soil moisture field, the stomatal part of ozone flux was calculated for two cases. The first represents a situation where the effect of soil moisture was neglected. This means that during the model run, the soil water stress function, $f_d(\theta) = 1$ was applied across the whole region. In line with this assumption, Figure 7 shows the distribution of stomatal ozone flux without considering spatial variability in soil moisture. This figure characterizes a theoretical well-watered situation, where the soil moisture content is considered to be equal to the field capacity soil water content for the whole country. It also represents a high flux case since the stomatal conductance is not limited by soil water deficiency. A more realistic distribution of predicted stomatal ozone flux can be seen in Figure 8, where in the model calculations, an estimated soil water content field (Figure 3) has been used.

In both cases the highest predicted stomatal fluxes are directly to the South East of Budapest and to the East of Hungary where the predicted ozone concentrations are over 100 ppb. Where soil wetness state is taken into account however, the predicted stomatal fluxes are substantially lower in most areas, reflecting the influence of soil water deficiency. The percentage differences between estimated stomatal fluxes for the two cases vary between 0 and 70 percent (Figure 9a). This term was calculated using $100 \cdot (F_{st1} - F_{st2})/F_{st1}$, where F_{st2} and F_{st1} are the stomatal fluxes with and without taking into account the effect of the soil moisture stress, respectively. Figure 9b shows the equivalent absolute differences in stomatal fluxes between the two cases.

Evidently, there are no differences over urban and water covered areas where the stomatal flux for the base case was effectively zero. The effect of soil wetness state however, influences the percentage differences between the two cases, as does the predicted ozone concentration.

The greatest relative and absolute differences are seen in the South Eastern part of the country where sand and loam soil types with low soil moisture content are present and the predicted ozone concentrations are over 80 ppb. High absolute differences are also seen directly to the South East of Budapest where the predicted ozone concentrations are high and again the soils are mainly sandy. Both of these regions are predominantly agricultural. High relative differences are seen in the South West of the country, although the absolute differences here are lower due to the lower predicted ozone concentrations (around 60 ppb) in this region. Much lower relative differences between the two cases are seen in regions of clay soils such as the North Eastern tip of Hungary, where θ is effectively higher.

Although the results refer to a single day case study, they serve to illustrate the importance of representing the spatial variability of soil moisture content in calculating stomatal ozone fluxes. Further conclusions about the importance of such effects over a longer period, such as a growing season, will be the subject of future investigations.

4. Conclusions

A chemical transport model and a dry deposition model were coupled for the purpose of simulating ozone fluxes over Hungary. Accurate estimation of both the ozone concentration and deposition velocity fields facilitates the calculation of stomatal ozone flux. This flux is an accurate measure of the effective ozone load and has been shown to differ from the ozone concentration field due to spatial variability in land use and soil type. The stomatal ozone flux depends on the atmospheric conditions, and the vegetation physiology. Previous investigations [15], have also shown that soil water content is another important factor which governs the deposition of ozone. The soil water deficiency can strongly reduce the stomatal conductance and so the ozone flux through it. In earlier studies, prescribed soil water fields had been used. In contrast, in this study the soil water field has been calculated using a simplified water-budget model. Stomatal ozone flux calculations were performed with and without taking into account the effect of the soil moisture stress on the ozone deposition.

The main conclusions that can be drawn from the study can be summerized as follows. For the hot, summer day tested, a significant difference in the spatial distribution of the stomatal flux between the two case studies was predicted. The obstructive effect of the soil wetness stress on the stomatal ozone deposition varies between 0 and 70 percent. These relative differences were shown to depend on both the atmospheric state, the vegetation type, and also strongly on soil types and soil characteristics. This suggests, that the effect of soil water content cannot be neglected in the continental climate region, especially in the hot summer period. However, a particular analysis of the influence of soil on overall ozone deposition requires additional model calculations. In the future, it is planned to couple the transport-deposition model with the ALADIN meso-scale limited area numerical weather prediction model to estimate ozone deposition over Hungary for a routine application. Such longer term predictions, coupled with sensitivity analyses, will allow more detailed investigations about the relationships between soil, vegetation and the resulting ozone fluxes over the growing season.

References

[1] Hjellbrekke, A-G., Solberg, S., 2002. Ozone measurments 2000. EMEP/CCC-Report 5/2002.

[2] Fuhrer, J., Skärby, L. Ashmore, M.R., 1997. Critical levels for ozone effects on vegetation in Europe. Environmental Pollution 97, 91–106.

[3] Emberson, L.D., Simpson, D., Tuovinen, J-P., Ashmore, M.R. Cambridge, H.M., 2000a. Towards a model of ozone deposition and stomatal uptake over Europe. EMEP MSC-W Note 6/00.

[4] Ács, F. and Hantel, M. (1998) 'The land-surface flux model PROGSURF', *Global and Planetary Change,* Vol. 19, pp. 19–34.

[5] Ács, F. and Hantel, M. (1999) 'The Penman-Monteith concept based land-surface model PMSURF', *Időjárás,* Vol. 103, pp. 19–36.

[6] Brook, J.R., Zhang, L., Di-Giovanni, F. and Padro, J. (1999) 'Description and evaluation of a model of deposition velocities for routine estimates of air pollutant dry deposition over North America. Part I: model development' *Atmospheric Environment,* Vol 33, pp. 5037–5051.

[7] Zhang, L., Moran, M.D., Makar, P.A., Brook, R. and Gong, S. (2002) 'Modelling gaseous dry deposition in AURAMS: a unified regional air-quality modelling system' *Atmospheric Environment,* Vol. 36, pp. 537–560.

[8] Grünhage, L. and Haenel, H.-D. (1997) 'PLATIN (PLant-ATmosphere INteraction) I: a model of plant-atmosphere interaction for estimating absorbed doses of gaseous air pollutants' *Environmental Pollution,* Vol 98, pp. 37–50.

[9] Meyers, T.P., Finkelstein, P., Clarke, J., Ellestad, T.G. and Sims, P.F. (1998) 'A multilayer model for inferring dry deposition using standard meteorological measurements' *Journal of Geophysical Research,* Vol. 103, pp. 22645–22661.

[10] Emberson, L.D., Ashmore, M.R., Cambridge, H.M., Simpson, D. and Touvinen, J.-P. (2000) 'Modelling stomatal ozone flux across Europe' *Atmospheric Pollution,* Vol. 109, pp. 403–413.

[11] Bassin, S., Calanca, P., Weidinger, T., Gerosa, G. and Fuhrer, J. (2004) 'Modeling seasonal ozone fluxes to grassland and wheat: model improvement, testing and application' *Atmospheric Environment,* Vol. 38, pp. 2349–2359.

[12] Calvet, J-C., Rivalland, V., Picon-Cochard, C. and Guehl, J-M. (2004) 'Modelling forest transpiration and CO_2 fluxes–response to soil moisture stress' *Agricultural and Forest Meteorology,* Vol. 124, pp. 143–156.

[13] Ács, F. (2005) 'On transpiration ans soil moisture content sensitivity to soil hydrophysical data' *Boundary Layer Meteorology,* Vol. 115, pp. 473–497.

[14] Smith, R.I., Fowler, D., Sutton, M.A., Flechard, C. and Coyle, M. (2000) 'Regional estimation of pollutant gas dry deposition int he UK: model description, sensitivity analyses and outputs' *Atmospheric Environment,* Vol. 34, pp. 3757–3777.

[15] Lagzi, I., Mészáros, R., Horváth, L., Tomlin, A., Weidinger, T., Turányi, T., Ács, F. and Haszpra, L. (2004) 'Modelling ozone fluxes over Hungary' *Atmospheric Environment,* Vol. 38, pp. 6211–6222.

[16] Mintz, Y. and Walker, G.K. (1993) 'Global fields of soil moisture and land surface evapotranspiration derived from observed precipitation and surface air temperature' *Journal of Applied Meteorology,* Vol. 32, pp. 1305–1334.

[17] Berzins, M., Dew, P.M. and Furzeland, R.M. (1989) 'Developing software for time-dependent problems using the method of lines and differential algebraic integrators', *Applied Numerical Mathematics,* Vol. 5, pp. 375–397.

[18] Berzins, M. and Furzeland, R.M. (1992) 'An adaptive Theta-method for the solution of stiff and nonstiff differential-equations', *Applied Numerical Mathematics,* Vol. 9, pp. 1–19.

[19] Berzins, M. and Ware, J. (1995) 'Positive cell-centered finite volume discretization methods for hyperbolic equations on irregular meshes', *Applied Numerical Mathematics,* Vol. 16, pp. 417–438.

[20] Berzins, M. and Ware, J. (1996) 'Solving convection and convection reaction problems using the method of lines', *Applied Numerical Mathematics,* Vol. 20, pp. 83–99.

[21] Azzi, M., Johnson, G.J. and Cope, M. (1992) 'An introduction to the generic reaction set photochemical smog mechanism', *Proceegings of the 11th Clean Air Conference and 4th Regional IUAPPA Conference,* Brisbane, Australia, pp. 451–462.

[22] National Atlas of Hungary (1989) Cartographia, Budapest

[23] Horányi, A., Ihász, I. and Radnóti, G. (1996) 'ARPEGE/ALADIN: A numerical Weather prediction model for Central-Europe with the participation of the Hungarian Meteorological Service' *Időjárás,* Vol. 100, pp. 277–301.

[24] Ács, F. and Szász, G. (2002) 'Characteristics of microscale evapotranspiration: a comparative analysis' *Theoretical and Applied Climatology,* Vol. 73, pp. 189–205.

[25] Hicks, B.B., Baldocchi, D.D., Meyers, T.P., Hosker, R.P. and Matt, D.R. (1987) 'A preliminary multiple resistance routine for deriving dry deposition velocities from measured quantities' *Water, Air and Soil Pollution,* Vol. 36, pp. 311–330.

[26] Jarvis, P.G. (1976) 'The interpretation of the variations in leaf water potential and stomatal conductance found in canopies in the field' Philosophical *Transactions of the Royal Society of London,* Series. B, Vol. 273, pp. 593–610.

[27] Zhang, L., Moran, M.D. and Brook, J.R. (2001) 'A comparison of models to estimate in-canopy photosynthetically active radiation and their influence on canopy stomatal resistance' *Atmospheric Environment,* Vol. 35, pp. 4463–4470.

[28] Wesely, M.L. (1989) 'Parameterization of surface resistances to gaseous dry deposition in regional-scale numerical models' *Atmospheric Environment,* Vol. 23, pp. 1293–1304.

[29]   Várallyay, Gy., Szűcs, L., Murányi, A., Rajkai, K. and Zilahy, P. (1980) 'Map of soil factors determining the agro-ecological potential of Hungary (1:100 000) II.' *Agrokémia és Talajtan,* Vol. 29, pp. 35–76 (in Hungarian).

[30]   Ács, F. (2003) 'On the relationship between the spatial variability of soil properties and transpiration' *Időjárás,* Vol. 107, pp. 257–272.

[31]   Antal, E. (1966) 'Potential evapotranspiration of certain agricultural vegetations' *Öntözéses Gazdálkodás* Vol. 4, pp. 69–86 (in Hungarian).
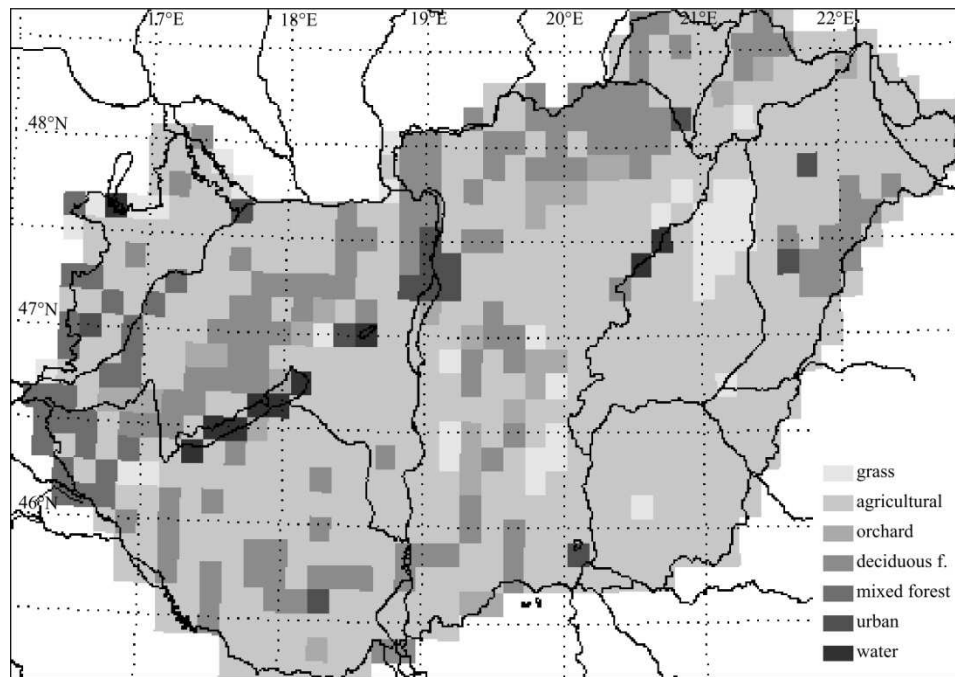
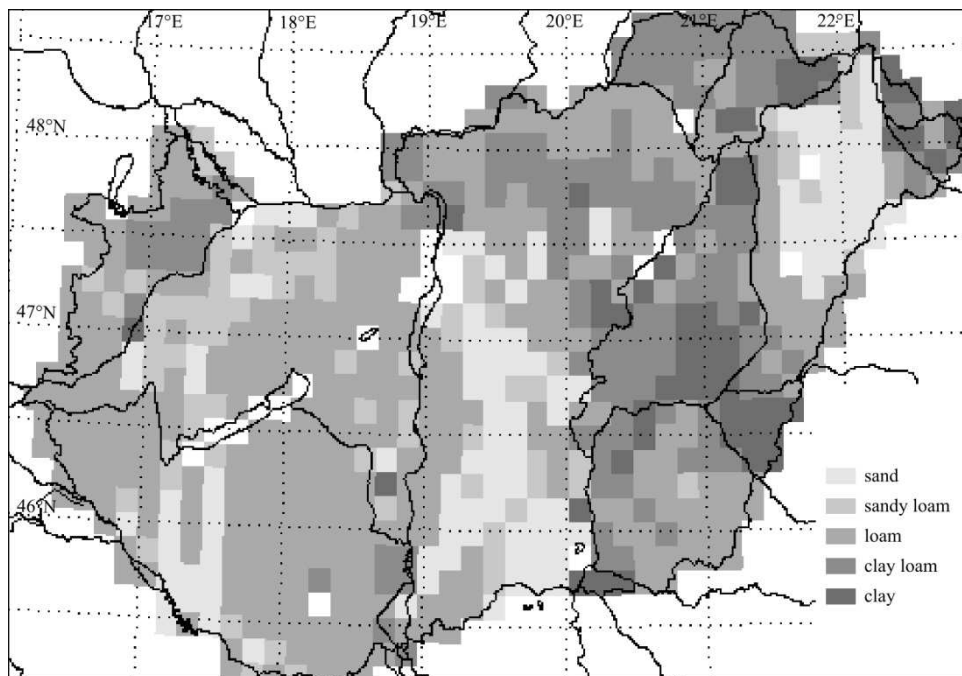**Figure 1** Land use categories in the model.

Figure 2 Soil types in the model.
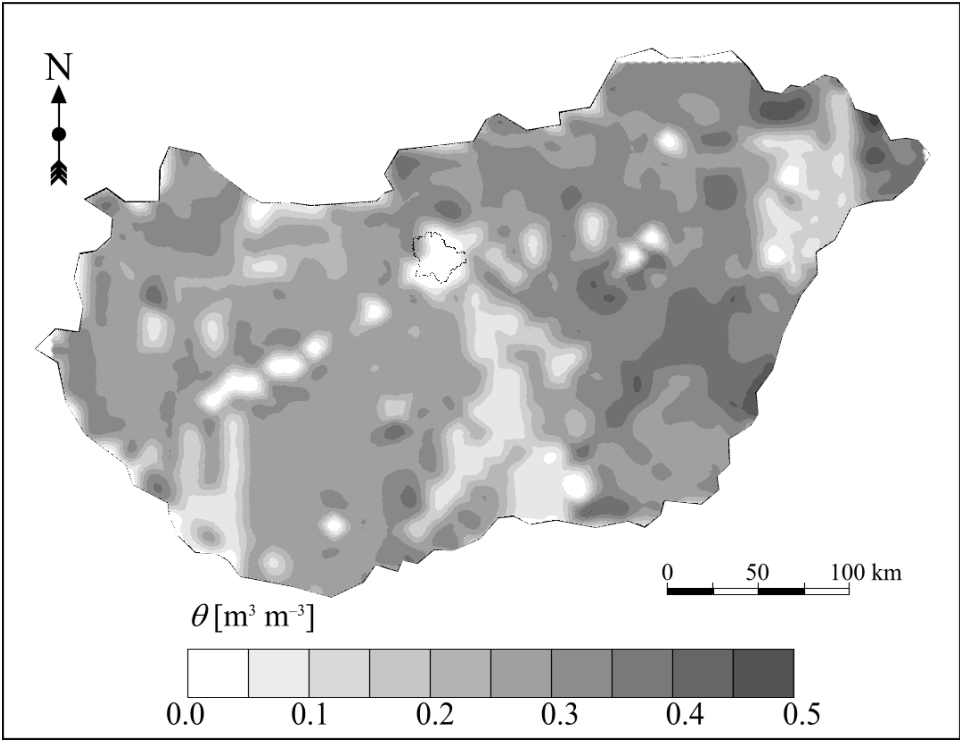
Figure 3 Calculated soil moisture content on 23 July 1998.
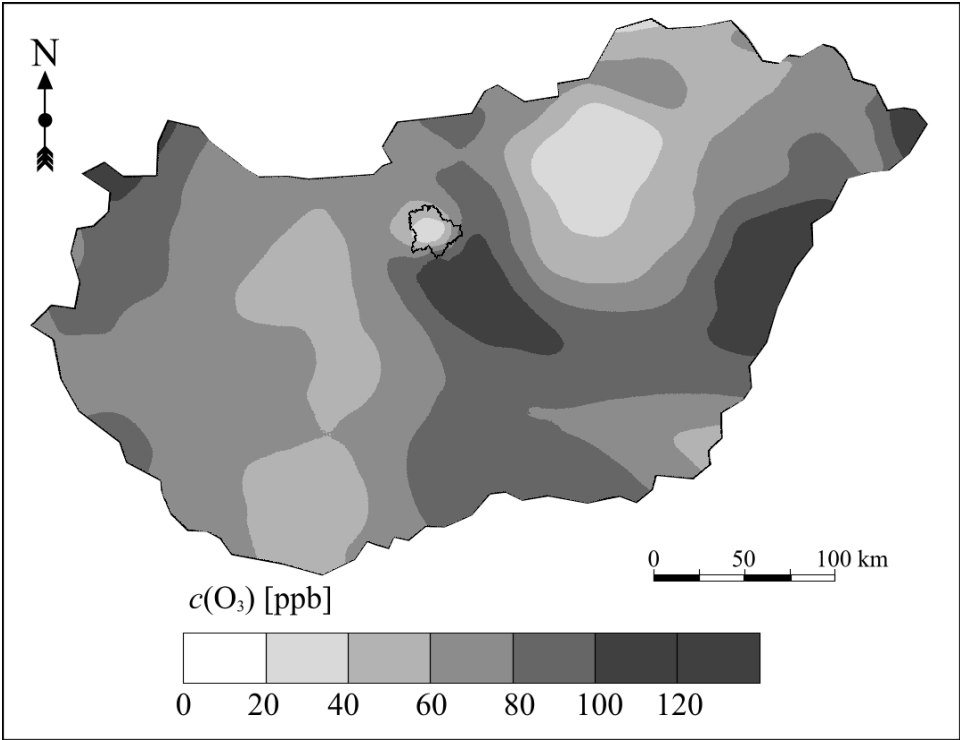
Figure 4 Calculated ozone concentration on 23 July 1998 at 12 UTC.

$v_d(O_3)$ [cm s^{-1}]

0.0   0.1   0.2   0.3   0.4   0.5   0.6
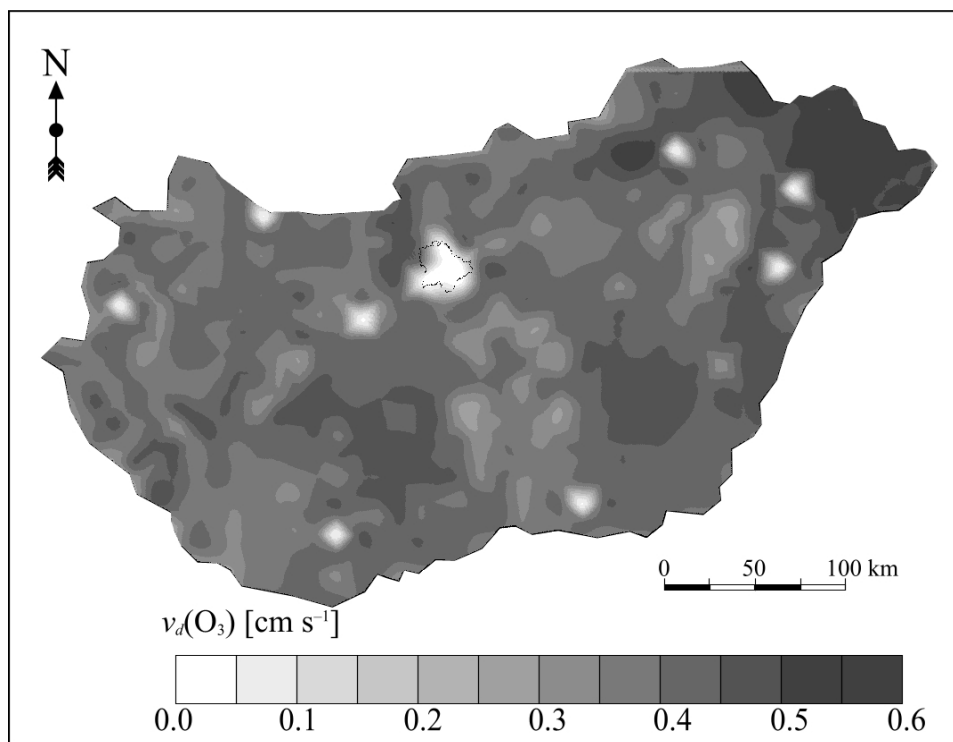
Figure 5 Calculated dry-deposition velocity of ozone on 23 July 1998 at 12 UTC.

$F(O_3)$-total [µg m^{-2} s^{-1}]

0.0   0.2   0.4   0.6   0.8   1.0
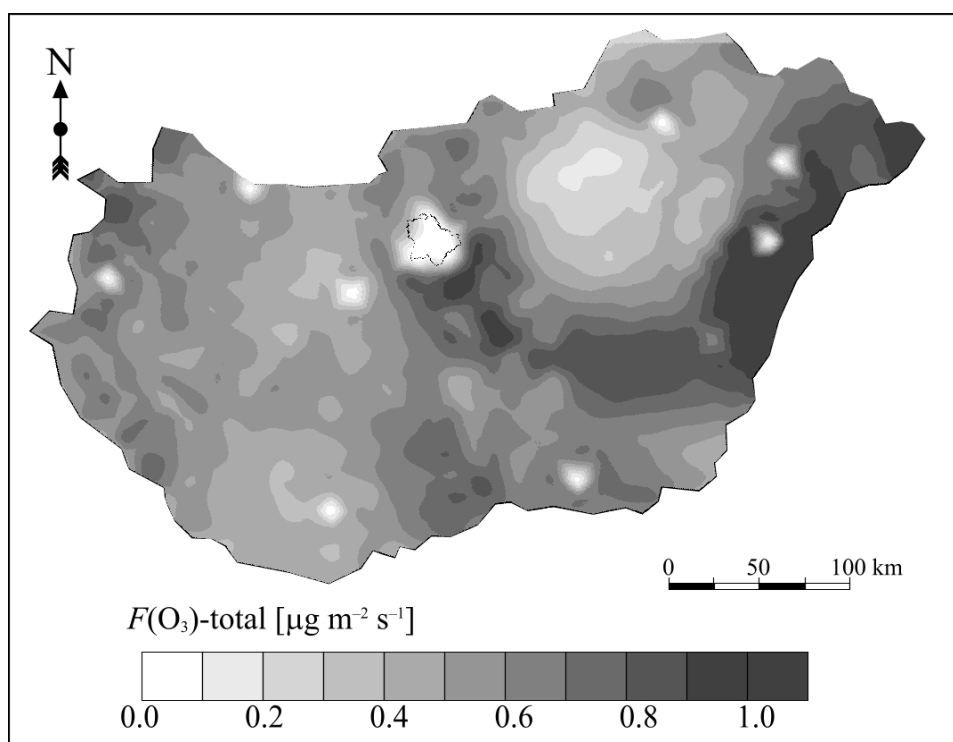
Figure 6 Calculated total ozone flux on 23 July 1998 at 12 UTC.
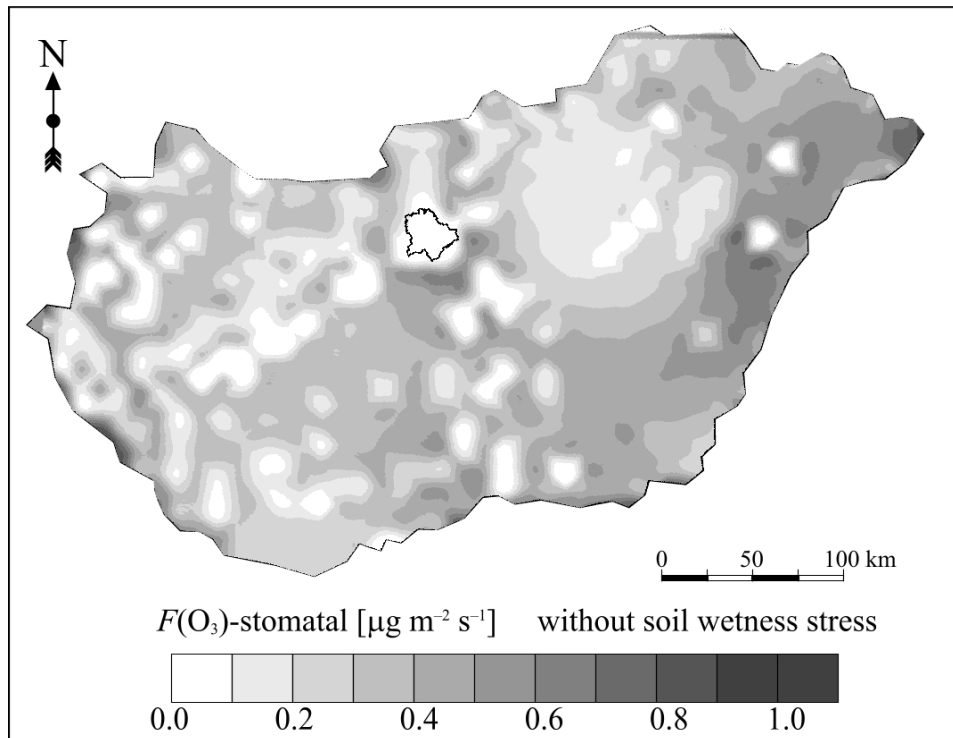
Figure 7 Calculated stomatal ozone flux on 23 July 1998 at 12 UTC. Result corresponds to a supposed condition with sufficient soil wetness.

Figure 8 Calculated stomatal ozone flux on 23 July 1998 at 12 UTC. Result corresponds to the effective soil wetness condition.

Figure 9 Effect of soil wetness state: (a) relative and (b) absolute differences of stomatal resistances with and without soil wetness stress.

Paper III

Evaluation of ozone deposition models over a subalpine forest in Niwot Ridge, Colorado
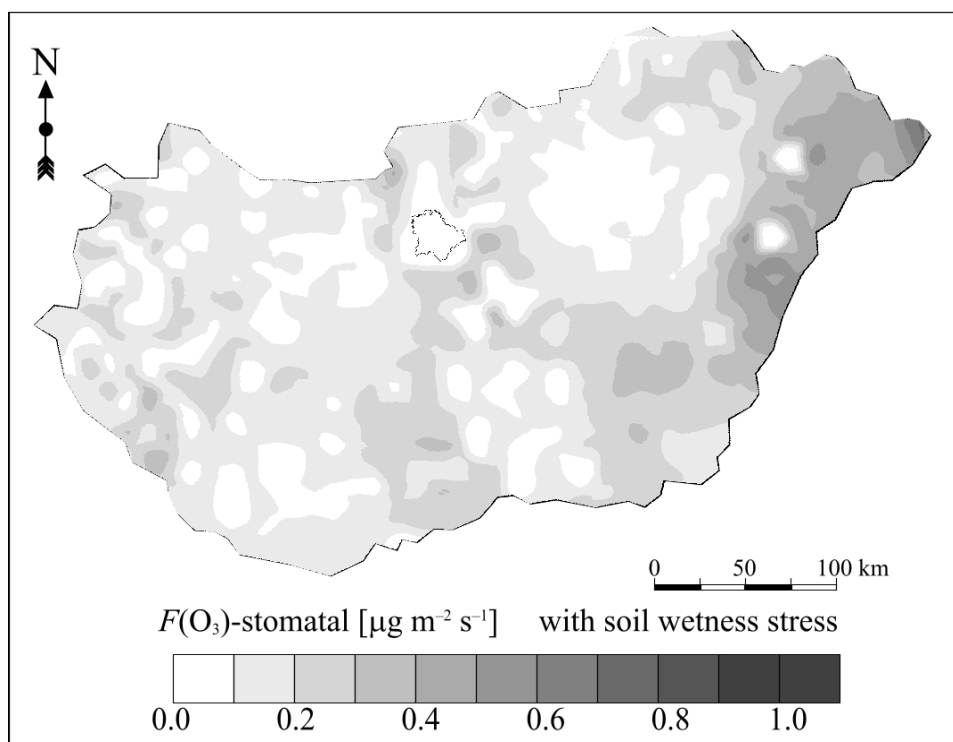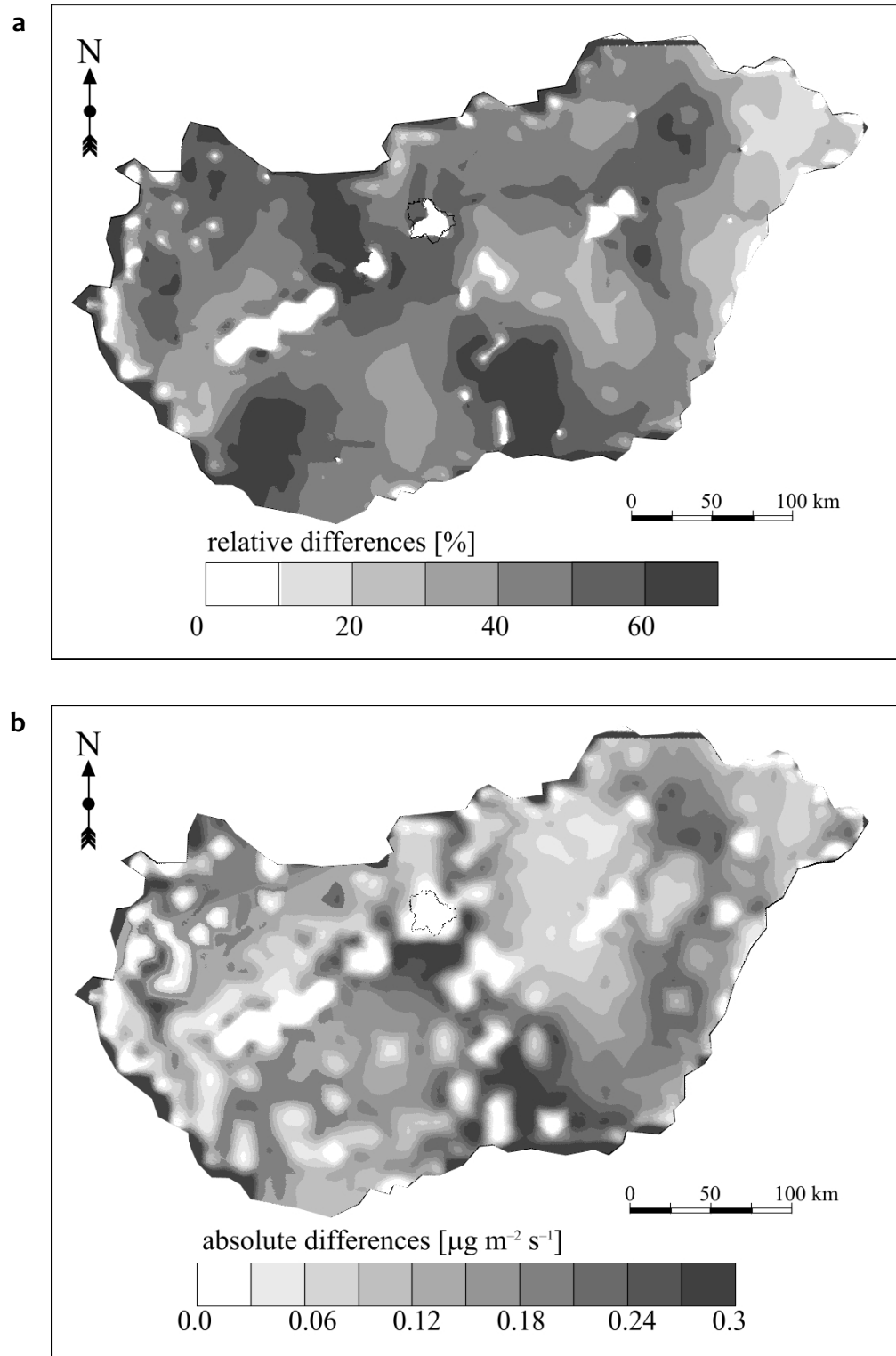
Szinyei D.[1,2], Gelybó Gy.[3], Guenther A. B.[4,5], Turnipseed A. A.[6], Tóth E.[3], Builtjes P. J. H.[7,8]

[1] MTA-PE Air Chemistry Research Group, University of Pannonia, Egyetem u. 10, 8200, Veszprém, Hungary

[2] Department of Geology and Meteorology, University of Pécs, Ifjúság útja 6, 7624, Pécs, Hungary

[3] Institute for Soil Sciences and Agricultural Chemistry, Centre for Agricultural Research, Hungarian Academy of Sciences, Herman Otto 15 út, 1022, Budapest, Hungary

[4] Pacific Northwest National Laboratory, Richland WA 99352, USA

[5] Department of Civil and Environmental Engineering, Washington State University, Pullman WA 99163, USA

[6] Atmospheric Chemistry Division, National Center for Atmospheric Research, P.O. Box 3000, Boulder, CO 80307-3000, USA

[7] TNO Built Environment and Geosciences, Air Quality and Climate Team, Princetonlaan 6, 3508 TA, Utrecht, The Netherlands

[8] Institute of Meteorology, Freie Universität Berlin, Carl-Heinrich-Becker Weg 6-10, 12165, Berlin, Germany

Abstract

The sophisticated interactions among atmospheric chemistry, ecosystem-, and climate processes are currently not represented in models in their full complexity. Emission and atmospheric processing of pollutants with anthropogenic origin is a high research priority due to their effect on the terrestrial biosphere and direct and indirect climatic forcing. However, large scale applications of surface-atmosphere exchange of reactive gases requires modelling results as accurate as possible to avoid nonlinear accumulation of errors in the spatially representative results. In this paper evaluation and comparison of three different modelling schemes of ozone gas deposition against measured data over a coniferous forest at Niwot Ridge AmeriFlux site (Colorado, USA) is carried out. Results show that in all three cases, model performance varies with time of the day, and the errors show a pronounced seasonal pattern as well. In order to explore possible reasons for model errors, we evaluated the driving variables of ozone deposition for hourly, daily

and monthly time steps based on measured ozone flux data at the study site. The results showed that measured gross primary production and ozone flux have a strong correlation although this relationship is not included in any of the investigated formulas of ozone deposition calculation.

Keywords
ozone fluxes, deposition model, big leaf models, coniferous forest, GPP

1. Introduction

Air quality monitoring and modelling is important not only to quantify the environmental stress on human health but also to understand the impact on terrestrial ecosystems. Many relevant studies, using field measurements and/or model results, have reported that tropospheric ozone can influence the health of the ecosystem (namely, Fares et al. [1], Loreto and Fares [2]). Ozone (O_3) like some other trace gases passes through the stomata into the mesophyll cells of plants and is toxic since it reacts with the liquid components of the apoplast to create reactive oxygen species [3]. These can oxidize the cell walls to start a cascade of reactions which lead, at the final stage, to cellular death [3]. Karnosky et al. [4, 5] reported significant ecosystem scale responses to elevated carbon dioxide (CO_2) and O_3 levels in the Aspen FACE Experiment. The changes were reflected in several ecosystem properties, including photosynthesis. Their results suggest that elevated O_3 at relatively low concentrations can significantly reduce the growth enhancement by elevated CO_2.

As forests can be long-term sinks of carbon [6], they play a key role in terrestrial ecosystem – atmosphere interactions. Any productivity changes caused e.g. by detrimental effects of the ozone can have serious effects on atmospheric CO_2 concentrations as well [7, 8]. Anav et al. [9] investigated the effects of tropospheric O_3 on photosynthesis and leaf area index on European vegetation using a land surface model (ORCHIDEE) coupled with a chemistry transport model (CHIMERE). Their results showed that the effect of ozone on vegetation leads to a reduction in yearly gross primary productivity (*GPP*) of about 22 % and a reduction in leaf area index (*LAI*) of 15–20 %. Decrease in *GPP* probably becomes more acute due to the harmful effect of tropospheric ozone as average global surface ozone concentration predicted to reach the amount of range of 38–71 ppb by 2060 and 42–84 ppb by 2100 compared to current annual average range of 20-45 ppb [10]. The resulting indirect radiative forcing by ozone effects on plants could contribute more to global warming than the direct radiative forcing of tropospheric ozone [11]. Therefore, investigation of ozone deposition has a high relevance especially in case of forests.

Although there is a global network of measurement sites (Ameriflux, Asiaflux, Euroflux) aiming at monitoring of fluxes of CO_2, a major greenhouse gas, this is not the

case with other trace gas flux and deposition measurements, where - especially continuous longterm - measurements are not common. For research aiming at the quantification of tropospheric ozone - climate feedbacks, reliable large scale information is required on ozone deposition. Besides direct flux measurements with limited availability and spatial representation, modelling efforts are of high importance, since they integrate field measurements of ozone concentration and fluxes to give a reliable estimation on ozone effects on ecosystems. Various 3-dimensional chemical transport models (CTMs) (e.g. AURAMS [12], CAMx [13], CHIMERE [14], EMEP MSC-W [15], GEOS-CHEM [16], LOTOS-EUROS [17], OFIS [18], RCG (RemCalGrid) [19], TAMP [20], WRF-CHEM [21] have been developed to estimate and investigate the environmental load of air pollutants. These models include embedded dry deposition modules (sub-models) that apply different approaches of parameterization schemes to calculate deposition of given trace gases or aerosols. The depositions models could be classified based on complexity of model in describing vegetation (one-, two- or multi-layered) and in the description and parameterization of exchange/deposition processes between the atmosphere and the surface (K-theory, higher order closure, non-local closure).

The choice is usually a compromise between application dependent requirements and data availability. The lack of measurements over different land use categories limits the validity of these modules [22].

The deposition velocity (v_d) which is commonly used to model or estimate deposition rate is defined in Eq. (1):

$$v_d = -\frac{F}{c} ,$$
(1)

where F is the atmosphere-surface flux of the given gas and (c) is the concentration of the given gas at a specified reference height [23]. Deposition velocity can be calculated as the reciprocal value of the residual of the resistances (analogous to Ohm's low for electricity) via parameterization of the aerodynamic (R_a), quasi-laminar boundary layer (R_b) and canopy resistance (R_c) where this latter term includes stomatal (R_{st}), mesophyll (R_{mes}), in-canopy (R_{inc}), cuticular (R_{cut}) and soil (R_{soil}) resistances. We describe resistance schemes later in Section 2.3. Most of the global models available in the literature estimate ozone deposition using the resistance analogy as well e.g. [11], and calculate the stomatal resistance using multiplicative algorithms as a function of meteorological parameters [24] or use physiological schemes, which link stomatal resistance to photosynthesis, so-called BWB-algorithm (Ball-Woodrow-Berry) [25]. There are few studies aiming to compare ozone deposition modules based on different approaches [26, 27], some studies compare different algorithms to estimate stomatal resistance [28, 29, 30, 31, 32], but a systematic comparative analysis of models is still lacking.

Therefore in this study three dry deposition models, all routinely applied in regional CTMs and characterized by different deposition schemes are evaluated. For the

evaluation of model results, measured ozone flux data were used for different time scales over the vegetation period. Since these ozone deposition models are widely used for estimation of ozone deposition over large areas e.g. [33] it is important to investigate model applicability over different land use categories (LUCs). We choose a land use category (LUC), for which none of the investigated models were calibrated. In order to explore discrepancies in results caused purely by the different deposition schemes, other basic parts of the models (not related to the deposition module, e.g. parameterization of meteorological variables) were standardized. The main questions addressed by this work are: (i) What environmental factors have impact on measured ozone deposition at the study site? (ii) What are the weaknesses of the investigated modules and how could they be improved?

The detailed in-depth evaluation of the discrepancies and their causes give an objective evaluation of performances of deposition schemes, and designate the direction of further improvements of the ozone deposition models.

2. Material and methods

2.1. Site description

For this study a six month dataset for the Niwot Ridge AmeriFlux site (Colorado, US) in the Roosevelt National Forest in the Rocky Mountains (40°1'58.4" N, 105°32'47.0" W, 3050 m a.s.l.) was used. Since the site lies on the hillside, the mountain-valley wind can effect meteorological parameters significantly. The soil of this site is mostly a glacial till, extremely rocky (granite) consisting primarily of mineral clays covered with a surface layer of organic material. During May (spring) when the annual snowmelt occurs the soils are fairly saturated with melt water. The mountain–valley winds predominate at this site (Figure 1), upslope flows from the east occur on many summer afternoons bringing high concentrations of anthropogenic pollutants, including ozone, from the Denver/Boulder Metropolitan area and have a profound effect on atmospheric ozone dynamics [34]. Table 1 contains the descriptive parameters of this site.

2.2. Measurements

2.2.1. Data used in the study

The main aim of this study is to evaluate different modelling schemes of ozone deposition over a coniferous forest ecosystem. Continuous ozone flux and meteorological measurements above a subalpine forest canopy (*Pinus contorta, Picea engelmannii, Abies lasiocarpa*) were carried out during the growing season (May-October) of 2003 at 21.5 m

height. Effect of short term variations in meteorological parameters has already been discussed in a previous publication [34]. The ozone flux was measured using the eddy-covariance (EC) technique above the canopy, detailed description of the experiment can be found in Monson et al. (2002) and Turnipseed et al. (2002, 2003, 2009). The meteorological data (air temperature (T), vapour pressure deficit (VPD), soil water content (SWC), photosynthetically active radiation (PAR), global radiation (SR) measurements), carbon-dioxide (CO_2) flux, gross primary productivity (GPP), net ecosystem exchange (NEE) data and additional information were obtained from Ameriflux (cdiac.ornl.gov/ftp/ameriflux/data/). Due to the lack of in-situ measurements of soil water retention, the value of wilting point (0.169 m^3m^{-3}) and field capacity soil moisture (0.396 m^3m^{-3}) were taken from the IGBP-DIS database (Global Gridded Surfaces of Selected Soil Characteristics (International Geosphere-Biosphere Programme - Data and Information System)) [35].

2.2.2. Data processing and quality assurance

Quality assurance of measured ozone flux data were carried out. Positive fluxes were not taken into account (ozone flux toward the ecosystem is negative by definition). After filtering the ozone flux data, the dataset contains 4013 records of the initially available 5243 half hourly values (23 % of the data being omitted) and 24 % of carbon-dioxide fluxes were excluded (initially 7142 data, after filtering 5395). Flux data were omitted during periods of precipitation and very low turbulence intensity where friction velocity (u^*) is less than 0.2 ms^{-1} after Coyle et al. [36], Hollinger and Richardson [37] and Turnipseed et al. [34]. In the case where data were available for more than 70 % of the day, gap filling of measured ozone flux was performed using monthly mean diurnal variations technique [38]. Daily accumulated ozone fluxes and daily averages of environmental parameters were calculated to eliminate the effect of diurnal variations of wind direction due to the mountain-valley wind system.

2.3. Modelling

The investigated dry deposition models are described in detail in Zhang et al. [39] (the ZHANG model), and in Stern [19] and in Schaap et al. [17] the DEPosition of Acidifying Compounds (DEPAC) model). These models are routinely applied in studies using regional CTMs that are described in the literature and applied over large spatial extents [40, 41], therefore it is important to examine the accuracy of their estimations. The ZHANG model is the deposition submodel of AURAMS CTM [12], and DEPAC is applied in RCG [19] and in LOTOS-EUROS [17] CTMs. Models were tested in site-specific mode, which employs local vegetation parameters and in situ meteorological observations as input data.

Alternatively, the investigated models can be run in regional mode, using the default vegetation parameters, even though these deposition models are not validated for all types of LUCs described by the simulations.

The dry deposition models are vertical (one-dimensional), one-layered models based on the so-called big-leaf concept as the canopy is treated as one big leaf surface and deposition velocity is calculated using resistance analogy:

$$v_d = \frac{1}{R_a + R_b + R_c} . \tag{2}$$

The differences in the schemes occur in parameterization of these resistances (Table 2). Calculation of R_a is very similar in both models, the ZHANG model uses the formula presented in Padro et al. [42] and the DEPAC model uses the parameterization of Wesely and Hicks [43]. R_b is parameterized using the same formula [44] in both models. To estimate R_c the following equations were used in the 'ZHANG model' Eq. 3 [39], and in the DEPAC model Eq. 4 [45]:

$$\frac{1}{R_c} = \frac{1 - W_{st}}{R_{st} + R_{mes}} + \frac{1}{R_{cut}} + \frac{1}{R_{inc} + R_{soil}} , \tag{3}$$

$$\frac{1}{R_c} = \frac{1}{R_{st} + R_{mes}} + \frac{1}{R_{cut}} + \frac{1}{R_{inc} + R_{soil}} , \tag{4}$$

where W_{st} is the fraction of stomatal blocking under wet conditions, and is calculated as:

$$W_{st} = \begin{cases} 0, & SR \leq 200\,\mathrm{Wm}^{-2} \\ \frac{(SR - 200)}{800}, & 200 \leq SR \leq 600\,\mathrm{Wm}^{-2} \\ 0.5, & SR > 600\,\mathrm{Wm}^{-2} \end{cases} . \tag{5}$$

One of the main differences between the models is the parameterization of stress functions of R_{st} (Table 2). The ZHANG model calculates R_{st} as described in Zhang et al. [27, 39], meanwhile DEPAC model has two different parameterizations for the stomatal resistance based on Baldocchi et al. [46] (referred to here as the DEPAC-Baldocchi model) and Wesely [47] (referred to here as the DEPAC-Wesely model), therefore three different modules are used in this study. Both the ZHANG model and the DEPAC-Baldocchi model calculate R_{st} using functions of air temperature ($f(T)$), vapor pressure deficit ($f(VPD)$) but water stress is described in different ways (for detailed description of model equations see Table 2). In the case of optimum environmental conditions, the canopy stress

functions are equal to one, representing no stress. In the ZHANG model water stress ($f(\psi)$) is a step function of leaf water potential, meanwhile in the DEPAC-Baldocchi model soil water stress ($f(\theta)$) has a constant value. In the DEPAC-Wesely model R_{st} depends on T and SR seasonally. During nighttime in all models, R_{st} has a high constant value of 12500 s m^{-1}, representing the closed stomata. R_{mes} has constant zero value in all models [39, 47]. In the ZHANG model R_{cut} depends on LAI, u^*, relative humidity (RH) and below a given temperature it is increasing as a function of temperature [39]. In the DEPAC model R_{cut} is constant [45]. R_{inc} depends on LAI and u^* in the ZHANG model [39] and depends on h, LAI and u^* in the DEPAC model [48]. R_{soil} has a constant value, but below a certain temperature this value changes as a function of temperature (the ZHANG model) [39] or has another constant value (the DEPAC model) [45].

Finally, model parameterization improvements were carried out. Many studies have shown that soil moisture is an important factor for controlling stomatal activity [49, 50]. It has been shown previously and also acknowledged in the literature that resistance based models are sensitive to moisture stress parameterization [51, 32]. Soil moisture content data is easy to obtain compared to the leaf water potential used in some modelling approach. Since none of the investigated models use soil moisture in the parameterization of stomatal resistance, model improvements were carried out (the ZHANG modified model and the DEPAC-Baldocchi modified model later on) with the introduction of a soil moisture ($f(\theta)$ in Eq. 6 stress function based on the work of e.g. Mészáros et al. [52] and Grünhage and Haenel [53]. The stress function introduced in the models for SWC is as follows:

$$f(\theta) = \begin{cases} 1 & \text{if } \theta > \theta_f \\ \max\left\{\dfrac{\theta - \theta_w}{\theta_f - \theta_w}, 0.05\right\} & \text{if } \theta_w < \theta \leq \theta_f \\ 0.05 & \text{if } \theta \leq \theta_w \end{cases} \quad , \tag{6}$$

where θ_w and θ_f denote soil moisture content corresponding to the wilting point and the field capacity, respectively.

To explore the performance of the different resistance schemes of the investigated models without influence of parameterization of environmental parameters, measured meteorological variables were used when it was possible and meteorological and astronomical parameterizations (e.g. characteristics of moist air and solar radiation) were synchronized using one common scheme in all other cases. Vapour pressure deficit was calculated using the approach of the World Meteorological Organization [54], density of moist air, specific heat of moist air was estimated after Grünhage and Haenel [53]. Solar zenith angle was calculated using the parameterization scheme provided by NASA [55].

2.4. Evaluation methodology

2.4.1. Measurement evaluation

In the first part of this work, analyses of in situ observations were carried out to explore the effect of environmental factors on ozone deposition. Climate impact studies and ecosystem studies are mainly focused on the accumulated pollutant load the ecosystem receives, i.e. the ozone uptake, to be able to qualitatively evaluate/predict its effect on photosynthetic activity [56, 57, 58].

We examined soil moisture, global radiation, photosynthetically active radiation, vapor pressure deficit and temperature as abiotic controlling factors of ozone flux, and *GPP*, *NEE* as biotic controlling factors. Half hourly measurements were quality checked and analyzed for the whole six month long period for changes in relationships between ozone fluxes and ozone deposition drivers throughout the vegetation season (May-October).

Besides abiotic environmental controls, we investigated how vegetation activity affects the ozone deposition. Daily accumulated ozone fluxes were compared to daily CO_2 exchange (mg C m^{-2} day^{-1}).

2.4.2. Model evaluation

In the second part of our study outputs of three deposition models were compared to measured ozone fluxes. Different model quality indicators were calculated to evaluate model performance using half hourly data on monthly and six months long time scale (Table 4). The statistical metrics used in this study (Pearson linear correlation coefficient (*R*), mean bias (*MB*), mean absolute error (*MAE*), root mean square error (*RMSE*), normalized mean square error (*NMSE*), index of agreement (*IA*) and modeling efficiency (*ME*) indicators) were calculated for the whole period both for daytime (when the solar zenith angle is greater than zero) and nighttime (when the solar zenith angle is less than or equal to zero). The equations of these metrics are given below [59, 60, 61, 62]:

$$R = \frac{\sum_{i=1}^{N}(O_i - \overline{O})(M_i - \overline{M})}{\sqrt{\sum_{i=1}^{N}(O_i - \overline{O})^2 \sum_{i=1}^{N}(M_i - \overline{M})^2}} \, , \tag{7}$$

$$MB = \frac{1}{N}\sum_{i=1}^{N}(O_i - M_i), \tag{8}$$

$$MAE = \frac{1}{N}\sum_{i=1}^{N}\left|M_i - O_i\right|, \tag{9}$$

$$RMSE = \sqrt{\frac{1}{N}\sum_{i=1}^{N}\left(M_i - O_i\right)^2}, \tag{10}$$

$$NMSE = \frac{\frac{1}{N}\sum_{i=1}^{N}\left(M_i - O_i\right)^2}{\overline{O}\cdot\overline{M}}, \tag{11}$$

$$IA = 1 - \frac{\sum_{i=1}^{N}\left(O_i - M_i\right)^2}{\sum_{i=1}^{N}\left(\left|O_i - \overline{O}\right| + \left|M_i - \overline{O}\right|\right)^2}, \tag{12}$$

$$ME = 1 - \frac{\sum_{i=1}^{N}\left(O_i - M_i\right)^2}{\sum_{i=1}^{N}\left(O_i - \overline{O}\right)^2}, \tag{13}$$

where O_i and M_i are the observed and modelled time series, overbar represents averages of observed or modelled data over the dataset, N the total number of data. R is the linear correlation between the observations and model results, values can vary between −1 and 1 (perfect correlation), 0 means the datasets are independent. MB is a measure of overall bias for variables, in case of perfect estimation it is 0. MAE is overall absolute bias of observed and modelled data and is less influenced by large errors and does not depend on the mean bias. $RMSE$ is the square root of the average squared bias of the modelled data, it is sensitive for extreme errors. $NMSE$ emphasizes the scatter in the entire data set since the deviations are summed instead of the differences. Smaller values of $NMSE$ denote better model performance. IA can vary between 0 and 1 and it is a metric of mean square error, in case of perfect agreement it is equal 1. ME has a range from 1 to −∞, and is a measure of the accuracy of model estimations to the mean of observations, any positive value means that estimation is better than means of measurements, in case of perfect agreement it is equal 1.

To explore the error dependency on environmental factors the daily mean absolute bias of measured and modeled ozone fluxes were compared to the daily mean of measured meteorological inputs.

3. Results and discussion

3.1. Measurements

In order to explore the effect of environmental factors on ozone deposition, relationships between environmental variables and CO_2 and energy fluxes were examined on a daily basis and on the original half hourly resolution using EC data. Daily mean of meteorological conditions (*T*, *SWC*, *VPD*) and daily sums of fluxes (*GPP*, *NEE*, *SR*, *PAR*) were compared against daily sums of ozone flux ($\mu mol\,m^{-2}\,day^{-1}$) to detect the most significant long-term drivers of ozone deposition.

3.1.1. Biotic controlling factors of ozone fluxes

The results showed that *GPP* and measured accumulated ozone flux are correlated for the whole period (Figure 2, R^2 = 0.33, p < 0.001) although this relationship is not included in any of the formulas of ozone deposition calculation. It is clarified by many authors in the literature that methods which calculate stomatal resistance as a function of photosynthetic rate can estimate stomatal resistances with higher accuracy [29, 30], so the relationship of gross primary production on ozone deposition should be considered as a way to improve these formulas. It should be mentioned that some studies have concluded that for present-day applications there is no obvious advantage in replacing the multiplicative with a BWB-algorithm for regional scale ozone deposition modelling schemes, but to include the influence of rising CO_2 concentrations and changing climate conditions might favour the photosynthesis-based algorithm [28].

Half hourly measured abiotic factors (*GPP*, *NEE*, CO_2 flux) were compared to half hourly measured ozone fluxes. Coefficients of determination are presented in Table 4 for the six month long time scale.

The strongest correlation was found with *GPP* (R^2 = 0.26, p < 0.001; Figure 3), although there is a relationship between ozone flux and *NEE* (R^2 = 0.21, p < 0.001) as well. The strong relationship with *GPP* can be explained by the fact that *GPP* is the gross CO_2 uptake which has a close relationship with ozone uptake due to both being under stomatal control. Note that only total ozone fluxes were used in this study, it was not partitioned to stomatal and non-stomatal components, they were not investigated separately, so there might be other effects superimposed on this relationship.

3.1.2. Abiotic controlling factors of ozone fluxes

Half hourly measured meteorological data were compared (*T, SWC, VPD, SR, PAR*) with half hourly measured ozone fluxes (Table 4). The examination of the relationship between ozone flux and abiotic drivers, such as *T, VPD* showed very poor correlation for the vegetation growing season (May-October) (R^2 = 0.012, p < 0.001 and R^2 = 0.05, p < 0.001 respectively)). The reason for this poor correlation is probably due to environmental conditions, such as temperature, being mostly in the optimal range during the season (between the minimum and the maximum values (Table 2 and 3)).

No relationship was found in case of *SWC*, which apparently was not a limiting factor for ozone deposition in the vegetation growing season of 2003 (R^2 < 0.02, p < 0.001). The soil moisture measured at 15 cm is probably not representative for the root zone at the study site (being a forest), therefore it does not reflect the moisture stress the vegetation receives. On the other hand, the soil at the site is more or less saturated with water during the vegetation growing season, therefore soil moisture is probably not a limiting factor during this particular study period.

In the case of *SR* and *PAR* the correlation is also very low (R^2 < 0.1, p < 0.001 for both factors) in the whole vegetation growing season. This indicates that radiation is not the main long-term driving factor of ozone deposition at Niwot Ridge for the measurement period.

3.2. Models

Model results were investigated on half hourly and daily time steps and model performance indicators were calculated based on measured and modelled ozone flux data.

The ZHANG model outperformed the other two model versions on the original half-hourly resolution, but one should be aware of the still poor correlation between measured and modelled ozone flux for the whole period (Table 5). In order to evaluate the average behaviour of models and how their performance varies with time of the day, mean diurnal variations of measured and modeled ozone fluxes were calculated. The ZHANG model provided the best results in capturing the ozone flux magnitude and dynamics as shown by mean diurnal variation (Figure 4A). The ZHANG modified model in Figure 4A will be addressed later in the paper.

The performances of the two versions of the DEPAC model stay below that of the ZHANG model as it is reflected by all model quality indicators listed in Table 5. Correlation is lower, the DEPAC-Baldocchi and the DEPAC-Wesely parameterization can only explain 15% and 7% of the observed variance. Model errors are significantly higher in case of the DEPAC-Baldocchi parameterization. It should be noted that although DEPAC-Wesely can explain even less of the observed variance of half hourly ozone deposition, its performance is comparable to that of the ZHANG model based on some other statistical measures (IA, ME, NMSE, RMSE).

Mean diurnal variation of ozone deposition modeled by different parameterizations of the DEPAC model are shown on Figure 5A together with measured ozone deposition. The DEPAC-Baldocchi model overestimates the measured fluxes (as also indicated by statistics based on the full half-hourly dataset, shown in Table 5). The most important difference between the ZHANG and DEPAC models lies in the parameterization of R_{st}. It has been reported by Mészáros et al. [52] that deposition models are sensitive to soil moisture content input. The soil moisture stress is not parameterized in the DEPAC-Baldocchi model, $f(\theta)$ has a fixed values of one, which assumes there is no water stress for the canopy. So, these results show that it is essential to include the soil moisture in the dry deposition models, consequently, the ZHANG model is to be preferred above the DEPAC models.

As it is presented on Figure 5A the DEPAC-Wesely model underestimates the measured fluxes, although model error is lower than in case of the DEPAC-Baldocchi parameterization (Table 5). The DEPAC-Baldocchi modified model in Figure 5A will be discussed later in the paper.

To explore if models capture long-term variabilities, monthly means of ozone fluxes were calculated (Figure 6). We separated data to daytime (Figure 6A) and nighttime (Figure 6B) parts, since the modeling approach is different for nighttime conditions (see Table 2). The calculated nighttime ozone deposition data reveal a very good agreement with measured flux (Figure 6B). Considering that nighttime ozone fluxes are mostly cuticular or soils, this good performance compared to the daytime performance of the models suggest that mostly the description of stomatal uptake is responsible for model errors. For observed ozone flux during nighttime, the DEPAC-Baldocchi model and the DEPAC-Wesely model results in the same values since the parameterizations are the same for nighttime conditions. For daytime data where stomatal resistance is calculated using the more sophisticated approach described in Table 2, the model performances diverge more. The relatively simple parameterization of the DEPAC-Wesely model simulated monthly average ozone deposition with the smallest bias in each month except June. It should be kept in mind, however, that only measured ozone flux data is considered here, i.e. this is not real average ozone deposition but the monthly average of available measured data.

The motivation for modeling ozone deposition is to simulate ozone load that the ecosystem receives on longer time scales. Therefore, model results were examined on a daily time step using accumulated ozone fluxes to simulate ozone load (Figure 4B, Figure 5B). This approach is used in most large scale studies. Results of the ZHANG model have a good correlation with measured accumulated ozone fluxes ($R^2 = 0.23$, $p < 0.05$, Table 6), but in case of DEPAC-Baldocchi, the model correlation cannot be detected ($R^2 = 0.05$, $p = 0.144$, Table 6).

This contradicting behaviour of three structurally identical models demonstrates the need for a careful interpretation of resistance based model results for sites where previous results reported in the literature regarding correlation and systematic model

errors. The performance of the ZHANG model has been evaluated for certain land use types (deciduous-forest, mixed-forest, grassland and vineyard) with R^2 = 0.14-0.51 in summertime using 1-3 month long datasets [27]. They showed that the model overestimated measurements in general, but in the case of mixed forest they found a slight underestimation in the early morning hours. Büker et al. [28] found a correlation (R^2) of 0.3 and overestimation for birch and an R^2 of 0.67 and underestimation for beech again, indicating the site specific behaviour of models. The evaluation of the DEPAC model was carried out for sulfur-dioxide over deciduous-forest, coniferous-forest, grassland and heathland with R^2 = 0.01-0.69 for wet and dry conditions using 1-10 months long datasets [45].

Results of the ZHANG modified model (Figure 4A) has a lower correlation (R^2 = 0.09, p < 0.001 instead of 0.26 in Table 5) with measurements using the full half hourly dataset, and RMSE value did not change (4.69 nmol m^{-2} s^{-1}). In case of the DEPAC-Baldocchi modified model (Figure 5A) R^2 decreased (0.05, p < 0.001 instead of 0.15 in Table 5), parallel RMSE decreased almost by half compared to the original parameterization (4.66 nmol m^{-2} s^{-1} versus 10.07 nmol m^{-2} s^{-1}). On a daily time step the DEPAC-Baldocchi modified model results showed better correlation with measured accumulated ozone fluxes than the original model (R^2 = 0.06, p = 0.140; Figure 5B). Comparing Figure 4B and Figure 5B we can conclude that the modified model results values are very similar, minimal differences can be detected. This can be explained by non-stomatal resistance (R_{cut}, R_{inc} and R_{soil}), since with implementation of $f(\theta)$ R_{st} has the same value in both modified models.

Mészáros et al. [52] carried out a sensitivity analysis of a multiplicative dry deposition model and found that soil moisture content is one of the most influential parameter in the model. This explains why the introduction of soil moisture stress parameterization in the DEPAC-Baldocchi model had such a dramatic effect on model results. However, as indicated by measurements, soil moisture was not a driving factor for ozone deposition at this site in the measurement period. This suggests that model constraints do not reflect real environmental circumstances, i.e. model results agree with measured ozone fluxes, but the model fails to explain short-term variability of ozone deposition, which led to a decrease in correlation between half hourly measured and modelled ozone fluxes. The use of soil moisture content data representative for the whole root zone when available, should improve model results.

4. Conclusion

In this study ecosystem-atmosphere ozone flux and its relation to environmental and ecosystem variables measured on site was examined, and simulated using three widely used deposition models. Due to the meteorological conditions climate of the site and the relatively short study period, we found no statistical correlation between environmental

variables and ozone deposition. Therefore, the effect of environmental drivers on ozone deposition as simulated in the models could not be fully evaluated against observations. Significant correlation was found, however between GPP and ozone flux, reflecting its relation to stomatal activity. This relation however is not included in any of the investigated models directly.

In spite of their wide acceptance [63, 64], the multiplicative models used in this study have not been tested for some important land cover types e.g. none of the above models have been tested for evergreen forests. In studies where these models are applied on large spatial scales, continents, countries [65, 66, 12] this can bias the results. Our study showed that even if we minimize input data errors using measured driving data when available, model results diverge when validated for a randomly selected geographical location and land use type. This suggests that in their current form these models are not adequate for all situations and reliable large scale modelling.

Our results showed, that the lack of calibration inhibits the use of these models in case of ecosystem types other than they have been calibrated for, and hence, their practicality in large scale studies where models are used over several ecosystems might be questionable. It was also shown that the ZHANG model is to be preferred especially when soil moisture is expected to be limiting and to be a driver of ozone deposition. Further investigations are required to optimize the model performance across ecosystems and scales.

Acknowledgement

The authors declare that there is no conflict of interests regarding the publication of this paper.

References

[1] S. Fares, R. Vargas, M. Detto et al., "Tropospheric ozone reduces carbon assimilation in trees: estimates from analysis of continuous flux measurements," *Global Change Biology*, vol. 19, no. 8, pp. 2427–2443, 2013.

[2] F. Loreto and S. Fares, "Is Ozone Flux Inside Leaves Only a Damage Indicator? Clues from Volatile Isoprenoid Studies," *Plant Physiology*, vol. 143, no. 3, pp. 1096–1100, 2007.

[3] S. Fares, A. Goldstein, and F. Loreto. "Determinants of ozone fluxes and metrics for ozone risk assessment in plants," *Journal of Experimental Botany*, vol. 61, no. 3, pp. 629–633, 2010.

[4] D. F. Karnosky, D. R. Zak, K. S. Pregitzer, and C. S. Awmack, "Tropospheric O3 moderates responses of temperate hardwood forests to elevated CO2: a synthesis of molecular to ecosystem results from the Aspen FACE project," *Functional Ecology*, vol. 17, no. 3, pp. 289–304, 2003.

[5] D. F. Karnosky, K. S. Pregitzer, and D. R. Zak, "Scaling ozone responses of forest trees to the ecosystem level in a changing climate," *Plant, Cell and Environment*, vol. 28, no. 8, pp. 965–981, 2005.

[6] Y. Pan, R. A. Birdsey, J. Fang et al., "A Large and Persistent Carbon Sink in the World's Forests," *Science*, vol. 333, no. 6045, pp. 988–993, 2011.

[7] M. R. Ashmore, "Assessing the future global impacts of ozone on vegetation," *Plant, Cell and Environment*, vol. 28, no. 8, pp. 949–964, 2005.

[8] J. Klingberg, M. Engardt, J. Uddling, P. Karlsson, and H. Pleijel, "Ozone risk for vegetation in the future climate of Europe based on stomatal ozone uptake calculations," *Tellus A*, vol. 63, no. 1, pp. 174–187, 2011.

[9] A. Anav, L. Menut, D. Khvorostyanov, and N. Viovy, "Impact of tropospheric ozone on the Euro-Mediterranean vegetation," *Global Change Biology*, vol. 17, no. 7, pp. 2342–2359, 2011.

[10] R. Vingarzan, 2004: "A review of surface ozone background levels and trends," *Atmospheric Environment*, vol. 38, no. 21, pp. 3431–3442, 2004.

[11] S. Sitch, P. M. Cox, W. J. Collins and C. Huntingford, "Indirect radiative forcing of climate change through ozone effects on the land-carbon sink," *Nature*, vol. 448, no. 7155, pp. 791–794, 2007.

[12] S. C. Smyth, W. Jiang, H. Roth, M. D. Moran, P. A. Makar, F. Yang, et al., "A comparative performance evaluation of the AURAMS and CMAQ air-quality modelling systems," *Atmospheric Environment*, vol. 43, no. 5, pp. 1059–1070, 2009.

[13] C. Emery, J. Jung, N. Downey et al., "Regional and global modeling estimates of policy relevant background ozone over the United States," *Atmospheric Environment*, vol. 47, pp. 206-217, 2012.

[14] L. Menut, B. Bessagnet, D. Khvorostyanov et al., "CHIMERE 2013: a model for regional atmospheric composition modelling," *Geosci. Model Dev.*, vol. 6, pp. 981–1028, 2013.

[15] D. Simpson, A. Benedictow, H. Berge, "The EMEP MSC-W chemical transport model – technical description," *Atmos. Chem. Phys.*, vol. 12, pp. 7825–7865, 2012.

[16] I. Bey, D. J. Jacob, R. M. Yantosca et al., "Global modeling of tropospheric chemistry with assimilated meteorology: Model description and evaluation," *J. Geophys. Res.*, vol. 106, no. D19, pp. 23073–23095, 2001.

[17] M. Schaap, R. M. A. Timmermans, M. Roemer et al. "The LOTOS–EUROS model: description, validation and latest developments,". *Int. J. Environment and Pollution*, vol. 32, no. 2, pp. 270–290, 2008.

[18] N. Moussiopoulos and I. Douros, "Efficient calculation of urban scale air pollutant dispersion and transformation using the OFIS model within the framework of CityDelta," *International Journal of Environment and Pollution*, vol. 24, nos. 1/2/3/4 pp. 64–74, 2005.

[19] R. Stern, "Das chemische Transportmodell REM-CALGRID. Model description," FU Berlin, p. 28, 2009. Online available: www.geo.fu-berlin.de/met/ag/trumf/RCG/RCG-Beschreibung.pdf?1373749582

[20] P. Hurley, "TAPM V4. Part 1: Technical Description," *CSIRO Marine and Atmospheric Research Paper*, no. 25, p. 59, 2008.

[21] G. A. Grell, S. E. Peckham, R. Schmitz et al., "Fully coupled 'online' chemistry in the WRF model," *Atmospheric Environment*, vol. 39, no. 37, pp. 6957–6976, 2005.

[22] J-P. Tuovinen, "Ozone flux modelling for risk assessment: status and research needs," *iForest – Biogeosciences and Forestry*, vol. 2, no.1, pp. 34–37, 2009. Online available: www.sisef.it/iforest/show.php?id=485

[23] A. C. Chamberlain, "Transport of Lycopodium Spores and Other Small Particles to Rough Surfaces," *Proceedings of the Royal Society of London, Series A, Mathematical and Physical Sciences*, vol. 296, no. 1444, pp. 45–70, 1967.

[24] P. G. Jarvis, "The interpretation of the variations in leaf water potential and stomatal conductance found in canopies in the field, " *Philosophical Transactions of the Royal Society of London*, vol. B 273, no. 927, pp. 593–610, 1976.

[25] J. T. Ball, I. E. Woodrow, and J. A. Berry, "A model predicting stomatal conductance and its contribution to the control of photosynthesis under different environmental conditions," In: J. Biggens (ed.), "Progress in Photosynthesis Research," vol. IV. Martinus Nijhoff, Dordrecht, pp. 221–224, 1987.

[26] T. P. Meyers and D. D. Baldocchi,"A comparison of models for deriving dry deposition fluxes of O_3 and SO_2 to a forest canopy," *Tellus* B, vol. 40, no. 4, pp. 270–284, 1988.

[27] L. Zhang, M. D. Moran, P. A. Makar, J. R. Brook, and S. Gong, "Modelling gaseous dry deposition in AURAMS: a unified regional air-quality modelling system," *Atmospheric Environment*, vol. 36, no. 3, pp. 537–560, 2002.

[28] P. Büker, L. D. Emberson, M. R. Ashmore et al., "Comparison of different stomatal conductance algorithms for ozone flux modelling," *Environmental Pollution*, vol. 146, no. 3, pp. 726–735, 2007.

[29] L. Misson, J. A. Panek, and A. H. Goldstein, "A comparison of three approaches to modeling leaf gas exchange in annually drought-stressed ponderosa pine forests," *Tree Physiology*, vol. 24, no. 5, pp. 529–541, 2004.

[30] D. S. Niyogi, S. Raman, and K. Alapaty, "Comparison of Four Different Stomatal Resistance Schemes Using FIFE Data. Part II: Analysis of Terrestrial Biospheric–Atmospheric Interactions," *J. Appl. Meteor.*, vol. 37, no. 10, pp. 1301–1320, 1998.

[31] J. Uddling, M. Hall, G. Wallin, and P. E. Karlsson, "Measuring and modelling stomatal conductance and photosynthesis in mature birch in Sweden," *Agricultural and Forest Meteorology*, vol. 132, no. 1–2, pp. 115–131, 2005.

[32] M. T. Van Wijk, S. C. Dekker, W. Bouten et al. "Modeling daily gas exchange of a Douglas-fir forest: comparison of three stomatal conductance models with and without a soil water stress function, " *Tree Physiology*, vol. 20, no. 2, pp. 115–122, 2000.

[33] R. Vautard, P. H. J. Builtjes, P. Thunis et al., "Evaluation and intercomparison of Ozone and PM10 simulations by several chemistry transport models over four European cities within the CityDelta project," *Atmospheric Environment*, vol. 41, no. 1, pp. 173–188, 2007.

[34] A. A. Turnipseed, S. P. Burns, D. J. P. Moore, J. Hu, A. B. Guenther, and R.K. Monson, "Controls over ozone deposition to a high elevation subalpine forest,". *Agricultural and Forest Meteorology*, vol. 149, no. 9, pp. 1447–1459, 2009.

[35] D. P. Turner, W. D. Ritts, and M. Gregory, "BigFoot NPP Surfaces for North and South American Sites, 2002-2004," Data set from Oak Ridge National Laboratory Distributed Active Archive Center, Oak Ridge, Tennessee, USA, 2006. Online available: daac.ornl.gov

[36] M. Coyle, E. Nemitz, R. Storeton-West, D. Fowler, and J. N. Cape, "Measurements of ozone deposition to a potato canopy, " *Agricultural and Forest Meteorology*, vol. 149, no. 3–4, pp. 655–665, 2009.

[37] D. Y. Hollinger and A. D. Richardson, "Uncertainty in eddy covariance measurements and its application to physiological models," *Tree Physiol.*, vol. 25, no. 7, pp. 873–885, 2005.

[38] E. Falge, D. Baldocchi, R. Olson et al., "Gap filling strategies for defensible annual sums of net ecosystem exchange," *Agricultural and Forest Meteorology*, vol. 107, no. 1, pp. 43–69, 2001.

[39] L. Zhang, J. R. Brook, and R. Vet, "A revised parameterization for gaseous dry deposition," *Atmos. Chem. Phys.*, vol. 3, pp. 2067–2082, 2003.

[40] R. Stern, P. Builtjes, M. Schaap et al., "A model inter-comparison study focussing on episodes with elevated PM10 concentrations," *Atmospheric Environment*, vol. 42, no. 19, pp. 4567–4588, 2008.

[41] S. Cho, P. A. Makar, W. S. Lee et al., "Evaluation of a unified regional air-quality modeling system (AURAMS) using PrAIRie2005 field study data: The effects of emissions data accuracy on particle sulphate predictions," *Atmospheric Environment*, vol. 43, no. 11, pp. 1864–1877, 2009.

[42] J. Padro, G. den Hartog, and H. H. Neumann, "An investigation of the ADOM dry deposition module using summertime O_3 measurements above a deciduous forest, " *Atmospheric Environment, Part A. General Topics*, vol. 25, no. 8, pp. 1689–1704, 1991.

[43] M. L. Wesely and B. B. Hicks, "Some factors that effect the deposition rates of sulfur dioxide and similiar gases on vegetation," *J. Air Pollut. Control Assoc.*, vol. 27, no.11, pp. 1110–1116, 1977.

[44] B. B. Hicks, In: "Critical assessment document on acid deposition, " Chapter VII, Dry deposition, ATDL Contribution file 81/24, Atmospheric Turbulence and Diffusion Laboratory, NOAA, Oak Ridge, Tennessee, USA, 1982.

[45] J. Erisman, A. Van Pul, and P. Wyers, "Parameterization of surface resistance for the quantification of atmospheric deposition of acidifying pollutants and ozone," *Atmospheric Environment*, vol. 28, no. 16, pp. 2595–2607, 1994.

[46] D. D. Baldocchi, B. B. Hicks, and P. Camara, "A canopy stomatal resistance model for gaseous deposition to vegetated surfaces," *Atmospheric Environment*, vol. 21, no. 1, pp. 91–101, 1987.

[47] M. Wesely, "Parameterization of surface resistance to gaseous dry deposition in regional-scale, numerical models," *Atmospheric Environment*, vol. 23, no.6, pp. 1293–1304, 1989.

[48] W. A. J. Van Pul and A. F. G. Jacobs, "The conductance of a maize crop and the underlying soil to ozone under various environmental conditions," *Boundary Layer Meteorology*, vol. 69, no. 1–2, pp. 83–99, 1994.

[49] L. M. Bates and A. E. Hall, "Stomatal Closure with Soil-Water Depletion No Associated with Changes in Bulk Leaf Water Status," *Oecologia*, vol. 50, pp. 62–65, 1981.

[50] T. Gollan, J. B. Passioura, and R. Munns, "Soil-Water Status Affects the Stomatal Conductance of Fully Turgid Wheat and Sunflower Leaves," *Australian Journal of Plant Physiology*, vol. 13, pp. 459–464, 1986.

[51] P. Büker, T. Morrissey, A. Briolat et al., "DO3SE modelling of soil moisture to determine ozone flux to forest trees," *Atmos. Chem. Phys.*, vol. 12, 5537–5562, 2012.

[52] R. Mészáros, D. Szinyei, C. Vincze et al., "Effect of the soil wetness state on the stomatal ozone fluxes over Hungary," *Int. J. Environment and Pollution*, vol. 36, nos. 1/2/3, pp. 180–194, 2009.

[53] L. Grünhage and H.-D. Haenel, "PLATIN PLant-ATmosphere Interaction model," *Landbauforschung*, Special Issue 319, p. 85, 2008.

[54] World Meteorological Organization, "Guide to meteorological instruments and methods of observation," Geneva, Switzerland: Secretariat of the World Meteorological Organization, 2008.

[55] W. B. Landsman, In "Astronomical Data Analysis Software and Systems II," *A.S.P. Conference Series*, vol. 52, ed. R. J. Hanisch, R. J. V. Brissenden, and Jeannette Barnes, p. 246, 1993.

[56] H. Harmens and G. Mills, "Ozone pollution: Impacts on carbon sequestration in Europe," ICP Vegetation Programme Coordination Centre. CEH Bangor, UK, ISBN: 978-1-906698-31-7, 2012.

[57] D. Lombardozzi, S. Levis, G. Bonan and J. P. Sparks, "Predicting photosynthesis and transpiration responses to ozone: decoupling modelled photosynthesis and stomatal conductance," Biogeosciences, vol. 9, no. 8, pp. 3113–3130, 2012.

[58] H. Tang, J. Pang, G. Zhang et al., "Mapping ozone risks for rice in China for years 2000 and 2020 with flux-based and exposure-based doses," Atmospheric Environment, vol. 86, pp. 74–83, 2014.

[59] J. Neter, W. Wasserman, and G. A. Whitmore, "Applied statistics," Allyn and Bacon, Inc., 3rd edition, p. 1006, 1988.

[60] J. C. Chang and S. R. Hanna, "Air quality model performance evaluation," *Meteorol Atmos Phys*, vol. 87, no. 1–3, pp. 167–196, 2004.

[61] A. R. Pereira, "The Priestley–Taylor parameter and the decoupling factor for estimating reference evapotranspiration", *Agricultural and Forest Meteorology*, vol. 125, no. 3–4, pp. 305–313, 2004.

[62] E. Falge, S. Reth, N. Brüggemann et al., "Comparison of surface energy exchange models with eddy flux data in forest and grassland ecosystems of Germany, "*Ecological Modelling*, vol. 188, no. 2–4, pp. 174–216, 2005.

[63] J. R. Brook, L. Zhang, Y. Li, and D. Johnson, "Description and evaluation of a model of deposition velocities for routine estimates of dry deposition over North America. Part II: review of past measurements and model results," *Atmospheric Environment*, vol. 33, no. 30, 5053–5070, 1999.

[64] J. Flemming and R. Stern, "Testing model accuracy measures according to the EU directives – examples using the chemical transport model REM-CALGRID," *Atmospheric Environment*, vol. 41, no. 39, pp. 9206–9216, 2007.

[65] A. Manders, E. van Meijgaard, A. Mues, R. Kranenburg, L.H. van Ulft, and M. Schaap, "The impact of differences in large-scale circulation output from climate models on the regional modeling of ozone and PM," *Atmospheric Chemistry and Physics*, vol. 12, 9441–9458, 2012.

[66] M. van Loon, R. Vautard, M. Schaap et al., "Evaluation of long-term ozone simulations from seven regional air quality models and their ensemble, "*Atmospheric Environment*, vol. 41, pp. 2083–2097, 2007.

[67] R. K. Monson, A. A. Turnipseed, J. P. Sparks et al., "Carbon sequestration in a high-elevation subalpine forest," *Global Change Biology*, vol. 8 no. 5, pp. 1–20, 2002.
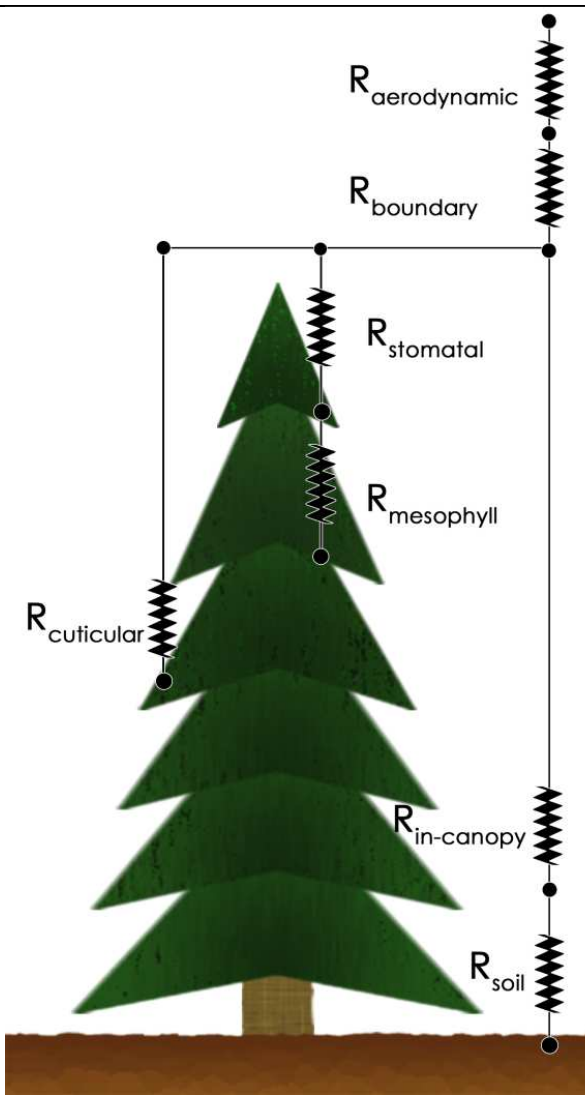
[68] A. A. Turnipseed, P. D. Blanken, D. E. Anderson, and R.K. Monson, "Energy budget above a high-elevation subalpine forest in complex topography," *Agricultural and Forest Meteorology*, vol. 110, no. 3, pp. 177–201, 2002.

[69] A. A. Turnipseed, D. E. Anderson, P. D. Blanken, W. Baugh, R. K. Monson, "Airflows and turbulent flux measurements in mountainous terrain. Part 1. Canopy and local effects," *Agricultural and Forest Meteorology*, vol. 119, no. 1–2, pp. 1–21, 2003.

[70] M. New, D. Lister, M. Hulme, and I. Makin, "A high-resolution data set of surface climate over global land areas," *Climate Research*, vol. 21, no. 1, pp. 1–25, 2002.

Table 1: Site characteristics.

Parameter	Value	Reference
Average height of canopy (h)	11.4 m	
Leaf area index (LAI)	4.2 $m^2\,m^{-2}$	[67, 68, 69]
Displacement height (d)	7.8 m	
Aerodynamic roughness (z_0)	1.6 m	
Average annual mean temperature	0.13 °C	1961-1990 mean, CRU CL 2.0 dataset [70]
Annual total precipitation	482 mm	
Mean (minimum, maximum) temperature (T)	9.41 °C (−14.17 °C, 23.63 °C)	2003 May-October, measured dataset
Total precipitation (P)	232 mm	
Mean (minimum, maximum) soil water content (SWC, θ)	0.152 $m^3\,m^{-3}$ (0.076 $m^3 m^{-3}$, 0.389 $m^3\,m^{-3}$)	

Table 2: Resistance networks.

	ZHANG model	DEPAC model

$$Ra = \frac{1}{\kappa \cdot u^*}\left[0.74 \cdot \ln\left(\frac{z_r}{z_0}\right) - \psi_h\right]$$

$$Ra = \frac{1}{\kappa \cdot u^*}\left[\ln\left(\frac{z_r}{z_0}\right) - \psi_h\right]$$

$$R_b = 1,31 \cdot \frac{5}{u^*}$$

$$R_{st} = \frac{1}{G_{st}(PAR) \cdot f(T) \cdot f(vpd) \cdot f(\psi) \cdot 0.637}$$

Baldocchi:

$$R_{st} = \frac{1}{G_{st}(PAR) \cdot f(T) \cdot f(vpd) \cdot f(\theta) \cdot 0.637}$$

Wesely:

$$R_{st} = 1,571 \cdot R_i \cdot \frac{400}{T \cdot (40 - T)} \cdot \left(1 + \left(\frac{200}{SR + 0.1}\right)^2\right)$$

if solar elevation < 0: R_{st} = 12500 $\left[sm^{-1}\right]$

$$R_{mes} = 0 \left[sm^{-1}\right]$$

$$R_{cut} = \frac{4000}{u^* \cdot LAI^{0.25} \cdot e^{0.03RH}}$$

$$R_{cut} = 1000 \left[sm^{-1}\right]$$

if T < –1°C: $R_{cut} = R_{cut} \cdot e^{0.2(-1-t)}$

$$R_{inc} = \frac{100 \cdot LAI^{0.25}}{(u^*)^2}$$

$$R_{inc} = 8 \cdot h \cdot \frac{LAI}{u^*}$$

$$R_{soil} = 200 \left[sm^{-1}\right]$$

$$R_{soil} = 100 \left[sm^{-1}\right]$$

if T< –1°C: $R_{soil} = R_{soil} \cdot e^{0.2(-1-t)}$

if T< 0°C: $R_{soil} = 2000 \left[sm^{-1}\right]$

R_aerodynamic, R_boundary, R_stomatal, R_mesophyll, R_cuticular, R_in-canopy, R_soil

ZHANG model	DEPAC model
$G_{st}(PAR) = \dfrac{LAI_s}{r_{st}(PAR_s)} + \dfrac{LAI_{sh}}{r_{st}(PAR_{sh})}$	$G_{st}(PAR) = \dfrac{LAI}{250 \cdot (1 + 25/PAR_{measured})}$
$r_{st}(PAR_x) = 250 \cdot (1 + 25/PAR_x)$	$R_i = 130;\ 250;\ 400;\ 250\ \left[\mathrm{sm}^{-1}\right]$
	summer, autumn, winter, spring

$$f(VPD) = 1 - b_{VPD} \cdot (e_s - e)$$

$$f(T) = \frac{T - T_{\min}}{T_{opt} - T_{\min}} \cdot \left(\frac{T_{\max} - T}{T_{\max} - T_{opt}}\right)^{b_T}$$

$$b_T = \frac{T_{\max} - T_{opt}}{T_{\max} - T_{\min}}$$

$f(\psi) = \begin{cases} 1 & \text{if } \psi > \psi_{c1} \\ \max\left(\dfrac{\psi - \psi_{c2}}{\psi_{c1} - \psi_{c2}}, 0.05\right) & \text{if } \psi_{c2} < \psi \leq \psi_{c1} \\ 0.05 & \text{if } \psi \leq \psi_{c2} \end{cases}$	$f(\theta) = 1$

<div align="center">

unstable   **unstable**

</div>

$$\Phi_h = 0.74 \cdot \ln\left(\frac{1 + \left(1 - \left(9 \cdot \frac{z_r}{L}\right)\right)^{0.25}}{2}\right) \qquad \Phi_h = \exp\left[0.598 + 0.39 \cdot \ln\left(-\frac{z_r}{L}\right) - 0.09 \cdot \left(\ln\left(-\frac{z_r}{L}\right)\right)^2\right]$$

<div align="center">

stable   **stable**

</div>

$$\Phi_h = -4.7\frac{z_r}{L} \qquad\qquad\qquad \Phi_h = -5\frac{z_r}{L}$$

<div align="center">

neutral

$$\Phi_h = 0$$

</div>

Table 3: Nomenclature.

ψ,	leaf-water-potential (MPa)
ψ_{c1}, ψ_{c2}	specify leaf-water-potential dependency parameters
Φ_h	dimensionless stability function
b_{VPD}	VPD constant (kPa^{-1})
e, e_s	ambient and saturation water vapour pressure (kPa), respectively
$G_{st}(PAR)$	unstressed leaf stomatal conductance ($m\,s^{-1}$)
κ	Karman constant (0.41)
L	Monin-Obukhov length (calculation method is not detailed here) (m)
PAR_s/PAR_{sh}	PAR received by sunlit and shaded leaves, respectively ($W\,m^{-2}$)
RH	relative humidity (0–100%)
$r_{st}(PAR)$	unstressed leaf stomatal resistance ($m\,s^{-1}$)
T_{min}, T_{max}, T_{opt}	minimum, maximum and optimum T for stomatal opening, respectively(–5 °C, 40 °C and 15 °C)
z_o	roughness length (m)
z_r	reference height (m)
W_{st}	fraction of stomatal blocking under wet conditions

Table 4: Coefficients of determination between biotic/abiotic factors against half hourly measured and daily accumulated ozone fluxes (May-October 2003), N is the number of available measured data, p is the level of significance, daytime, when solar elevation greater than 0, nighttime, when solar elevation is less than zero.

	Period	O_3 flux [nmol m^{-2} s^{-1}]			Acc. O_3 flux [nmol m^{-2} day^{-1}]		
		R^2	p	N	R^2	p	N
	All data	0.004	0.000	4013	0.000	0.927	39
T [Celsius]	Daytime	0.001	0.071	2599			
	Nighttime	0.035	0.000	1414			
	All data	0.057	0.000	4013	0.098	0.052	39
VPD [hPa]	Daytime	0.045	0.000	2599			
	Nighttime	0.043	0.000	1414			
	All data	0.019	0.000	3879	0.003	0.746	38
SWC [m^3 m^{-3}]	Daytime	0.009	0.000	2565			
	Nighttime	0.006	0.000	1314			
	All data	0.090	0.000	4013	0.007	0.607	39
PAR [W m^{-2}]	Daytime	0.090	0.000	2599			
	Nighttime	0.111	0.000	1414			
	All data	0.081	0.000	4013	0.001	0.861	39
SR [W m^{-2}]	Daytime	0.081	0.000	2599			
	Nighttime	0.081	0.000	1414			
	All data	**0.257**	0.000	3866	**0.333**	0.000	36
GPP [mg CO$_2$ m^{-2} s^{-1}]	Daytime	0.246	0.000	2474			
	Nighttime	0.257	0.000	1392			
	All data	**0.212**	0.000	3866	0.050	0.189	36
NEE [mg CO$_2$ m^{-2} s^{-1}]	Daytime	0.214	0.000	2474			
	Nighttime	0.200	0.000	1392			

Table 5: Model quality indicators based on half hourly measured ozone fluxes (May-October 2003), daytime is defined when solar elevation greater than zero, nighttime is defined when solar elevation is less than zero.

Model name	Period	R^2	p	N	MB [nmol m^{-2} s^{-1}]	MAE [nmol m^{-2} s^{-1}]	RMSE [nmol m^{-2} s^{-1}]	NMSE [nmol m^{-2} s^{-1}]	IA	ME
ZHANG model	All data	0.256	0.000	3877	1.389	3.206	4.445	0.520	0.681	0.082
	Daytime	0.168	0.000	2796	1.828	3.765	4.911	0.444	0.592	-0.033
	Nighttime	0.065	0.000	1081	0.254	1.758	2.917	0.930	0.467	-0.153
DEPAC-Baldocchi model	All data	0.154	0.000	3877	7.302	8.085	10.066	1.438	0.457	-3.707
	Daytime	0.045	0.000	2796	9.837	10.467	11.716	1.289	0.371	-4.876
	Nighttime	0.018	0.000	1081	0.744	1.926	2.903	0.799	0.310	-0.145
DEPAC-Wesely model	All data	0.066	0.000	3877	-0.498	3.032	4.550	0.751	0.420	0.038
	Daytime	0.012	0.000	2796	-0.978	3.460	5.045	0.706	0.341	-0.089
	Nighttime	0.018	0.000	1081	0.744	1.926	2.903	0.799	0.310	-0.145

Table 6: Model quality indicators based on daily measured accumulated ozone fluxes (May-October 2003).

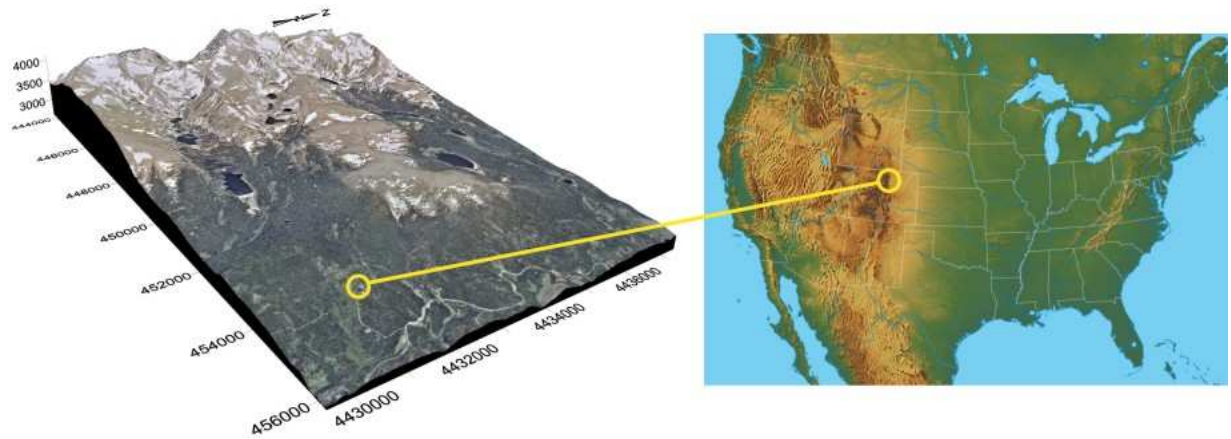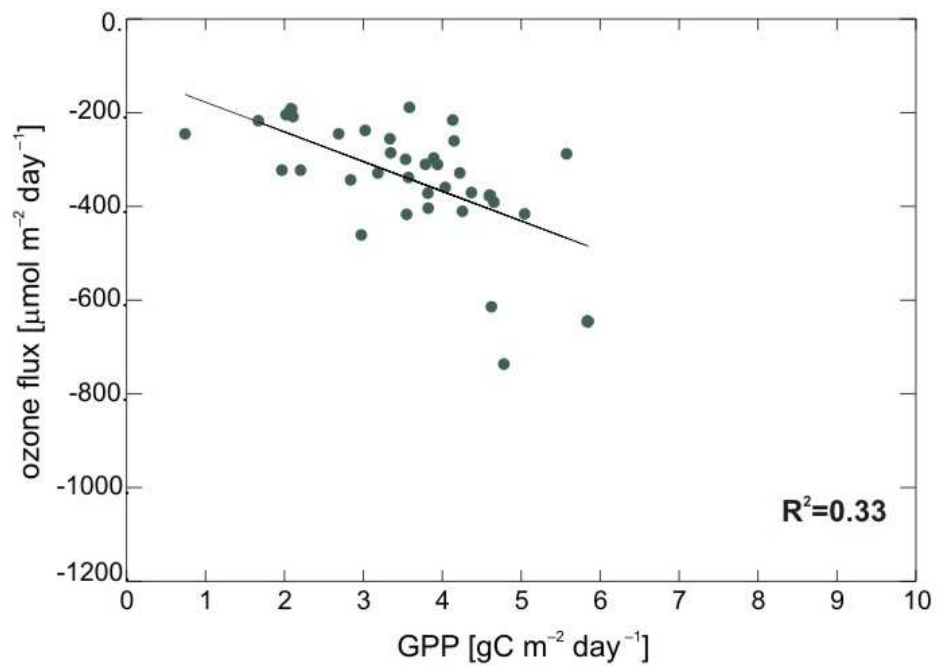| Model name	R^2	p	N	MB [μmol m^{-2} day^{-1}]	MAE [μmol m^{-2} day^{-1}]	RMSE [μmol m^{-2} day^{-1}]	NMSE [nmol m^{-2} day^{-1}]	IA	ME
ZHANG model	0.224	0.002	39	148.918	171.066	218.657	0.286	0.995	0.964
DEPAC-Baldocchi model	0.057	0.144	39	548.170	552.926	585.115	1.130	0.983	0.513
DEPAC-Wesely model	0.023	0.358	39	61.143	119.427	151.741	0.168	0.998	0.994

Figure 1: Landscape and location of the Niwot Ridge Ameriflux site.

Figure 2: Daily accumulated measured ozone flux against daily sums of gross primary production (May-October 2003).
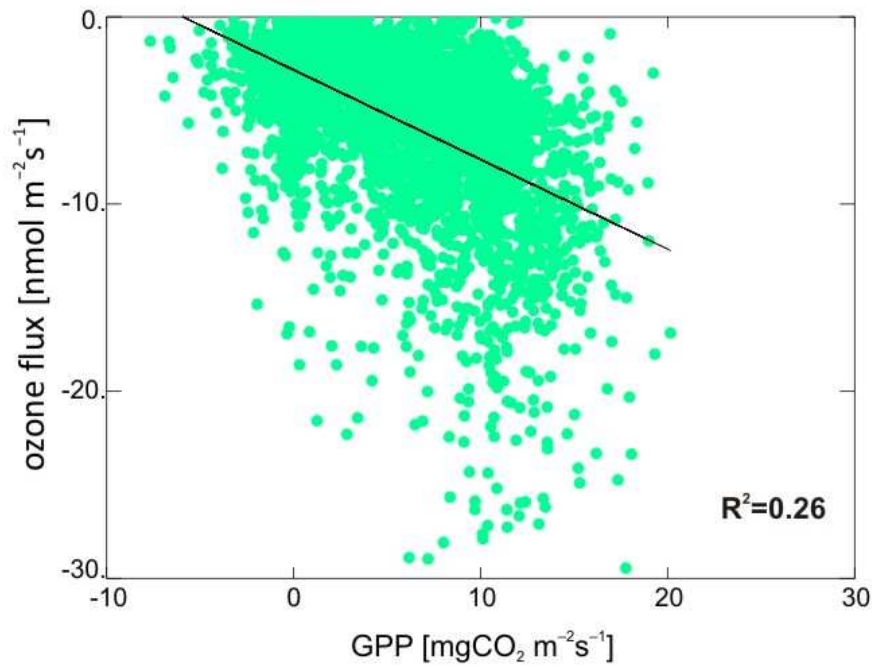
Figure 3: Half hourly measured ozone flux against half hourly measured (May-October 2003) gross primary production.
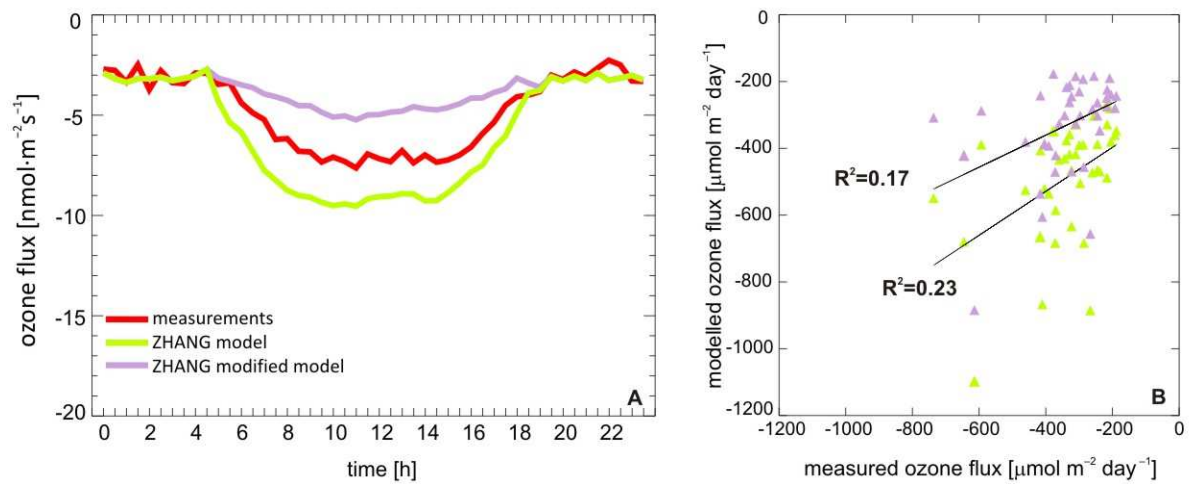

Figure 4: Performance of the ZHANG model and the ZHANG modified model (May-October 2003) (A) mean diurnal variation of half hourly measured and modeled ozone flux (B) daily accumulated measured and modeled ozone flux.

Figure 5: Performance of the DEPAC-Baldocchi model, the DEPAC-Wesely model and the DEPAC-Baldocchi modified model (May-October 2003) (A) mean diurnal variation of half hourly measured and modeled ozone flux (B) daily accumulated measured and modeled ozone flux.
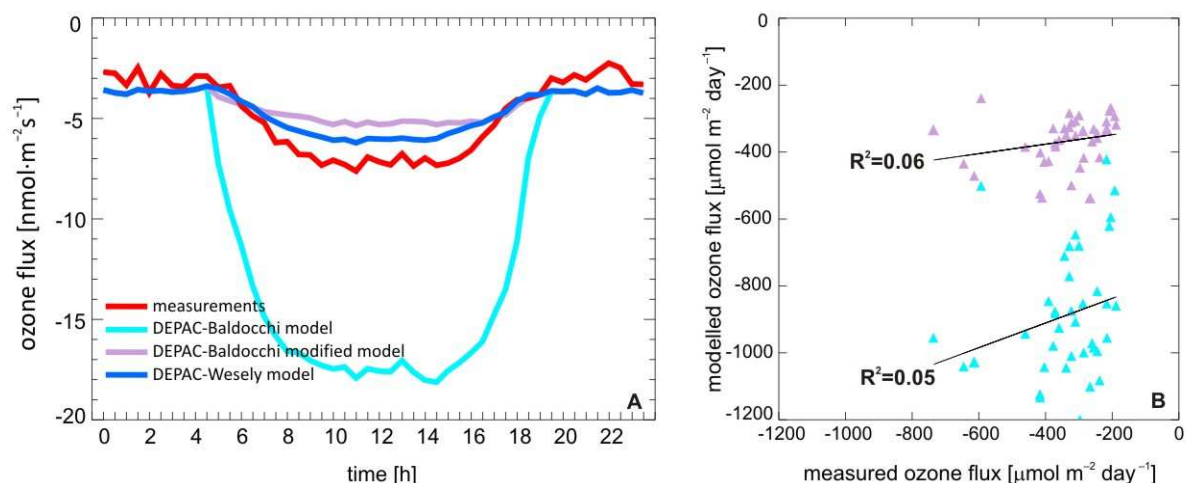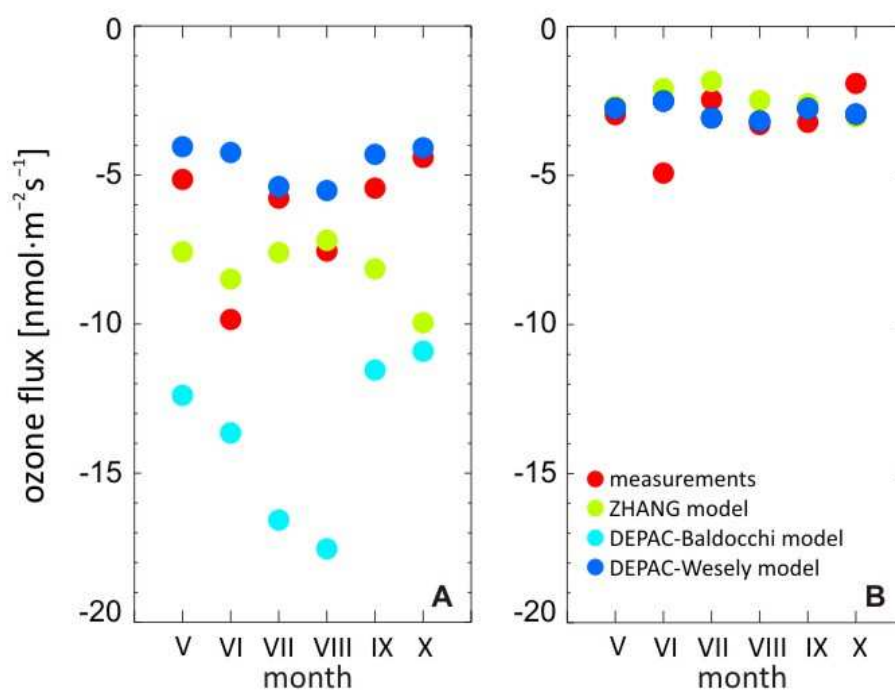

Figure 6: Monthly means of half hourly ozone flux (May-October 2003) (A) daytime, when solar elevation greater than 0, (B) nighttime, when solar elevation is less than zero.

III. Overall conclusions

In this study modelling and evaluation of ozone dry deposition models were carried out focusing on research question addressed in Chapter I. In the following the main conclusions from the previous chapters are summarized.

The behaviour of a deposition model in a temperate climate in the Central European region and the effects of input parameters on the calculated total and stomatal depositions are investigated in the first paper. Two global statistical methods, the Monte Carlo and the Morris analyses were used. With the Monte Carlo method it was possible to characterize the probability distribution of the total and stomatal depositions. The Morris method provided individual contributions of the investigated input variables to the daytime total and stomatal deposition velocity of ozone. Based on these sensitivity analyses, important and unimportant input data were defined. Since long-term prediction of atmospheric variables and feedbacks are very difficult to determine precisely, the sensitivity analyses can be effective tools to decrease the uncertainty of estimations. This investigation showed that the stomatal deposition velocity has a larger variability than the total deposition velocity. Under some conditions, when environmental stresses hit the vegetation, stomatal uptake is nearly zero, while under optimum circumstances the stomatal deposition approaches its vegetation dependent maximum. One of the main results is that the type of the soil slightly affects the deposition velocity; however, root-zone soil moisture is one of the most crucial factors of deposition in the continental climate region.

To answer the second question coupled transport-deposition model was applied for a simulation period from noon 22nd July to midnight 23rd July, 1998. This case study was chosen because during the selected days, the high temperature, low cloud cover and low wind speed resulted in high photooxidant levels in Hungary. To analyze the influence of the soil moisture on the ozone flux, the soil water content has been calculated by a simplified water-budget model. To utilize the soil moisture field, the stomatal part of ozone flux was calculated for two cases. One of them represents a situation, when the effect of soil moisture was neglected, assuming a theoretical well-watered situation, as if the soil moisture content would be equal to the field capacity soil water content at the whole country. In the second case in the model calculations an estimated soil water content field have been used, which provided a more realistic distribution of stomatal ozone flux. It seems that the differences between stomatal fluxes for both taking and without taking into account the effect of the soil moisture stress are conspicuous and varies between 0–70%. Differences depends on both atmospheric state and vegetation, and also strongly on soil types and soil

characteristics. This suggests that the effect of soil water content cannot be neglected in the continental climate region, especially in the hot summer period.

In the third study ecosystem-atmosphere ozone flux and its relation to environmental and ecosystem variables measured on site was examined, and simulated using three widely used deposition models. Due to the meteorological conditions climate of the investigated site (subalpine forest) and the relatively short study period (half year), no statistical correlation between environmental variables and ozone deposition was found. Therefore, the effect of environmental drivers on ozone deposition as simulated in the models could not be fully evaluated against observations. Significant correlation was found, however between GPP (gross primary production) and ozone flux, reflecting its relation to stomatal activity. This study showed that even if we minimize input data errors using measured driving data when available, model results diverge when validated for a randomly selected geographical location and land use type. The results showed, that the lack of calibration inhibits the use of these models in case of ecosystem types other than they have been calibrated for, and hence, their practicality in large scale studies where models are used over several ecosystems might be questionable. Models have to be subjected to rigorous tests of their calculations before drawing serious scientific conclusions. The widely used modelling methods applied in this study have been not yet investigated in such detail. This pioneer work created a major step forward in the study and understanding of atmosphere-plant interaction.

Since models have important role in mapping surface ozone concentrations and investigating direct and indirect consequences of changing tropospheric ozone concentration their continuous development is a general directive.

IV. Outlook

The biosphere of the Earth has been continuously changing for millions of years due to prevailing circumstances formed by interconnected processes. In addition, any changes in this system infer changes of other spheres and depending on their response time could affect on the recent environmental conditions. As indicated by measurements the composition of atmosphere is changing due to the increasing trace gases concentrations of natural and anthropogenic origin. Changing composition impacts the energy balance of the atmosphere and enhances harmful effect of toxic elements. Tropospheric ozone is considered to be one of these elements, can have negative effects on living and non-living environment. Due to the reduced ecosystem productivity tropospheric ozone has a huge influence on carbon sequestration, biodiversity and food security.

This highlights the importance of accurate future predictions regarding tropospheric ozone concentration and the combined effect of ozone and climate change on biospheric carbon sequestration. Since ozone is a secondary pollutant, abundance of its precursors basically determines local concentration patterns. The local and yet transboundary nature of ozone pollution requires international as well as national efforts to effectively reduce emissions of nitrogen oxides and volatile organic compounds (Harmens and Mills, 2012). Such emission reductions would have co-benefits for climate change and human health. Our knowledge is limited regarding current emissions, and even more limited regarding future emission inventories. This can introduce significant errors in future predictions.

Furthermore, investigation of future indirect radiative forcing of ozone is difficult due to the different resistance times of ozone and carbon dioxide. According to Fiore et al. (2002) the ozone lifetime is only a 3–5 days in the continental boundary layer in summer and based on estimation of Šakalys and Girgždienė (2010) groundlevel ozone lifetime under rural conditions during different seasons are in the range of 3–6 hours. Therefore, ozone concentration is very difficult to predict for longer time scales. Mathematical descriptions of these processes included in current ozone deposition models limit the accuracy of future predictions. Uncertainty of climate model predictions together with the difficulties presented above reduces reliability of estimations and inhibit development of effective mitigation strategies.

Humans have more chance than ever to prepare for these changes e.g. using prediction of climate models with new energy solutions and developing more resistant crops. However, mitigation efforts increasingly rely on model simulations, therefore the aim is to have more accurate predictions, hence the developing and evaluation of models are required. The discovery and description the interactions between climate, ecosystems and tropospheric ozone are the key step on this way.

Based the results of the thesis it is suggested that further development of the resistance scheme is desirable, with special attention given to stomatal resistance. A new development direction can be to estimate stomatal resistance with GPP based scheme (like BWB-algorithm) or with combined stress functions. Grünhage and Haenel (2008) presented an example of this latter. Since plants under water stress react more sensitive to vapour pressure deficit, they applied a combined function of vapour pressure deficit and soil moisture which accounts for the interaction effect.

In addition, further evaluations are required to optimize the deposition submodels performance over different land use ecosystems and long data sets.

V. Summary

In connection to the recent climate change the large scale researches based on models are playing increasingly important role. To detect the level of current and future ozone deposition on ecosystem measurements and modelling simulations are carried out. The deposition models differ in describing and parameterization of energy exchange, air and surface resistances or chemical mechanism. Since these models are frequently applied in regional mode evaluation of model outputs is required. To achieve this goal a complex study presented here were carried out.

First, a sensitivity analyses of a detailed ozone dry deposition model was performed for five soil types and four land use categories to reveal the variability of some environmental parameters and data on the estimation of ozone deposition velocity. Deposition velocity and ozone flux depend on the weather situation, physiological state of the plants and numerous surface-, vegetation-, and soil-dependent parameters. The input data and the parameters of deposition calculations all have higher or lower spatial and temporal variability. We investigated the effect of the variability of the meteorological data (cloudiness, relative humidity and air temperature), plant-dependent (leaf area index and maximum stomatal conductance) and soil-dependent (soil moisture) parameters on ozone deposition velocity. To evaluate this effect, two global methods, the Morris method and the Monte Carlo analysis with Latin hypercube sampling were applied. Additionally, local sensitivity analyses were performed to estimate the contribution of non-stomatal resistances to deposition velocity. Using the Monte Carlo simulations, the ensemble effect of several nonlinear processes can be recognised and described. Based on the results of the Morris method, the individual effects on deposition velocity are found to be significant in the case of soil moisture and maximum stomatal conductance. Temperature and leaf area index are also important factors; the former is primarily in the case of agricultural land, while the latter is for grass and coniferous forest. The results of local sensitivity analyses reveal the importance of nonstomatal resistances.

In the second study a coupled photochemical reaction-transport model and a detailed ozone dry deposition model have been utilised for the estimation of stomatal ozone fluxes over Hungary assuming different soil wetness conditions. Ozone concentrations were modelled on an unstructured triangular grid using a method of lines approach to the solution of the reaction–diffusion–advection equations describing ozone formation, transport and deposition. The model domain covers Central-Europe including Hungary, which was located at the centre of the domain and covered by a high resolution nested grid. The dry deposition velocity of ozone was calculated based on the aerodynamic, quasi-laminar boundary layer and canopy resistance. The effect of soil water content on the stomatal ozone flux was analysed. The stomatal ozone flux

calculations were performed for two cases, with and without taking into account the effect of the soil moisture stress on the ozone deposition. The meteorological data were generated by the ALADIN meso-scale limited area numerical weather prediction model. It was found that soil water deficiency can strongly reduce the stomatal conductance and hence the ozone flux through it.

Finally, detailed evaluation of three different deposition schemes was carried out to investigate model applicability. The sophisticated interactions among atmospheric chemistry, ecosystem-, and climate processes are currently not represented in models in their full complexity. Emission and atmospheric processing of pollutants with anthropogenic origin is a high research priority due to their effect on the terrestrial biosphere and direct and indirect climatic forcing. However, large scale applications of surface-atmosphere exchange of reactive gases require modelling results as accurate as possible to avoid nonlinear accumulation of errors in the spatially representative results. In this paper evaluation and comparison of three different modelling schemes of ozone gas deposition against measured ozone flux data over a coniferous forest at Niwot Ridge AmeriFlux site (Colorado, USA) is carried out. Results show that in all three cases, model performance varies with time of the day, and the errors show a pronounced seasonal pattern as well. During daytime both over- and underestimation occurred depending on the season and low correlation was detected between measured and modelled ozone flux for the whole period. In order to explore possible reasons for model errors, we evaluated the driving variables of ozone deposition for hourly, daily and monthly time steps based on measured ozone flux data at the study site. The results showed that measured gross primary production and ozone flux have a strong correlation although this relationship is not included in any of the investigated formulas of ozone deposition calculation. Finally, model parameterization improvements were carried out in case of two models. With modification of soil moisture parameterisation (using the full half hourly dataset) bias did not change in case of one modell, although in case the other model bias decreased almost by half compared to the original parameterization.

Since models have important role in mapping surface ozone concentrations and investigating direct and indirect consequences of changing tropospheric ozone concentration their continuous development is a general directive.

VI. Zusammenfassung

Die auf Modellen basierenden weitreichenden Forschungen spielen im Zusammenhang mit der derzeitigen Klimaänderung eine zunehmend wichtige Rolle. Es werden Messungen und Modellsimulationen durchgeführt, um das Maß der derzeitigen und zukünftigen Ozondeposition auf das Ökosystem festzustellen. Die Depositionsmodelle unterscheiden sich in der Beschreibung und Parametrisierung des Energieaustausches, des Luft- und Oberflächenwiderstandes oder des chemischen Mechanismus. Da diese Modelle regional angewandt werden, ist eine Evaluierung der Modelle erforderlich. Um dieses Ziel zu erreichen, wurde die hier beschriebene komplexe Studie durchgeführt.

Als erstes wurden gründliche Sensitivitätsanalysen eines detaillierten Trockendepositionsmodelles für fünf Bodentypen und vier Landnutzungskategorien durchgeführt, um die Variabilität einiger Umweltparameter und -Daten bei der Berechnung der Ozondepositionsgeschwindigkeit zu untersuchen. Die Depositionsgeschwindigkeit und der Ozonfluss hängen von der Wetterlage, dem physiologischen Zustand von Pflanzen und zahlreichen oberflächen-, vegetations- und bodenabhängigen Parameter ab. Die Eingangsdaten und die Parameter der depositionbezogenen Berechnungen haben höhere oder niedrigere räumliche und zeitliche Variabilität. Die Wirkung der Variabilität meteorologischer Daten (Bewölkung, Luftfeuchte und Lufttemperatur), pflanzenabhängiger Parameter (Blattflächenindex und maximale stomatäre Leitfähigkeit) und eines bodenabhängigen Parameters (Bodenfeuchte) auf die Ozondepositionsgeschwindigkeit wurde untersucht. Um diesen Effekt zu bewerten, wurden zwei globale Methoden, die Morris-Methode und die Monte-Carlo-Analyse mit Latin Hypercube Stichprobe angewendet. Zusätzlich wurden lokale Sensitivitätsanalysen durchgeführt, um den Beitrag nichtstomatärer Widerstände der Depositionsgeschwindigkeit abzuschätzen. Mit Hilfe der Monte-Carlo-Simulationen kann die Ensemblewirkung mehrerer nichtlinearer Prozesse erkannt und beschrieben werden. Die Ergebnisse der Morris-Methode ergaben, dass die einzelnen auf die Depositionsgeschwindigkeit wirkenden Effekte im Falle der Bodenfeuchtigkeit und der maximalen stomatären Leitfähigkeit signifikant sind. Temperatur und Blattflächenindex sind ebenfalls wichtige Faktoren; die erstere spielt vor allem bei landwirtschaftlichen Flächen eine wichtige Rolle, während Blattflächenindex für Gras und Nadelwald wichtig ist. Die Ergebnisse der lokalen Sensitivitätsanalysen zeigen die Bedeutung nichtstomatärer Widerstände.

In der zweiten Studie wurden ein Chemie-Transportmodell und ein detailliertes Ozondepositionsmodell für die Schätzung stomatärer Ozonflüsse über Ungarn unter verschiedenen Bodenfeuchtigkeiten verwendet. Die Ozonkonzentrationen wurden auf einem unstrukturierten Dreiecksgitter mit einem Linienmethodeansatz zur Lösung der

Reaktion-Diffusion-Advektionsgleichungen von Ozonbildung, Transport und Deposition modelliert. Der Modellbereich umfasst Mitteleuropa einschließlich Ungarn, welches in der Mitte des Untersuchungsgebietes liegt und von einem hochaufgelösten verschachtelten Gitter bedeckt ist. Die Ozondepositionsgeschwindigkeit wurde auf der Grundlage turbulenter, quasi-laminarer Transferwiderstände und des Oberflächenwiderstands berechnet. Die Wirkung der Bodenfeuchtigkeit auf den stomatären Ozonfluss wurde analysiert. Die stomatären Ozonflussberechnungen wurden für zwei Fälle durchgeführt, mit und ohne Berücksichtigung der Wirkung der Bodenfeuchtigkeitsbelastung der Ozondeposition. Die meteorologischen Daten wurden mit dem numerischen Wettervorhersagemodell ALADIN erzeugt. Es wurde festgestellt, dass das Bodenfeuchtigkeitsdefizit die stomatäre Leitfähigkeit stark reduzieren kann, und dass dadurch auch der Ozonfluss nachlassen kann.

Zuletzt wurde die detaillierte Auswertung drei verschiedener Depositionsschemata durchgeführt, um die Anwendbarkeit der Modelle zu untersuchen. Die anspruchsvollen Interaktionen zwischen Luftchemie-, Ökosystem- und Klimaprozessen werden derzeit in Modellen nicht in ihrer ganzen Komplexität dargestellt. Emission und atmosphärische Verarbeitung von anthropogenen Schadstoffen ist ein großer Forschungsschwerpunkt aufgrund ihrer Wirkung auf die terrestrische Biosphäre und ihrer direkten und indirekten Klimagewalt. Allerdings, großräumige Anwendungen des Oberflächen-Atmosphären-Austausches reaktiver Gasen erfordern möglichst akkurate Modellierungsergebnisse, um nichtlineare Anhäufungen von Fehlern räumlich repräsentativer Ergebnisse zu vermeiden. In dieser Arbeit wurde die Evaluierung und der Vergleich dreier verschiedener Modellschemata der Ozondeposition gegen Messdaten über einem Nadelwald am Standort Niwot Ridge Ameriflux (Colorado, USA) durchgeführt. Die Ergebnisse zeigen, dass die Modellleistung in allen drei Fällen mit der Tageszeit variiert, und dass die Fehler ein ausgeprägtes saisonales Muster zeigen. Am Tag treten abhängig von der Jahreszeit Über- und Untersätzungen auf und die Korrelation zwischen den gessungenen und modellierten Ozoneflüssen ist für die gesamte Periode gering. Um mögliche Gründe für Modellfehler zu erforschen, wurden die treibenden Variablen der Ozondeposition in stündlichen, täglichen und monatlichen Zeitschritten basierend auf gemessenen Ozonflussdaten am Standort untersucht. Die Ergebnisse zeigen, dass die gemessene Bruttoprimärproduktion und der gemessene Ozonfluss eine starke Korrelation haben, obwohl diese Beziehung in keiner der untersuchten Formeln von Ozondepositionsberechnung einbezogen wird. Zuletzt werden in zwei unterschiedlichen Modellen Modellparametrisierungsentwicklungen druchgeführt. Durch die Modifikation der Bodenfeuchtigkeitsparametrierung (benutzte halbstündliche Daten) blieb der Fehler in einem der beiden Modelle unändern, obwohl im Falle des anderen Modells der Bias im Vergleich zur ursprünglichen Parametrierung um fast die Hälfte verringert wurde . Da Modelle im Mapping der Oberflächenkonzentration von Ozon und in der Untersuchung direkter sowie indirekter Folgen der Veränderung troposphärischer Ozonkonzentration eine wichtige Rolle spielen, ist ihre kontinuierliche Entwicklung eine generelle Direktive.

References

Amann, M., Bertok I., Cofala J., Gyarfas F., Heyes C., Klimont Z., Schöpp W., Winiwarter W., 2005. Baseline Scenarios for the Clean Air for Europe (CAFE.) Programme Final Report, Royal Society, 65–66.

Anav A., Menut L., Khvorostyanov D., Viovy N., 2011. Impact of tropospheric ozone on the Euro-Mediterranean vegetation. Global Change Biology, 17, 2342–2359.

Ashworth K., Wild O., Hewitt C. N., 2013. Impacts of biofuel cultivation on mortality and crop yields. Nature Climate Change, 3, 492–496.

Baldocchi D. D., Hicks B. B., Camara P., 1987. A canopy stomatal resistance model for gaseous deposition to vegetated surfaces. Atmospheric Environment, 21, 91–101.

Bassin S., Volk M., Fuhrer J., 2007. Factors affecting the ozone sensitivity of temperate European grasslands: an overview. Environmental Pollution, 146, 678–691.

Bey I., Jacob D. J., Yantosca R. M., Logan J. A., Field B. D., Fiore A. M., Li Q., Liu H. Y., Mickley L. J., Schultz M. G., 2001. Global modeling of tropospheric chemistry with assimilated meteorology: Model description and evaluation. Journal of Geophysical Research: Atmospheres, 106, D19, 23073–23095.

Bytnerowicz A., Omasa K., Paoletti E., 2007. Integrated effects of air pollution and climate change on forests: A northern hemisphere perspective. Environmental Pollution, 147, 438–445.

Collins W. J., Sitch S., Boucher O., 2010. How vegetation impacts affect climate metrics for ozone precursors. Journal of Geophysical Research: Atmospheres, 115, D23, D23308.

Coyle M., Nemitz E., Storeton-West R., Fowler D., Cape J. N., 2009. Measurements of ozone deposition to a potato canopy. Agricultural and Forest Meteorology, 149, 655–665.

EEA Technical report No 5/2007. Air pollution by ozone in Europe in summer 2006. Overview of exceedances of EC ozone threshold values for April–September 2006.

Emery C., Jung J., Downey N., Johnson J., Jimenez M., Yarwood G., Morris R., 2012. Regional and global modeling estimates of policy relevant background ozone over the United States. Atmospheric Environment, 47, 206–217.

Fares S., Goldstein A., Loreto F., 2010a. Determinants of ozone fluxes and metrics for ozone risk assessment in plants. Journal of Experimental Botany, 61, 629–633.

Fares S., McKay M., Holzinger R., Goldstein A. H., 2010b. Ozone fluxes in a Pinus ponderosa ecosystem are dominated by non-stomatal processes: Evidence from long-term continuous measurements. Agricultural and Forest Meteorology, 150, 420–431.

Felzer B. S. F., Kicklighter D. W., Melillo J. M., Wang C., Zhuang Q., Prinn R. G., 2004. Effects of ozone on net primary production and carbon sequestration in the conterminous United States using a biogeochemistry model. Tellus, 56B, 230–248.

Felzer B. S., Cronin T., Reilly J. M., Melillo J. M., Wang X., 2007. Impacts of ozone on trees and crops. Comptes Rendus Geoscience, 339, 784–798.

Fiore A. M., Jacob D. J., Bey I., Yantosca R. M., Field B. D., Fusco A. C., Wilkinson J. G., 2002. Background ozone over the United States in summer: Origin, trend, and contribution to pollution episodes. Journal of Geophysical Research: Atmospheres, 107, D15, ACH 11-1–ACH 11-25.

Foken T., Dlugi R., Kramm, G., 1995. On the determination of dry deposition and emission of gaseous compounds at the biosphere-atmosphere interface. Meteorologische Zeitschrift, 4, 91–118.

Forster, P., Ramaswamy V., Artaxo P., Berntsen T., Betts R., Fahey D. W., Haywood J., Lean J., Lowe D. C., Myhre G., Nganga J., Prinn R., Raga G., Schulz M., Van Dorland R., 2007. Changes in Atmospheric Constituents and in Radiative Forcing. In: Climate Change 2007: The Physical Science Basis. Contribution of Working Group I to the Fourth Assessment Report of the Intergovernmental Panel on Climate Change [Solomon, S., Qin D., Manning M., Chen Z., Marquis M., Averyt K. B., Tignor M., Miller H. L. (eds.)]. Cambridge University Press, Cambridge, United Kingdom and New York, NY, USA.

Fowler, D., Amann, M., Anderson, R., Ashmore, M., Cox, P., Depledge, M., Derwent, D., Grennfelt, P., Hewitt, N., Hov, O., Jenkin, M., Kelly, F., Liss, P., Pilling, M., Pyle, J., Slingo, J., Stevenson, D., 2008. Ground-level ozone in the 21st century: future trends, impacts and policy implications. Royal Society Policy Document 15/08, London: The Royal Society.

Grell G. A., Peckham S. E., Schmitz R., McKeen S. A., Frost G., Skamarock W. C., Eder B., 2005. Fully coupled 'online' chemistry in the WRF model. Atmospheric Environment, 39, 6957–6976.

Grünhage L. and Haenel H.-D., 2008. PLATIN PLant-ATmosphere Interaction model. Landbauforschung, Special Issue, 319, p. 85.

Harmens H. and Mills G., 2012. Ozone pollution: Impacts on carbon sequestration in Europe. ICP Vegetation Programme Coordination Centre, Centre for Ecology and Hydrology, Bangor, UK.

Hartmann, D. L., Klein Tank A. M. G., Rusticucci M., Alexander L. V., Brönnimann S., Charabi Y., Dentener F. J., Dlugokencky E. J., Easterling D. R., Kaplan A., Soden B. J., Thorne P. W., Wild M., Zhai P. M., 2013. Observations: Atmosphere and Surface. In: Climate Change 2013: The Physical Science Basis. Contribution of Working Group I to the Fifth Assessment Report of the Intergovernmental Panel on Climate Change [Stocker, T. F., Qin D., Plattner G.-K., Tignor M., Allen S. K., Boschung J., Nauels A., Xia Y., Bex V., Midgley P. M. (eds.)]. Cambridge University Press, Cambridge, United Kingdom and New York, NY, USA.

Hayes F., Wagg S., Mills G., Wilkinson S., Davies W., 2012. Ozone effects in a drier climate: implications for stomatal fluxes of reduced stomatal sensitivity to soil drying in a typical grassland species. Global Change Biology, 18, 948–959.

Hurley P., 2008. TAPM V4. Part 1: Technical Description. CSIRO Marine and Atmospheric Research Paper, 25, 59.

Karnosky D. F., Pregitzer K. S., Zak D. R., 2005. Scaling ozone responses of forest trees to the ecosystem level in a changing climate, Plant, Cell and Environment, 28, 965–981.

Karnosky D. F., Zak D. R., Pregitzer K. S., Awmack C. S., 2003. Tropospheric O3 moderates responses of temperate hardwood forests to elevated CO2: a synthesis of molecular to ecosystem results from the Aspen FACE project, Functional Ecology, 17, 289–304.

LRTAP Convention, 2010. Mapping Manual 2004. Manual on methodologies and criteria for modelling and mapping critical loads & levels and air pollution effects, risk and trends. Chapter 3. Mapping critical levels for vegetation. 2010 revision, Available at: http://icpvegetation.ceh.ac.uk.

Menut L., Bessagnet B., Khvorostyanov D., Beekmann M., Blond N., Colette A., Coll I., Curci G., Foret G., Hodzic A., Mailler S., Meleux F., Monge J.-L., Pison I., Siour G., Turquety S., Valari M., Vautard R., Vivanco M. G., 2013. CHIMERE 2013: a model for regional atmospheric composition modelling. Geoscientific Model Development, 6, 981–1028.

Mills G., Wagg S., Harmens H., 2013. Ozone pollution: Impacts on ecosystem services and biodiversity. ICP Vegetation Programme Coordination Centre, Centre for Ecology and Hydrology, Bangor, UK.

Mills, G. and Harmens, H., 2011. Ozone pollution: A hidden threat to food security. ICP Vegetation Programme Coordination Centre, Centre for Ecology and Hydrology, Bangor, UK.

Monteith J. L., Unsworth M. H., 2008. Principles of Environmental Physics, 3rd ed., Elsevier, Academic Press.

Moussiopoulos N. and Douros I., 2005. Efficient calculation of urban scale air pollutant dispersion and transformation using the OFIS model within the framework of CityDelta. International Journal of Environment and Pollution, 24, 64–74.

References

Musselman R. C.,Lefohn A. S., Massman W. J., R. L. Heath, 2006. A critical review and analysis of the use of exposure- and flux-based ozone indices for predicting vegetation effects. Atmospheric Environment, 40, 1869–1888.

Pan Y., Birdsey R. A., Fang J., Houghton R., Kauppi P. E., Kurz W. A., Phillips O. L., Shvidenko A., Lewis S. L., Canadell J. G., Ciais P., Jackson R. B., Pacala S. W., McGuire A.D. , Piao S., Rautiainen A., Sitch S., Hayes D., 2011. A Large and Persistent Carbon Sink in the World's Forests, Science, 333, 988–993.

Panek J. A., Kurpius M. R., Goldstein A. H., 2002. An evaluation of ozone exposure metrics for a seasonally drought- stressed ponderosa pine ecosystem. Environmental Pollution, 117, 93–100.

Prather M., Ehhalt D., Dentener F., Derwent R., Dlugokencky E., Holland E., Isaksen I., Katima J., Kirchhoff V., Matson P., Midgley P., Wang M., 2001. Chapter 4: Atmospheric chemistry and greenhouse gases. In: Houghton J. T., Ding Y., Griggs D. J., Noguer M., van der Linden P. J., Dai X., Maskell K., Johnson C. A. (Eds.), Climate Change 2001: The Scientific Basis. Contribution of Working Group 1 to the Third Assessment Report of the Intergovernmental Panel on Climate Change. Cambridge University Press, Cambridge, pp. 239–287.

Šakalys J. and Girgždienė R., 2010. Estimation of the ground-level ozone lifetime under rural conditions. Lithuanian Journal of Physics, 50, 247–254.

Samoli E., Zanobetti A., Schwartz J., Atkinson R., LeTertre A., Schindler C., Pérez L., Cadum E., Pekkanen J., Paldy A., Touloumi G., Katsouyanni K., 2009. The temporal pattern of mortality responses to ambient ozone in the APHEA project. Journal of Epidemiology and Community Health, 63, 960-966.

Sandermann H., Ernst D., Heller W., Langebartels, C., 1998. Ozone: An abiotic elicitor of plant defence reactions. Trends in Plant Science, 3, 47–50.

Schaap M., Timmermans R. M. A., Roemer M., Boersen G. A. C., Builtjes P. J. H., Sauter F. J., Velders G. J. M., Beck J. P., 2008. The LOTOS–EUROS model: description, validation and latest developments. International Journal of Environment and Pollution, 32, 270–290.

Schimel D. S., 1995. Terrestrial ecosystems and the carbon cycle. Global Change Biology, 1, 77–91.

Seinfeld J. H. and Pandis S. N., 2012. Atmospheric Chemistry and Physics: From Air Pollution to Climate Change. Wiley-Interscience, John Wiley & Sons, Inc.

Seinfeld J.H. and Pandis S.N., 2012. Atmospheric Chemistry and Physics: From Air Pollution to Climate Change. Wiley-Interscience, John Wiley & Sons, Inc.

Simpson D., Benedictow A., Berge H., 2012. The EMEP MSC-W chemical transport model – technical description. Atmospheric Chemistry and Physics, 12, 7825–7865.

Sitch S., Cox P. M., Collins W. J., Huntingford C., 2007. Indirect radiative forcing of climate change through ozone effects on the land-carbon sink. Nature, 448, 791–794.

Smithson, P. A., 2002. IPCC Climate Change 2001: the scientific basis. Contribution of Working Group 1 to the Third Assessment Report of the Intergovernmental Panel on Climate Change, edited by J. T. Houghton, Y. Ding, D. J. Griggs, M. Noguer, P. J. van der Linden, X. Dai, K. Maskell, C. A. Johnson (eds). Cambridge University Press, Cambridge, UK, and New York, USA.

Smyth S. C., Jiang W., Roth H., Moran M. D., Makar P. A., Yang F., Bouchet V. S., Landry H., 2009. A comparative performance evaluation of the AURAMS and CMAQ air-quality modelling systems. Atmospheric Environment, 43, 1059–1070.

Stern R., 2009. Das chemische Transportmodell REM-CALGRID. Model description. Freie Universität Berlin. Online available: www.geo.fu-berlin.de/met/ag/trumf/RCG/RCG-Beschreibung.pdf?1373749582

Stevenson D. S., Dentener F. J., Schultz M. G., Ellingsen K., van Noije T. P. C., Wild O., Zeng G., Amann M., Atherton C. S., Bell N., Bergmann D. J., Bey I., Butler T., Cofala J., Collins W. J., Derwent R. G., Doherty R. M., Drevet J., Eskes H. J., Fiore A. M., Gauss M., Hauglustaine D. A., Horowitz L. W., Isaksen I. S. A., Krol M. C., Lamarque J.-F., Lawrence M. G., V. Montanaro, Müller J.-F., Pitari G., Prather M. J., Pyle J. A., Rast S., Rodriguez J. M., Sanderson M. G., Savage N. H., Shindell D. T., Strahan S. E., Sudo K.,Szopa S., 2006. Multimodel ensemble simulations of present-day and near-future tropospheric ozone. Journal of Geophysical Research: Atmospheres, 111, D8, D08301.

Stöckhardt J.H., 1871. Untersuchungen über die schädlichen Einwirkungen des Hütten-und Steinkohlenrauches auf das Wachsthum der Pflanzen, insbesondere der Fichten und Tannen. Tharandter Forstliches Jahrbuch, 21, 218–254.

Van Dingenen, R., Dentener, F. J., Raes, F., Krol, M. C., Emberson, L., Cofala, J., 2009. The global impact of ozone on agricultural crop yields under current and future air quality legislation. Atmospheric Environment, 43, 604–618.

Vieno M., Dore A. J., Stevenson D. S., Doherty R., Heal M. R., Reis S., Hallsworth S., Tarrason L., Wind P., Fowler D., Simpson D., Sutton M. A., 2010. Modelling surface ozone during the 2003 heat-wave in the UK. Atmospheric Chemistry and Physics, 10, 7963–7978.

Volk M., Bungener P., Contat F., Montani M., Fuhrer J., 2006. Grassland yield declined by a quarter in 5 years of free-air ozone fumigation. Global Change Biology, 12, 74–83.

Warneck P., 2000. Chemistry of the natural atmosphere. International Geophysics series, 71, Academic press.

Wesely M. L. and Hicks B. B., 2000. A review of the current status of knowledge on dry deposition. Atmospheric Environment, 34, 2261–2282.

References

Wittig, V. E., Ainsworth, E. A., Naidu, S. L., Karnosky, D. F., Long, S. P., 2009. Quantifying the impact of current and future tropospheric ozone on tree biomass, growth, physiology and biochemistry: a quantitative meta-analysis. Global Change Biology, 15, 396–424.

World Health Organization Regional Office for Europe, 2006. Air quality guidelines global update 2005: Particulate matter, ozone, nitrogen dioxide, and sulfur dioxide. Copenhagen: World Health Organization Regional Office for Europe.

Appendix containing the contribution to the study

Contribution to the paper I and II:

The main work of these studies has been done at the Department of Meteorology, Eötvös University (Hungary). The set-up for paper I was mainly developed by István Gyula Zsély and István Lagzi. I carried out, in cooperation with the other autors, the interpretation and discussion of simulation results including plotting of figures and the analyses of results. The paper I was mainly written by Róbert Mészáros.

The model development for paper II was mainly perfomed by Róbert Mészáros and István Lagzi. I performed, in cooperation with my colleagues at the Department of Meteorology the adaption of the soil wetness routine to the deposition model, based on my previous research results. The literature studies and collection of data were mainly conducted by myself. The paper was mainly written by Róbert Mészáros, I contributed to the interpretation and the discussion of the results.

Contribution to the paper III:

The set-up of the study was performed by myself in discussions with colleagues at Freie Universität Berlin. I adopted the dry deposition submodels of DEPAC and ZHANG model to address the scientific questions. A new common environment was constructed by myself to explore the performance of the different resistance schemes of these models. The improved process descriptions of soil stress function were adapted to the models system and implemented in the model by myself. The literature studies, model simulations, post-processing of model and measurement data including plotting of figures and the analyses of results were mainly conducted by myself. The data which I used in this study were provided by Russel Monson (PI at Niwot Ridge AmeriFlux site) with kind cooperation of Alex Guenther and Andew Turnipseed. The paper was written by myself in cooperation with Györgyi Gelybó.

List of publications

Journal papers

Szinyei D., Gelybó Gy., Guenther A. B., Turnipseed A. A., Tóth E., Builtjes P. J. H., 2014. Evaluation of ozone deposition models over a subalpine forest in Niwot Ridge, Colorado. Submitted to Advances in Meteorology.

Mészáros R., Zsély I. Gy., Szinyei D., Vincze Cs., Lagzi I., 2009. Sensitivity analysis of ozone deposition model. Atmospheric Environment, 43, 663–672.

Mészáros R., Szinyei D., Vincze Cs., Lagzi I., Turányi T., Haszpra L., Tomlin A. S., 2009. Effect of the soil wetness state on the stomatal ozone fluxes over Hungary. International Journal of Environment and Pollution, 36, 180–194.

Mészáros R., Lagzi I., Juhász Á., Szinyei D., Vincze Cs., Horányi A., Kullmann L., Tomlin A.S., 2006. Description and evaluation of a coupled Eulerian transport-exchange model: Part II: Sensitivity analysis and application. Időjárás, 110, 365–337.

Conference presentations

Szinyei D., Gelybó Gy., Guenther A., Turnipseed A., Czigány Sz., Pirkhoffer E., Builtjes P.H.J., 2013. Evaluation of ozone deposition models over a subalpine forest. 13th Annual Meeting of the European Meteorological Society and 11th European Conference on Applications of Meteorology (ECAM), 9–13 September 2013, Reading, United Kingdom.

Szinyei D., Czender Cs., Lagzi I., Mészáros R., Vincze Cs., Zsély I. Gy., 2007. Uncertainty analysis of a dry deposition model. 7th Annual Meeting of the European Meteorological Society and 8th European Conference on Applications of Meteorology (ECAM), 1–5 October 2007, San Lorenzo de El Escorial, Spain.

Szinyei D., Mészáros R., Vincze Cs., Lagzi I., 2007. Parameterization of dry deposition velocity, ozone fluxes and air quality model development. ECONET Meeting of Modern Techniques in Atmospheric Physics and Chemistry, 2–4 May 2007, Szeged, Hungary.

Conference posters

Szinyei D., Gelybó Gy., Guenther A., Turnipseed A., Czigány Sz., Pirkhoffer E., Builtjes, P.H.J., 2013. Evaluation of ozone deposition models over a subalpine forest. 13th Annual Meeting of the European Meteorological Society and 11th European Conference on Applications of Meteorology (ECAM), 9–13 September 2013, Reading, United Kingdom.

Szinyei D., Gelybó G., Guenther A., Turnipseed A. A., Grünhage L., Kerschbaumer A., Builtjes P. H. J., 2010. Estimation of ozone deposition over subalpine forest in Niwot Ridge, Colorado. 29th Conference on Agricultural and Forest Meteorology, Keystone, Colorado, Amer. Meteor. Soc., P1.15.

Mészáros R., Lagzi I., Szinyei D., Vincze Cs., Zsély I. Gy., 2008: Uncertainties of input parameters of an ozone deposition model. 8th Annual Meeting of the European Meteorological Society and 7th European Conference on Applications of Climatology (ECAC), 29 September–3 October 2008, Amsterdam, The Netherlands.

Juhász Á., Czender Cs., Komjáthy E., Antal K., Mészáros R., Lagzi I., Vincze Cs., Szinyei D., 2007. Current state of the TREX deposition model and the main line of the further development. 7th Annual Meeting of the European Meteorological Society and 8th European Conference on Applications of Meteorology (ECAM), 1–5 October 2007, San Lorenzo de El Escorial, Spain.

Vincze Cs., Zsély I. Gy., Szinyei D., Mészáros R., Lagzi I., 2007. Uncertainty analysis of ozone deposition model. 5th International Conference on Sensitivity Analysis of Model Output (SAMO 2007), 18–22 June 2007, Eötvös University, Budapest, Hungary.

Komjáthy E., Lagzi I., Mészáros R., Vincze Cs., Szinyei D., 2007. Estimation of ozone deposition with TREX (TRansport-Exchange) model. European Geosciences Union, General Assembly 2007, 15–20 April 2007, Vienna, Austria.

Lagzi I., Mészáros R., Vincze Cs., Juhász Á., Szinyei D., Komjáthy E., Antal K., 2006. Recent developments and application of TREX (TRansport-EXchange) model. 6th Annual Meeting of the European Meteorological Society and 8th European Conference on Applications of Meteorology (ECAM), 4–8 September 2006, Ljubljana, Slovenia.

Szinyei D., Mészáros R., Lagzi I., 2006. Estimation of energy-balance components for a photochemical reaction-transport model. European Geosciences Union, General Assembly 2006, 3–7 April 2006, Vienna, Austria.

Szinyei D., Vincze Cs., Mészáros R., Lagzi I., Ács F., Pintér K., Haszpra L., 2005. Estimation of root-zone soil water content by a simple bucket model: applications on Hungarian datasets. 5th Annual Meeting of the European Meteorological Society and 7th European Conference on Applications of Meteorology (ECAM), 12–16 September 2005, Utrecht, The Netherlands.

Juhász Á., Mészáros R., Lagzi I., Vincze Cs., Szinyei D., Ács F., Horányi A., Kullmann L., 2005. Estimating stomatal ozone fluxes using a coupled transport-deposition model. 5th Annual Meeting of the European Meteorological Society and 7th European Conference on Applications of Meteorology (ECAM), 12–16 September 2005, Utrecht, The Netherlands.

Lagzi I., Mészáros R., Ács F., Szinyei D., Vincze Cs., Tomlin A. S., Turányi T., Haszpra L., 2006. Effect of the soil wetness state on the stomatal ozone fluxes in continental region. European Geosciences Union, General Assembly 2005, 24–29 April 2005, Vienna, Austria.

Acknowledgement

I would like to thank ALL who contribute to this work for their assistance, instructions, guidance, energy and time.

My special thanks go to ...

… my supervisors, my co-authors of articles used in this dissertation and my colleagues for their leadership, common work and help, namely: Peter Builtjes, Róbert Mészáros, Györgyi Gelybó, István Lagzi, Csilla Vincze, István Zsély, Tamás Turányi, László Haszpra, Alison Tomlin, Alex Guenther, Andrew Turnipseed, Eszter Tóth, Eberhard Reimer, Rainer Stern, Andreas Kerschbaumer, Jürgen Fath, Sabine Banzhaf, Andrea Mues, Szabolcs Czigány, Ervin Pirkhoffer, István Geresdi, Noémi Sarkadi, András Gelencsér.

… project leaders to involve me their projects and for financial supports, namely: Róbert Mészáros, István Lagzi, Eberhard Reimer, István Geresdi, András Gelencsér, Szabolcs Czigány, Ervin Pirkhoffer.

… Györgyi Gelybó for her indispensable, professional and loyal co-operation.

… DAAD and BERL♥N.

… my Family and my Friends in present and past, who believe me and help me to be on the road all the time, specially my Parents, my Brothers and my Cousins. I dedicate my thesis to Them.

My endless thanks go to my Ironman **Father** who is my ideal for teaching me how to become a finisher and to my beloved **Attila** for his never-ending inspiration.